WL-TR-92-2125

ROTORDYNAMIC AND LEAKAGE CHARACTERISTICS OF A 4-STAGE BRUSH SEAL

K. J. CONNER
D. W. CHILDS

TURBOMACHINERY LABORATORIES
MECHANICAL ENGINEERING DEPARTMENT
TEXAS A&M UNIVERSITY
COLLEGE STATION, TEXAS 77843-3123

DECEMBER 1992

FINAL REPORT FOR PERIOD OCTOBER 1988 - AUGUST 1990

APPROVED FOR PUBLIC RELEASE; DISTRIBUTION UNLIMITED

AERO PROPULSION & POWER DIRECTORATE
WRIGHT LABORATORY
AIR FORCE MATERIEL COMMAND
WRIGHT-PATTERSON AIR FORCE BASE, OHIO 45433-7649

NOTICE

When Government drawings, specifications, or other data are used for any purpose other than in connection with a definitely Government-related procurement, the United States Government incurs no responsibility or any obligation whatsoever. The fact that the government may have formulated or in any way supplied the said drawings, specifications, or other data, is not to be regarded by implication, or otherwise in any manner construed, as licensing the holder, or any other person or corporation; or as conveying any rights or permission to manufacture, use, or sell any patented invention that may in any way be related thereto.

This report is releasable to the National Technical Information Service (NTIS). At NTIS, it will be available to the general public, including foreign nations.

This technical report has been reviewed and is approved for publication.

Constance A. Dolwer

CONSTANCE A. DOLWER, Capt, USAF
Project Engineer, Compressor Research
Technology Branch
Turbine Engine Division
Aero Propulsion & Power Directorate

Marvin A. Stibich

MARVIN A. STIBICH
Chief, Compressor Research Section
Technology Branch
Turbine Engine Division
Aero Propulsion & Power Directorate

Richard J. Hill

RICHARD J. HILL
Acting Deputy for Technology
Turbine Engine Division
Aero Propulsion & Power Directorate

If your address has changed, if you wish to be removed from our mailing list, or if the addressee is no longer employed by your organization please notify WL/POTX, WPAFB, OH 45433-7649 to help us maintain a current mailing list.

Copies of this report should not be returned unless return is required by security considerations, contractual obligations, or notice on a specific document.

REPORT DOCUMENTATION PAGE

Form Approved
OMB No. 0704-0188

1. AGENCY USE ONLY *(Leave blank)*

2. REPORT DATE
DEC 1992

3. REPORT TYPE AND DATES COVERED
FINAL 10/30/88--08/30/92

4. TITLE AND SUBTITLE
ROTORDYNAMIC AND LEAKAGE CHARACTERISTICS
OF A 4-STAGE BRUSH SEAL

5. FUNDING NUMBERS
C F33615-88-C-2908
PE 62203
PR 3066
TA 11
WU 69

6. AUTHOR(S)
J. CONNER
D. W. CHILDS

7. PERFORMING ORGANIZATION NAME(S) AND ADDRESS(ES)
TURBOMACHINERY LABORATORY
MECHANICAL ENGINEERING DEPARTMENT
TEXAS A&M UNIVERSITY
COLLEGE STATION TX 77843-3123

8. PERFORMING ORGANIZATION REPORT NUMBER

9. SPONSORING/MONITORING AGENCY NAME(S) AND ADDRESS(ES)
AERO PROPULSION AND POWER DIRECTORATE
WRIGHT LABORATORY
AIR FORCE MATERIEL COMMAND
WL/POTX, Attn: DOWLER 513-2558210

10. SPONSORING/MONITORING AGENCY REPORT NUMBER
WL-TR-92-2125

11. SUPPLEMENTARY NOTES
THIS IS A CORRECTED VERSION OF A FINAL REPORT PREVIOUSLY PUBLISHED AS REPORT WL-TR-91-2013.

12a. DISTRIBUTION/AVAILABILITY STATEMENT
APPROVED FOR PUBLIC RELEASE; DISTRIBUTION IS UNLIMITED.

DISTRIBUTION STATEMENT A
Approved for public release
Distribution Unlimited

12b. DISTRIBUTION CODE

13. ABSTRACT *(Maximum 200 words)*

Experimental results are presented for the direct and cross-coupled stiffness and damping coefficients as well as the leakage performance for a 4-stage brush seal. Variable test parameters include the inlet pressure, pressure ratio, shaft speed, fluid pre-rotation, and seal spacing. Direct damping is shown to increase with running speed; otherwise, the rotordynamic coefficients are relatively insensitive to changes in the test parameters. Cross-coupled stiffness is generally unchanged by increasing the inlet tangential velocity to the seals, suggesting that the brush seal is not affected by inlet swirl. Direct stiffness is shown to increase with frequency; however, the magnitudes of direct stiffness are always positive. Cross-coupled stiffness increases slightly with frequency; yet not as drastically as direct stiffness. Comparisons of test results for the 4-stage brush seal with an 8-cavity labyrinth showed superior rotordynamics performance for the brush seal; viz., larger values for direct stiffness and lower values for the (destabilizing) cross-coupled stiffness coefficient. The damping for brush seals is smaller, but comparable to labyrinth seals. The whirl-frequency ratio is always smaller for the brush seal.

14. SUBJECT TERMS
BRUSH SEAL, ROTORDYNAMICS, SEAL, TURBINE

15. NUMBER OF PAGES
147

16. PRICE CODE

17. SECURITY CLASSIFICATION OF REPORT	18. SECURITY CLASSIFICATION OF THIS PAGE	19. SECURITY CLASSIFICATION OF ABSTRACT	20. LIMITATION OF ABSTRACT
UNCLASSIFIED	UNCLASSIFIED	UNCLASSIFIED	UL

TABLE OF CONTENTS

CHAPTER | Page

I INTRODUCTION 1

Rotordynamic Coefficient Definition. 3

II EXPERIMENTAL SETUP 6

Rotordynamic Coefficient Identification 10

Test Apparatus Modifications 12

Experimental Uncertainty Analysis 17

III TEST RESULTS 25

Test Parameters 25

Inter-Stage Pressure Profiles 27

Leakage Characteristics 38

Direct Stiffness 46

Cross-Coupled Stiffness 53

Direct Damping 57

Whirl-Frequency Ratio 64

Comparison to a Tooth-on-Rotor Labyrinth Seal 68

Torque Imposed on the Shaft Due to Friction 72

IV CONCLUSIONS 74

REFERENCES 77

APPENDIX

A Impedance Function Plots 79

B Tabulation of Test Conditions and Test Results 107

C Tabulation of Rotordynamic Coefficients and the expected Uncertainties 117

LIST OF FIGURES

Page

Figure 1 - Axial and cross-section views of a brush seal. 2

Figure 2 - Forces on whirling rotor. 4

Figure 3 - Air seal test apparatus. 7

Figure 4 - Front detail of test rig showing hydraulic shaker unit. 8

Figure 5 - Support and position of the seal stator within the test housing. ... 9

Figure 6 - Cross section of test rig. 12

Figure 7 - Cross-section detail of seal stator. 13

Figure 8 - Maximum and intermediate swirl vanes. 16

Figure 9 - Time and Frequency traces of F_X, F_Y, and X. 22

Figure 10 - Scatter comparison of direct and cross-coupled damping data. ... 24

Figure 11 - Seal configurations. 26

Figure 12 - Pressure distribution for seal 2 with no inlet swirl. 29

Figure 13 - Pressure distribution for seal 2 with intermediate swirl. 30

Figure 14 - Pressure distribution for seal 2 with high inlet swirl. 31

Figure 15 - Pressure distribution for seal 3 with no inlet swirl. 32

Figure 16 - Pressure distribution for seal 3 with intermediate swirl. 33

Figure 17 - Pressure distribution for seal 3 with high swirl. 34

Figure 18 - Delta P across each stage with no inlet swirl for seal 3. 35

Figure 19 - Delta P across each stage with intermediate inlet swirl for seal 3. 36

Figure 20 - Delta P across each stage with high inlet swirl for seal 3. 37

Figure 21 - Inlet tangential velocity vs. inlet pressure and rotor speed for seal 1. 39

Figure 22 - Inlet tangential velocity vs. inlet pressure and rotor speed for seal 2. 40

Figure 23 - Inlet tangential velocity vs. inlet pressure and rotor speed for seal 3. 41

Figure 24 - Mass flow rate vs. inlet circumferential velocity ratio for seal 1. .. 42

Figure 25 - Mass Flow rate vs. inlet circumferential velocity ratio for seal 2. . 43

	Page
Figure 45 - Leakage rate comparison between a 4-stage brush seal and a 9-cavity tooth-on-rotor labyrinth seal.	69
Figure 46 - Direct stiffness comparison between labyrinth and brush seals.	69
Figure 47 - Cross-coupled stiffness comparison for labyrinth and brush seals.	70
Figure 48 - Direct damping comparison for labyrinth and brush seals.	71
Figure 49 - Whirl frequency comparison for labyrinth and brush seals.	71
Figure 50 - Time traces of the load cell output in volts.	73
Figure 51 - Direct stiffness impedance graph for seal 1 with no fluid pre-rotation.	80
Figure 52 - Direct stiffness impedance graph for seal 1 with intermediate fluid pre-rotation.	81
Figure 53 - Direct stiffness impedance graph for seal 1 with high fluid pre-rotation.	82
Figure 54 - Cross-coupled stiffness impedance graph for seal 1 with no fluid pre-rotation.	83
Figure 55 - Cross-coupled stiffness impedance graph for seal 1 with intermediate fluid pre-rotation.	84
Figure 56 - Cross-coupled stiffness impedance graph for seal 1 with high fluid pre-rotation.	85
Figure 57 - Direct damping impedance graph for seal 1 with no fluid pre-rotation.	86
Figure 58 - Direct damping impedance graph for seal 1 with intermediate fluid pre-rotation.	87
Figure 59 - Direct damping impedance graph for seal 1 with high fluid pre-rotation.	88
Figure 60 - Direct stiffness impedance graph for seal 2 with no fluid pre-rotation.	89
Figure 61 - Direct stiffness impedance graph for seal 2 with intermediate fluid pre-rotation.	90
Figure 62 - Direct stiffness impedance graph for seal 2 with high fluid pre-rotation.	91
Figure 63 - Cross-coupled stiffness impedance graph for seal 2 with no fluid pre-rotation.	92
Figure 64 - Cross-coupled stiffness impedance graph for seal 2 with intermediate fluid pre-rotation.	93

Page

Figure 26 - Mass flow rate vs. inlet circumferential velocity ratio for seal 3. . . 44

Figure 27 - Mass flow rate vs. inlet pressure. 45

Figure 28 - Direct stiffness as a function of frequency. 48

Figure 29 - Intercept of $Re(\hat{F}/\hat{X})$ vs. inlet velocity ratio. 49

Figure 30 - Mean value of K vs. inlet circumferential velocity ratio for seal 1. 50

Figure 31 - Mean value of K vs. inlet circumferential velocity ratio for seal 2. 51

Figure 32 - Mean value of K vs. inlet circumferential velocity ratio for seal 3. 52

Figure 33 - Cross-coupled stiffness versus inlet circumferential velocity ratio for seal 1. 54

Figure 34 - Cross-coupled stiffness versus inlet circumferential velocity ratio for seal 2. 55

Figure 35 - Cross-coupled stiffness versus inlet circumferential velocity ratio for seal 3. 56

Figure 36 - Direct damping versus inlet circumferential velocity ratio for seal 1. 58

Figure 37 - Direct damping versus inlet circumferential velocity ratio for seal 2. 59

Figure 38 - Direct damping versus inlet circumferential velocity ratio for seal 3. 60

Figure 39 - $Im(\hat{F}_X/\hat{X})$ intercept at $\omega=0$ versus inlet circumferential velocity ratio for seal 1. 61

Figure 40 - $Im(\hat{F}_X/\hat{X})$ intercept at $\omega=0$ versus inlet circumferential velocity ratio for seal 2. 62

Figure 41 - $Im(\hat{F}_X/\hat{X})$ intercept at $\omega=0$ versus inlet circumferential velocity ratio for seal 3. 63

Figure 42 - Whirl frequency ratio versus inlet circumferential velocity ratio for seal 1. 65

Figure 43 - Whirl frequency ratio versus inlet circumferential velocity ratio for seal 2. 66

Figure 44 - Whirl frequency ratio versus inlet circumferential velocity ratio for seal 3. 67

LIST OF TABLES

Page

Table 1 - Test parameters. 26

Table 2 - Rotor growth as a function of speed. 27

Table B1 - Static and dynamic test data for seal 1 cases with no fluid pre-rotation. 108

Table B2 - Static and dynamic test data for seal 1 cases with intermediate fluid pre-rotation. 109

Table B3 - Static and dynamic test data for seal 1 cases with high fluid pre-rotation. 110

Table B4 - Static and dynamic test data for seal 2 cases with no fluid pre-rotation. 111

Table B5 - Static and dynamic test data for seal 2 cases with intermediate fluid pre-rotation. 112

Table B6 - Static and dynamic test data for seal 2 cases with high fluid pre-rotation. 113

Table B7 - Static and dynamic test data for seal 3 cases with no fluid pre-rotation. 114

Table B8 - Static and dynamic test data for seal 3 cases with intermediate fluid pre-rotation. 115

Table B9 - Static and dynamic test data for seal 3 cases with high fluid pre-rotation. 116

Table C1a - Rotordynamic coefficient test data and uncertainties for seal 1 cases with no fluid pre-rotation. 117

Table C1b - Static and dynamic test data for seal 1 cases with no fluid pre-rotation. 118

Table C2a - Rotordynamic coefficient test data and uncertainties for seal 1 cases with intermediate fluid pre-rotation. 119

Table C2b - Static and dynamic test data for seal 1 cases with intermediate fluid pre-rotation. 120

Table C3a - Rotordynamic coefficient test data and uncertainties for seal 1 cases with high fluid pre-rotation. 121

Table C3b - Static and dynamic test data for seal 1 cases with high fluid pre-rotation. 122

Table C4a - Rotordynamic coefficient test data and uncertainties for seal 2 cases with no fluid pre-rotation. 123

Page

Figure 65 - Cross-coupled stiffness impedance graph for seal 2 with high fluid pre-rotation. 94

Figure 66 - Direct damping impedance graph for seal 2 with no fluid pre-rotation. 95

Figure 67 - Direct damping impedance graph for seal 2 with intermediate fluid pre-rotation. 96

Figure 68 - Direct damping impedance graph for seal 2 with high fluid pre-rotation. 97

Figure 69 - Direct stiffness impedance graph for seal 3 with no fluid pre-rotation. 98

Figure 70 - Direct stiffness impedance graph for seal 3 with intermediate fluid pre-rotation. 99

Figure 71 - Direct stiffness impedance graph for seal 3 with high fluid pre-rotation. 100

Figure 72 - Cross-coupled stiffness impedance graph for seal 3 with no fluid pre-rotation. 101

Figure 73 - Cross-coupled stiffness impedance graph for seal 3 with intermediate fluid pre-rotation. 102

Figure 74 - Cross-coupled stiffness impedance graph for seal 3 with high fluid pre-rotation. 103

Figure 75 - Direct damping impedance graph for seal 3 with no fluid pre-rotation. 104

Figure 76 - Direct damping impedance graph for seal 3 with intermediate fluid pre-rotation. 105

Figure 77 - Direct damping impedance graph for seal 3 with high fluid pre-rotation. 106

NOMENCLATURE

C, c	Direct and cross-coupled damping coefficients.
CPM	Shaft angular velocity (cycles/minute).
$\delta(x)$	Uncertainty of variable x.
$f = k/C\omega$	Whirl frequency ratio.
F_{RX}, F_{RY}	Reaction forces, equation (1).
F_X, F_Y	Fluid forces imposed on the seal.
$\hat{F}_X$, $\hat{F}_Y$	Complex fluid forces imposed on the seal.
M	Stator mass.
$\dot{m}$	Mass flow rate (kg/s).
ω	Frequency.
K, k	Direct and cross-coupled stiffness coefficients.
P_o	Inlet stagnation pressure.
P_b	Exit stagnation pressure.
$P_{cav\,x}$	Stagnation pressure in cavity 1, 2, or 3.
SEE	Standard error of estimate.
$U_{\theta o}$	Inlet circumferential velocity (m/s).
$u_{\theta o}$	Inlet circumferential velocity ratio.
w_f	Total uncertainty in a result, f.
X, Y	Position coordinates of the rotor relative to the stator.

Page

Table C4b - Static and dynamic test data for seal 2 cases with no fluid pre-rotation. 124

Table C5a - Rotordynamic coefficient test data and uncertainties for seal 2 cases with intermediate fluid pre-rotation. 125

Table C5b - Static and dynamic test data for seal 2 cases with intermediate fluid pre-rotation. 126

Table C6a - Rotordynamic coefficient test data and uncertainties for seal 2 cases with high fluid pre-rotation. 127

Table C6b - Static and dynamic test data for seal 2 cases with high fluid pre-rotation. 128

Table C7a - Rotordynamic coefficient test data and uncertainties for seal 3 cases with no fluid pre-rotation. 129

Table C7b - Static and dynamic test data for seal 3 cases with no fluid pre-rotation. 130

Table C8a - Rotordynamic coefficient test data and uncertainties for seal 3 cases with intermediate fluid pre-rotation. 131

Table C8b - Static and dynamic test data for seal 3 cases with intermediate fluid pre-rotation. 132

Table C9a - Rotordynamic coefficient test data and uncertainties for seal 3 cases with high fluid pre-rotation. 133

Table C9b - Static and dynamic test data for seal 3 cases with high fluid pre-rotation. 134

NOMENCLATURE

C, c	Direct and cross-coupled damping coefficients.
CPM	Shaft angular velocity (cycles/minute).
$\delta(x)$	Uncertainty of variable x.
$f=k/C\omega$	Whirl frequency ratio.
F_{RX}, F_{RY}	Reaction forces, equation (1).
F_X, F_Y	Fluid forces imposed on the seal.
$\hat{F}_X$, $\hat{F}_Y$	Complex fluid forces imposed on the seal.
M	Stator mass.
$\dot{m}$	Mass flow rate (kg/s).
ω	Frequency.
K, k	Direct and cross-coupled stiffness coefficients.
P_o	Inlet stagnation pressure.
P_b	Exit stagnation pressure.
$P_{cav\,x}$	Stagnation pressure in cavity 1, 2, or 3.
SEE	Standard error of estimate.
$U_{\theta o}$	Inlet circumferential velocity (m/s).
$u_{\theta o}$	Inlet circumferential velocity ratio.
w_f	Total uncertainty in a result, f.
X, Y	Position coordinates of the rotor relative to the stator.

CHAPTER I

INTRODUCTION

Current designs for high performance turbomachinery require higher pressures, temperatures, and rotational speeds. This trend has caused almost universal use of labyrinth seals due to the low leakage performance in comparison to other seals. Some seals, however, cause a rotordynamic instability in the shaft. Instability is caused by a driving force in the tangential direction of a whirling rotor. This force has been proven to be caused by tangential fluid flow induced in labyrinth and similar seals. Therefore, more research and development into different types of seals using current state-of-the-art technology is being done on a continuing basis.

An alternative to labyrinth and similar seals is the brush seal. Figure 1 is a drawing of a brush seal in cross-section and axial views. This seal consists of a front and back plate, with wire bristles sandwiched in-between. The bristles point radially inward and contact the shaft at an angle. The internal diameter of the seal used in the present tests is 129.4 mm and the external diameter is 158.7 mm. The seals were fabricated by Cross Manufacturing Co. The bristle material is inconel X750, and the side plates are nimonic 75 HR 203.

The journal model for this thesis is the Transactions of the ASME, Journal of Tribology.

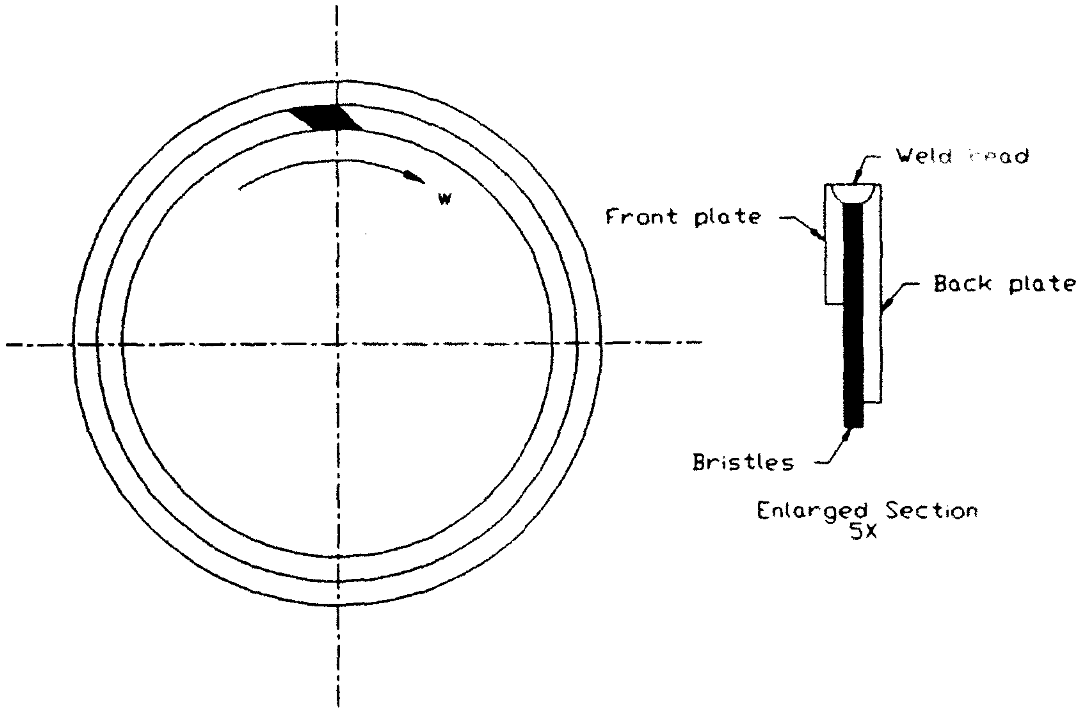

Figure 1 - Axial and cross-section views of a brush seal.

The rotor is coated with a hard ceramic coating to prevent the bristles from wearing a groove into the rotor. The coating is machined smooth to prevent erosion of the bristles. Because the bristles contact the shaft at an angle, the bristles tend to bend instead of buckle when changes in the relative radial position of the shaft occur.

Ferguson (1988) compares leakage performance of the brush seal to various five-finned labyrinth seal designs. Comparative data showed that the leakage rates of the brush seal were dramatically lower, as low as 5% in comparison to a vertical fin, 0.75 mm clearance labyrinth seal. Braun et al. (1990) have published flow-

visualization results in an attempt to explain the flow phenomena involved in the superior leakage performance of brush seals. Chupp and Nelson (1990) performed an evaluation of replacing current labyrinth seals with brush seals in limited life engines. Their results showed that brush seals offer significant sealing improvements over labyrinth seals. It was also shown that brush seals have an initial wear-in period, yet retain significantly reduced leakage rates over labyrinth seals for times exceeding limited-life applications. Holle and Krishnan (1990) have investigated the utilization of various high temperature brush seals in several test engines. Results indicate that leakage reductions in comparison to labyrinth seals approach an order of magnitude. Yet, they have a concern about the application of brush seals is the wear and durability characteristics on uncoated rotors. They concluded that wear rates are on the order of hundreds of hours, not the thousands of hours desirable for reusable engines. Flower (1990) has proposed several different designs of brush seals. These include an abradable back-plate design, a strip seal, which uses metal strips instead of bristles, and a segmented seal which would aid in maintenance and assembly. To the author's knowledge, the present work is the first investigation of the rotordynamic characteristics of brush seals.

Definition of Rotordynamic Coefficients

Previous publications (Childs and Scharrer, 1986, and Scharrer, 1987] have proven that forces in annular seals can influence the stability of the shaft. The forces

on a whirling rotor can be expressed in terms of radial and tangential components as shown in Figure 2.

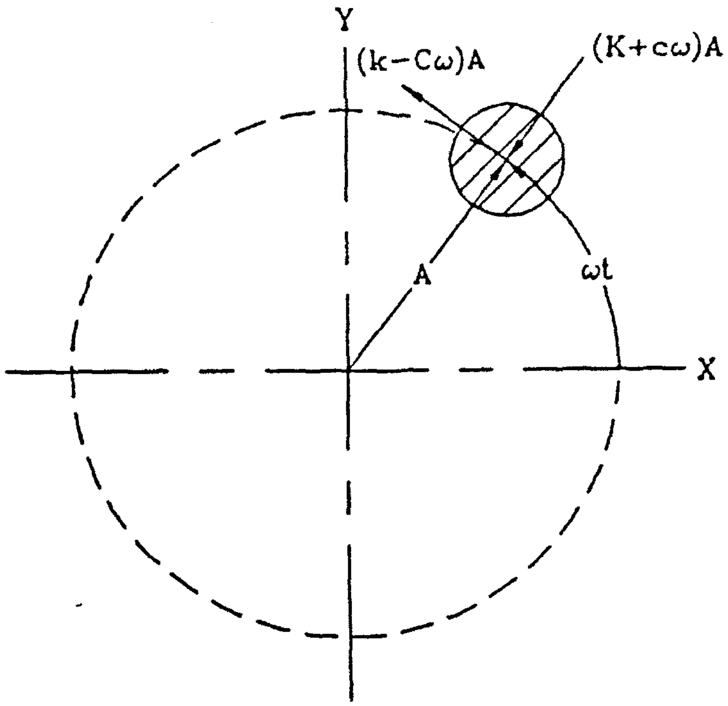

Figure 2 - Forces on a whirling rotor.

The reaction forces arising for an annular seal exhibiting small motion about the centered position can be modeled as:

$$\begin{Bmatrix} F_{RX} \\ F_{RY} \end{Bmatrix} = \begin{bmatrix} K & k \\ -k & K \end{bmatrix} \begin{Bmatrix} X \\ Y \end{Bmatrix} + \begin{bmatrix} C & c \\ -c & C \end{bmatrix} \begin{Bmatrix} \dot{X} \\ \dot{Y} \end{Bmatrix} \qquad (1)$$

Where X and Y define the motion of the rotor relative to the stator, and F_{RX} and F_{RY} are the reaction forces acting on the rotor. K, k, C, and c are the direct stiffness, cross-coupled stiffness, direct damping, and cross-coupled damping coefficients, respectively.

The cross-coupled stiffness k is the source of destabilizing forces in labyrinth annular seals and arises due to fluid rotation within the seal. This destabilizing effect is aggravated when the fluid enters the seal with a "swirl" or tangential velocity component in the direction of rotation. Various investigations (Childs, Baskharone, and Ramsey, 1990, and Childs and Ramsey, 1990) have demonstrated that k can be reduced or even reversed if an inlet "swirl brake" is placed upstream of the seal to reduce or reverse the inlet tangential velocity to the seal.

The nature of a brush seal is such that it would appear to be both a seal and a swirl brake; i.e., intuitively, the closely packed bristles should reduce or eliminate the inlet tangential velocity. The present research was motivated by this optimistic thought and has the objective of measuring rotordynamic coefficients of brush seals.

CHAPTER II

EXPERIMENTAL SETUP

The test apparatus and facility used in this study were developed as part of an extended, joint, NASA-USAF funded research program for annular gas seal research. J.B. Dressman of the University of Louisville completed the original design of the test rig in 1982. Several modifications to both the test apparatus and the supporting facilities have been made since that time. A detailed description of the test facility and the basic configuration have been discussed in earlier publications [8,9].

The test rig uses air as the fluid medium and can identify the rotordynamic coefficients of various types of annular gas seals. Figure 3 shows that the high speed test shaft is suspended in a pendulum fashion from a rigidly mounted pivot shaft. This configuration allows side-to-side motion of the test shaft for both static positioning and dynamic excitation. The upper pivot shaft has an eccentric cam which allows static vertical positioning of the rotor. Figure 4 shows how the rotor is statically centered and horizontally excited about its center by a hydraulic shaker head, which acts on the shaft housing against a return spring. Forces encountered by the seal stator during this excitation are measured by three piezo-electric, tri-axial, load cells, which support the stator in a trihedral fashion as shown in Figure 5. The shake frequency is varied using a swept sine wave from 35 to 70 Hz. with an amplitude of approximately 0.089 mm. Theoretically, the rotordynamic coefficients

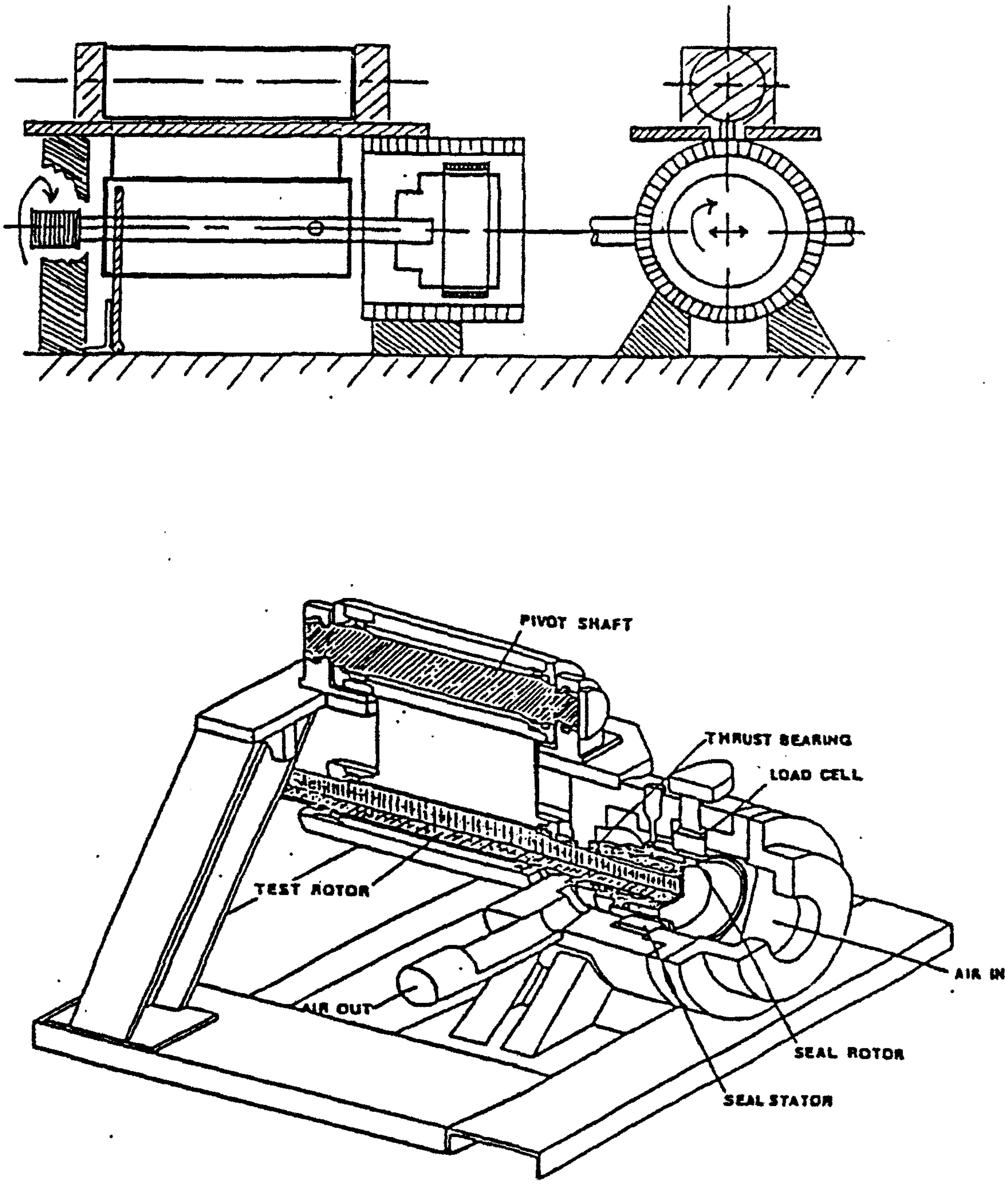

Figure 3 - Air seal test apparatus.

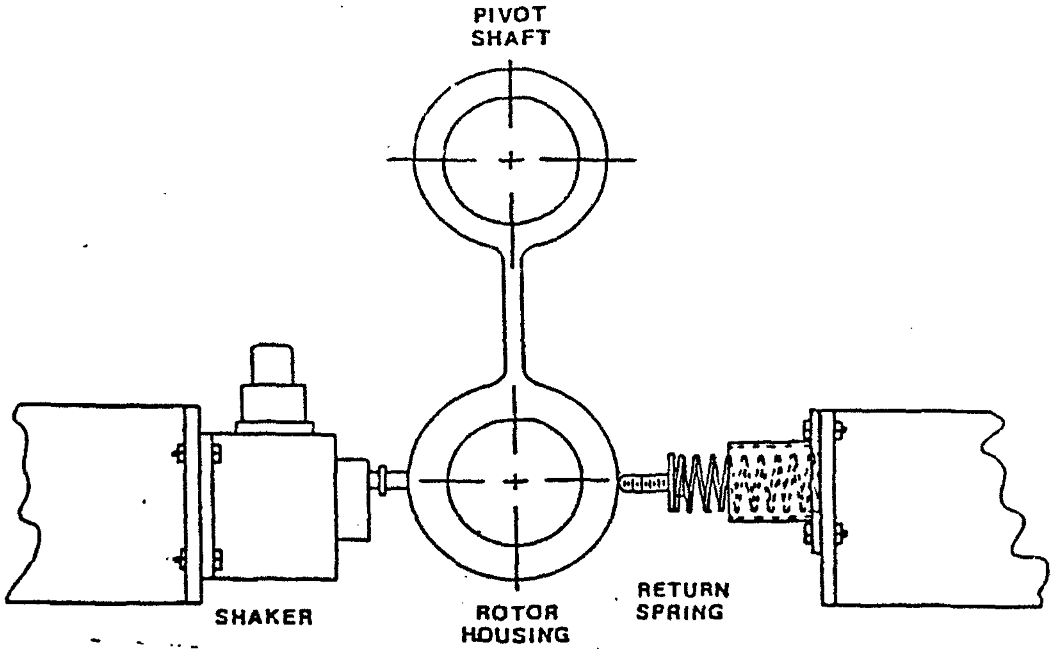

Figure 4 - Front detail of test rig showing hydraulic shaker unit.

should be independent of shake frequency. However, previous testing has shown that the coefficients of some seals depend on frequency. The swept-sine-wave excitation used here is patterned after the procedure followed by Bolleter et al. (1987).

The excitation lasts for approximately one second during which the gas forces and rotor position data are taken. After each shake, a two second time interval allows residual vibration in the system to be damped out and also allows the computer and data acquisition unit to calculate and record the needed data. Spurious or random data is reduced by time averaging the response signals over 35 sweeps.

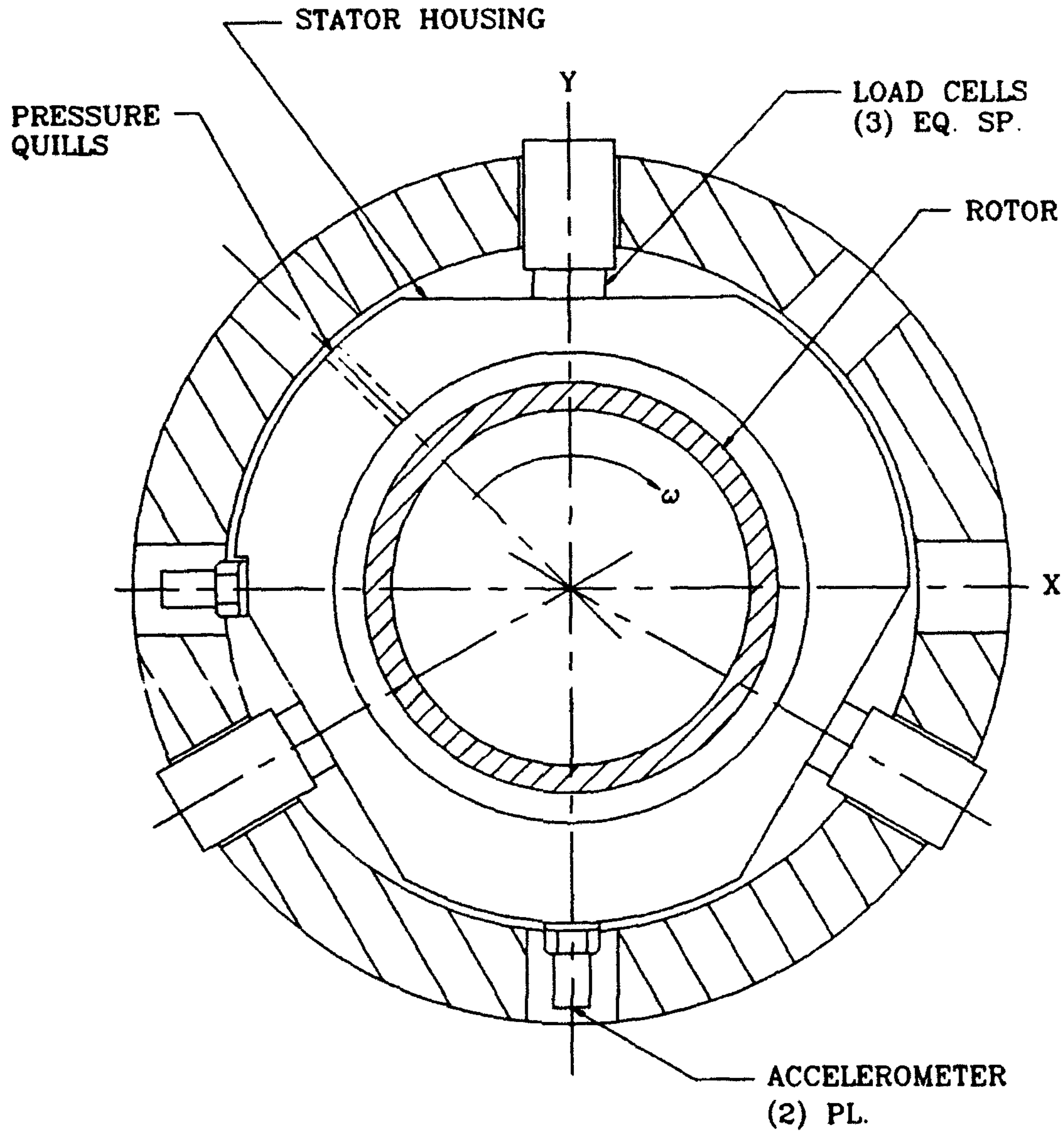

Figure 5 - Support and position of the seal stator within the test housing.

The time averaged traces of force and position data are used in the analysis of the rotordynamic coefficients. A complete discussion of swept sine wave excitation for modal identification is provided by Ewins (1986).

Rotordynamic Coefficient Identification

The rotordynamic coefficients are found experimentally by the following method. Consider the equations of motion for the brush seal housing:

$$M\begin{Bmatrix} \ddot{X} \\ \ddot{Y} \end{Bmatrix} = \begin{Bmatrix} F_{RX} \\ F_{RY} \end{Bmatrix} - \begin{bmatrix} K & k \\ -k & K \end{bmatrix}\begin{Bmatrix} X \\ Y \end{Bmatrix} - \begin{bmatrix} C & c \\ -c & C \end{bmatrix}\begin{Bmatrix} \dot{X} \\ \dot{Y} \end{Bmatrix} \tag{2}$$

In this model, F_{RX}, F_{RY}, X, and Y are the reaction forces and acceleration components of the stator housing, and M is the mass of the seal stator. The rotordynamic model defined in equation (2) is simplified because the motion of the shaft is assumed to be in the horizontal or X direction only; hence, equation (2) becomes:

$$\begin{Bmatrix} F_{RX} - M\ddot{X} \\ F_{RY} - M\ddot{Y} \end{Bmatrix} = \begin{Bmatrix} F_X \\ F_Y \end{Bmatrix} = \begin{bmatrix} K \\ -k \end{bmatrix} X + \begin{bmatrix} C \\ -c \end{bmatrix} \dot{X} \tag{3}$$

The response forces, F_X and F_Y, are generated by an analog circuit which sum F_{RX} and F_{RY} vectorially from the three load cells and subtracts the M X and M Y terms. The acceleration components are measured by accelerometers positioned as shown in 5. Proximity probes, which are located 90 degrees apart, are used to measure the horizontal and vertical position of the rotor, and to measure the position

of the rotor during the shake. The data acquisition unit records 1024 data points of F_X, F_Y, and X as a function of time during the 1 second excitation of the rotor. As mentioned before, the data used for analysis is the time averaged trace of 35 excitations at a set condition of test parameters. The Fourier transform version of equation (3) is:

$$\begin{Bmatrix} \hat{F}_X \\ \hat{F}_Y \end{Bmatrix} = \begin{bmatrix} K + jCw \\ -k - jcw \end{bmatrix} \hat{X} = \begin{bmatrix} Z_c \\ z_c \end{bmatrix} \hat{X} \tag{4}$$

where the ^ symbol indicates the Fourier transform of the variable. The rotordynamic coefficients are defined as:

$$K = Re(\hat{Z}) = Re\left(\frac{\hat{F}_X}{\hat{X}}\right) \qquad C = \frac{Im(\hat{Z})}{\omega} = \frac{Im\left(\frac{\hat{F}_X}{\hat{X}}\right)}{\omega}$$
$$k = Re(\hat{z}) = Re\left(\frac{\hat{F}_Y}{\hat{X}}\right) \qquad c = \frac{Im(\hat{z})}{\omega} = \frac{Im\left(\frac{\hat{F}_Y}{\hat{X}}\right)}{\omega} \tag{5}$$

Only data between 40 and 65 Hz were used in the analysis of the coefficients. The real and imaginary parts of Z and $\hat{z}$ are plotted with respect to shake frequency. The average over frequency of Re(Z) and Re($\hat{z}$) define K and k, and the slope of Im(Z) and Im($\hat{z}$) versus frequency define C and c.

Test Apparatus Modifications

Recent modifications to the flow field upstream and downstream of the seal were made in order to accommodate brush seals. A variable length, back-pressure, labyrinth seal allowed a wider range of available pressure ratios. This back-pressure seal is internally ported to allow the operator to withdraw or inject air in the gap between the back-pressure seal and the test seal. Other modifications include a new rotor, stator, and inlet pre-swirl vanes. Figure 6 is a cross-sectional view of the test rig which shows these modifications.

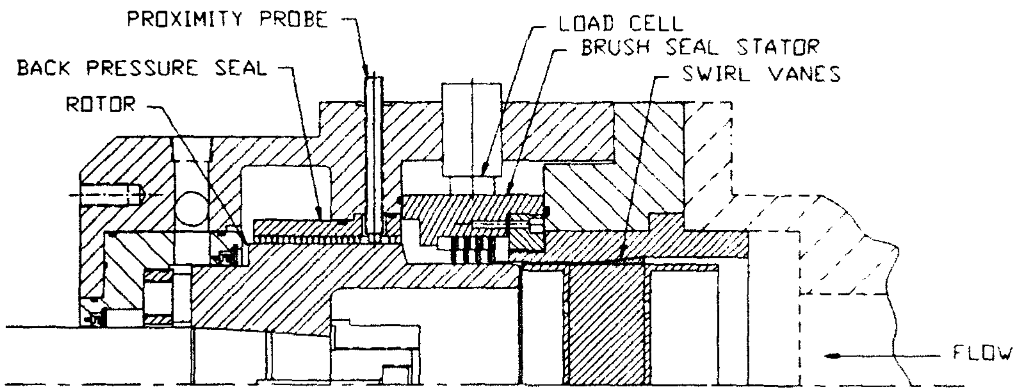

Figure 6 - Cross section of test rig.

The rotor is made of 17-4PH stainless steel and is attached to the test shaft with a hydraulic taper fit. A ceramic coating was applied to the rotor on the brush seal surface and machined to a thickness of 0.127 mm., a surface finish of 0.1 μm (4 μin), and a finished diameter of 129.4 mm. This diameter corresponds to the internal

diameter of the brush seal, chosen to simulate worn-in conditions. The rotor was initially coated with chromium carbide, which wore through to the base material after about 40 hours of testing. A coatings specialist suggested chromium oxide, which is harder, and has a lower coefficient of friction. This material also has a tendency to wear smooth, or become smoother as it wears down. This coating performed very well and showed little wear.

Figure 7 shows how the stator, or seal housing, holds the seals in place via a retaining ring, which applies an axial pre-load to the seal group.

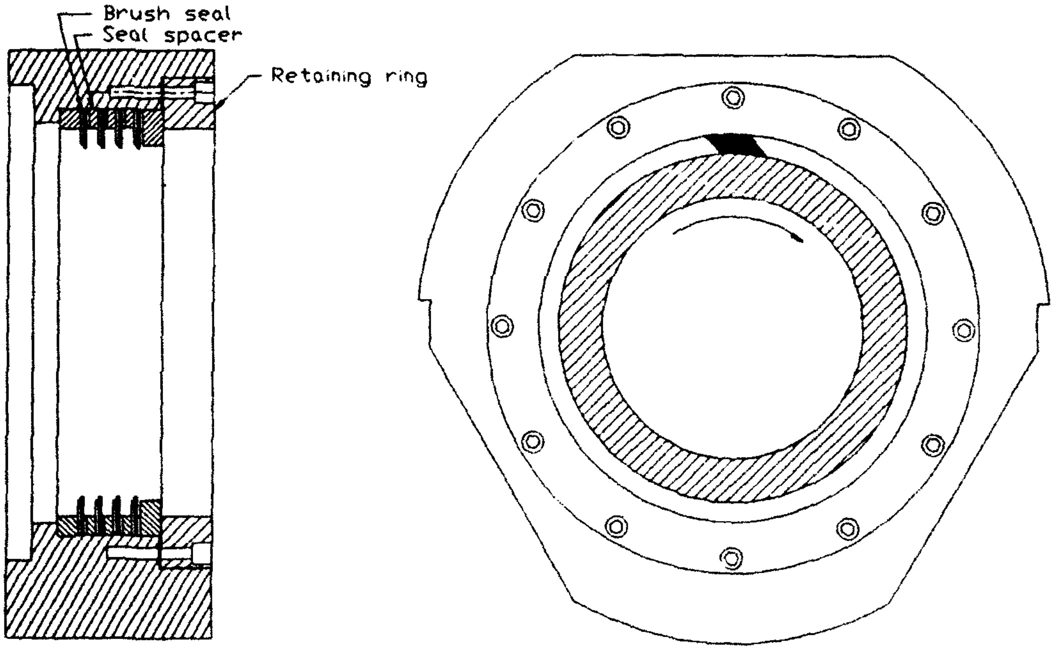

Figure 7 - Cross-section detail of seal stator.

A group of four brush seals was used to create a sufficiently large reaction force to measure reliably. To test the effect of between-seal spacings, the seals were tested with no spacer and two different spacer widths. For the two configurations with spacers between the seals, pressure taps were inserted to measure the axial pressure distribution. Temperatures were also recorded at the inlet and exit of the test section. Leakage measurements were performed by a 12.65 mm turbine flow meter.

Modifications were made to the analog circuit used to perform the vector sum of the X and Y forces to measure the torque imposed on the shaft. The load cells are positioned such that the shear force measured by the load cells in the tangential direction would be the force caused by the friction of the bristles. The tangential force of each load cells are simply recorded as a function of time. In theory, the three forces could be summed, and multiplied by the radial distance to the load cell location, with the result being the torque imposed on the seal by the rotation of the shaft. It will be shown in Chapter 3, however, that torque measurement was not possible due to equipment limitations.

Inlet swirl of the flow is induced by a set of guide vanes placed in front of the seal section. These guide vanes are similar in shape to a turbine stator blade. A computer code developed by NASA was used to generate the blade shape. Previous research showed that the flow velocities would be very low; therefore, by aerodynamically contouring the tips of the blades, the vanes were designed with an

inlet-to-exit area ratio of 3 to 1. This design reduces the boundary layer effect on the flow. Two sets of swirl vanes, shown in Figure 8, were designed to provide high and intermediate tangential velocities.

The high velocity vanes have an exit angle of 75 degrees and the intermediate set has an exit angle of 61.8 degrees. The intermediate set provides one half the tangential velocity of the 75 degree vanes at the same flow rate.

Even though the exit area of the swirl vanes is small, partial admission had to be utilized to raise the tange ial velocity due to the extremely low flow rate. Partial admission was implemented by blocking two out of three blade-to-blade passages. It is assumed that the rotational velocity component of the flow is conserved and the losses occur in the axial direction. Using this assumption, the tangential velocity component of the flow at the inlet to the test seals was predicted in the following manner. Conservation of momentum is assumed in the tangential direction; hence, the tangential velocity component of the flow at the exit of the nozzle equals the tangent velocity at the inlet to the seal. Viscous losses are also assumed to be low in the gap between the inlet of the swirl vanes to the inlet of the seal.

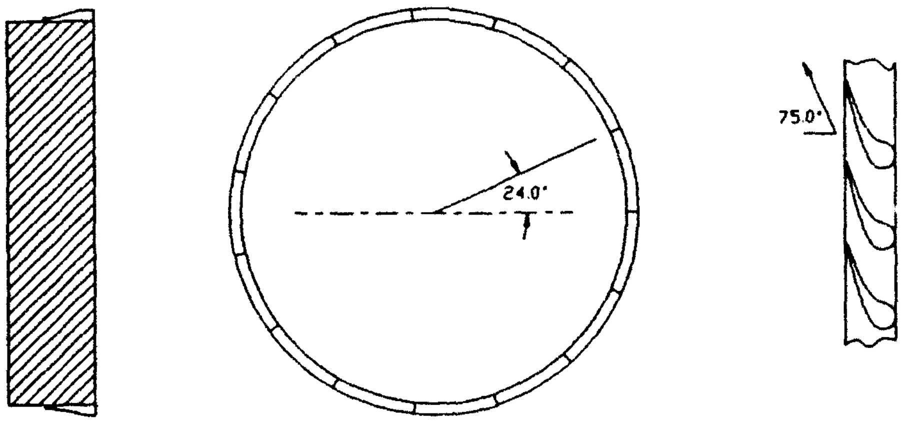

Maximum Swirl Vanes

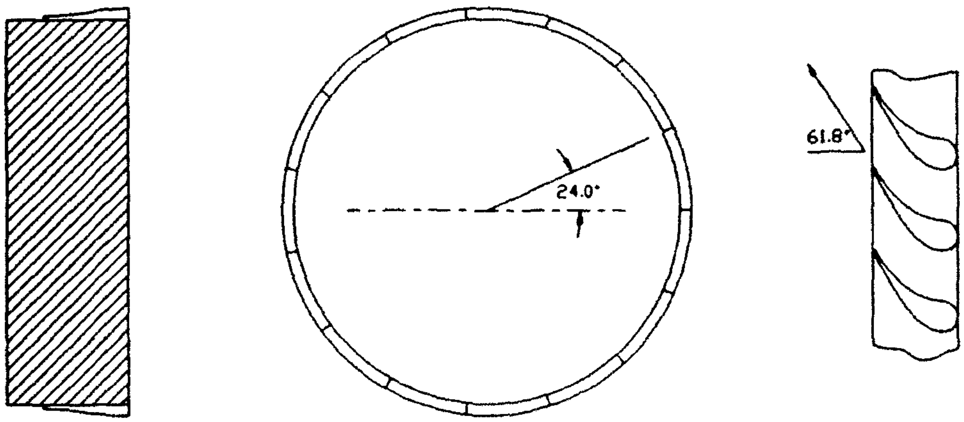

Intermediate Swirl Vanes

Figure 8 - Maximum and intermediate swirl vanes.

The volumetric flow rate, q, is easily computed at the exit of the nozzle, knowing the measured values of mass flow rate, temperature, and pressure. Dividing q by the exit area of the nozzle yielded the average magnitude of the exit velocity. Since the exit angle of the nozzle is known, the tangential component is found by simple geometry. In order to reduce jetting of the flow into the seal and to allow mixing of the flow, the guide vanes were placed approximately 6 cm. upstream of the seal section. Actual tangent velocities depend on the volumetric flow rate. A set of straight vanes were also tested to provide a benchmark parameter of no fluid pre-rotation.

Experimental Uncertainty Analysis

All experimentally measured values have a statistical level of uncertainty, which is comprised of two parts. One part of the total uncertainty is the accuracy uncertainty, which is the statistical deviation in a group of measured values. The other type of uncertainty is precision uncertainty, which is the error associated with the instrument used for the measurement. For example, the diameter of an atom cannot be measured with a standard ruler because of the precision uncertainty. Holman (1978) describes a method for calculating a total uncertainty of a parameter value. This total uncertainty expression is shown in equation (6).

$$w_f = \left[(f_{x1} w_1)^2 + (f_{x2} w_2)^2 + \ldots + (f_{xn} w_n)^2 \right]^{\frac{1}{2}} \tag{6}$$

where w_f is the total uncertainty in a result, f, which is a function of n primary measurements $x_1, x_2, \ldots, x_n$ with uncertainties $w_1, w_2, \ldots, w_n$.

To calculate the precision uncertainty values, resolutions for the various instruments use for measurement have to be identified. The flow meter used to measure the volumetric flow rate through the seal has a resolution of 0.5% l/s, while the pressure transducer and thermocouple have resolutions of 0.05% and 0.3 C respectively. The analog to digital board channels which are used to record the pressures and temperatures have resolutions of 0.00117 bar and 0.08 C respectively. The forces on the stator are measured by load cells and accelerometers which have resolutions of 0.01 N and 0.0001 g's respectively. The force resolution of the accelerometer is determined by multiplying its resolution by the stator mass, 10.335 kg. The resolution is then found to be 0.103 N. The resolution of the motion probes are 0.00254 mm.

For quantities such as mass flow rate, temperature, and pressure measurements, the total uncertainty is found by direct application of the Holman theory. The rotordynamic coefficients, however, are mathematically calculated from complex expressions in the frequency domain. This frequency domain expression is the result of performing a fourier transform on the time domain signals of force in the X and Y directions, and motion in the X direction. The magnitude of the accuracy uncertainty in the measured force and motion values result from time

averaging 35 separate sweep cycles. Each of the 1024 points of the averaged trace have a standard deviation associated with it, because each point in the final signal is the average of that same point in time from 35 separate waves. Experience has shown that the value of this standard deviation is relatively constant from point to point on the final wave; therefore, the average of the 1024 standard deviations is used as a measure of the accuracy uncertainty. Expressions for the total uncertainty in the direct and cross-coupled stiffness values are:

$$\delta(K) = \left[\mathrm{Re}\left(\frac{\delta K}{\delta \hat{F}_X}\right)^2 (\delta \hat{F}_X)^2 + \mathrm{Re}\left(\frac{\delta K}{\delta \hat{X}}\right)^2 (\delta \hat{X})^2 \right]^{\frac{1}{2}} \tag{7}$$

$$\delta(k) = \left[\mathrm{Re}\left(\frac{\delta k}{\delta \hat{F}_Y}\right)^2 (\delta \hat{F}_Y)^2 + \mathrm{Re}\left(\frac{\delta k}{\delta \hat{X}}\right)^2 (\delta \hat{X})^2 \right]^{\frac{1}{2}} \tag{8}$$

where:

$$\frac{\delta K}{\delta \hat{X}} = -\frac{\hat{F}_X}{\hat{X}^2} \tag{9}$$

$$\frac{\delta k}{\delta \hat{X}} = -\frac{\hat{F}_Y}{\hat{X}^2} \tag{10}$$

$$\frac{\delta K}{\delta \hat{F}_X} = \frac{\delta k}{\delta \hat{F}_Y} = \frac{1}{\hat{X}} \tag{11}$$

Expressions for the total uncertainty in the direct and cross-coupled damping coefficients are:

$$\delta(C) = \left[Im\left(\frac{\delta C}{\delta \hat{F}_X}\right)^2 (\delta \hat{F}_X)^2 + Im\left(\frac{\delta C}{\delta \hat{X}}\right)^2 (\delta \hat{X})^2 \right]^{\frac{1}{2}} \tag{12}$$

$$\delta(c) = \left[Im\left(\frac{\delta c}{\delta \hat{F}_X}\right)^2 (\delta \hat{F}_X)^2 + Im\left(\frac{\delta c}{\delta \hat{X}}\right)^2 (\delta \hat{X})^2 \right]^{\frac{1}{2}} \tag{13}$$

where:

$$\frac{\delta C}{\delta \hat{F}_X} = -\frac{\delta c}{\delta \hat{F}_Y} = \frac{1}{\omega \hat{X}} \tag{14}$$

$$\frac{\delta c}{\delta \hat{X}} = -\frac{\hat{F}_Y}{\omega \hat{X}^2} \tag{15}$$

$$\frac{\delta C}{\delta \hat{X}} = -\frac{\hat{F}_X}{\omega \hat{X}^2} \tag{16}$$

The above equations are complex and in the frequency domain. The values of the accuracy and precision uncertainty which are known in the time domain had to be correctly transformed to the frequency domain. This had to be done because the magnitude of the value is mathematically attenuated as a function of the fast Fourier transform, and the fast swept sine wave mathematics. A detailed description of the mathematics of the fast swept sine wave is presented by White and Pennington

(1982). For example, the motion probes have a resolution of 0.00254 mm (.1 mil), and the amplitude of the motion trace is on the order of 0.05 mm (2.0 mils) peak to peak, which is a 5.0% error. Figure 9 shows that the amplitude of motion observed in the frequency domain has a magnitude of 0.006 mm (.24 mils). Naturally, no energy has been lost in the mathematics, but the magnitudes of the values have been changed. Therefore, the values of the accuracy and precision uncertainty for each point are mathematically attenuated in the same manner as the wave form in question. This allows meaningful application of the Holman theory in the frequency domain. Appendix A contains the impedance plots which graphically show the data from which the rotordynamic coefficients are formed. The accuracy uncertainty is obtained from the data by applying an expression from Holman [11, 12]:

$$\sigma_Y = \left[\frac{\sum_{i=1}^{n} (y_i - y_m)^2}{n - 1} \right]^{\frac{1}{2}} \tag{17}$$

Where y_m is the value of the coefficient in question and y_i are the values of the coefficient at a given frequency in the range from 40 to 65 Hz.

Another measure of the accuracy uncertainty for the damping coefficients is the amount of scatter of the data about the defined line given by the regression analysis. Coleman and Steele (1989) formed a statistic called the standard error of estimate (SEE):

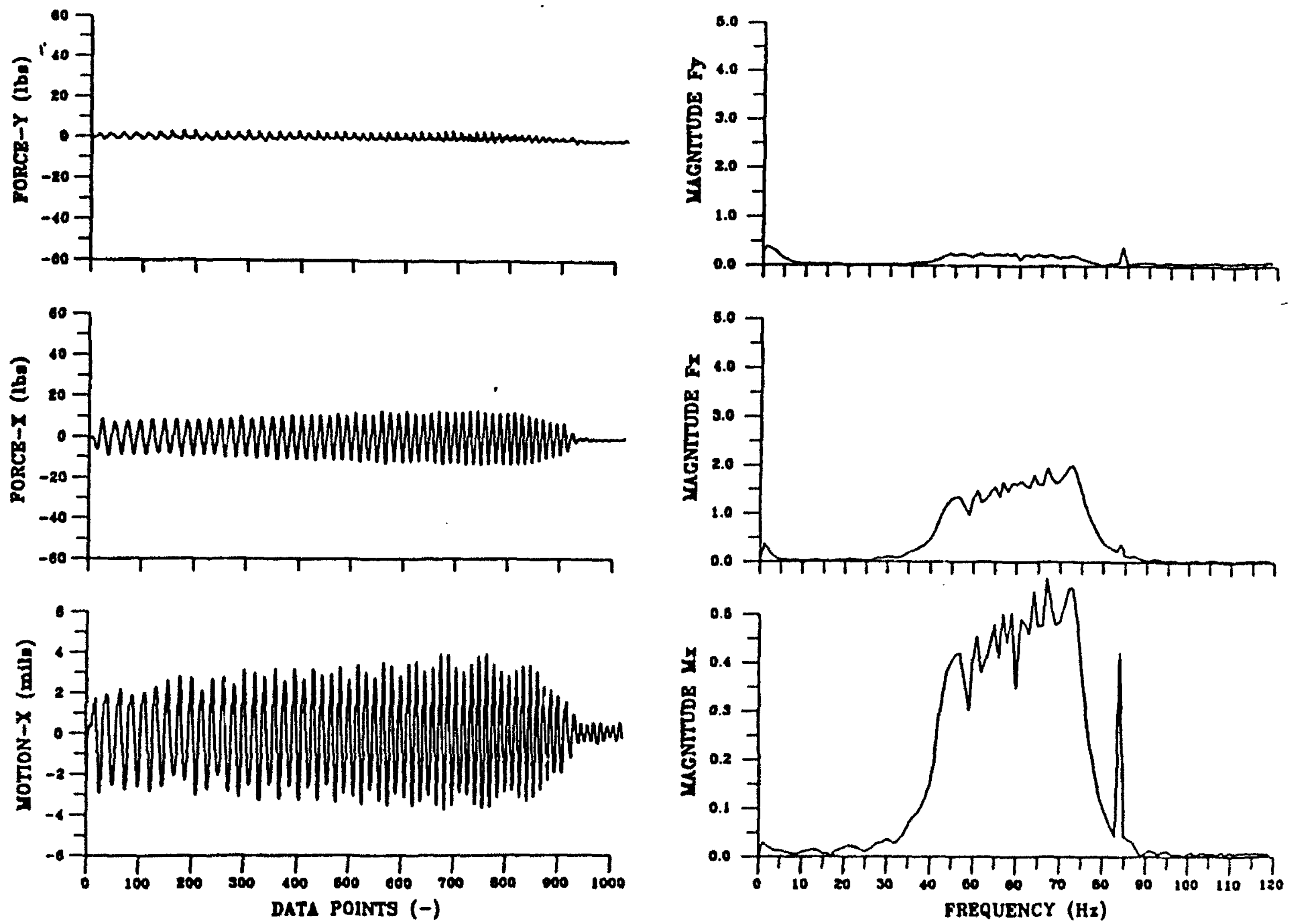

Figure 9 - Time and Frequency traces of F_X, F_Y, and X.

$$SEE = \left\{ \frac{\sum_{i=1}^{N} [Y_i - (aX_i + b)]^2}{N - 2} \right\}^{\frac{1}{2}} \tag{18}$$

This has the general form of a precision index and is a measure of the scatter of the data points about the linear curve fit. The 2 subtracted from N in the denominator arises because two degrees of freedom are lost from the set of N data pairs (X_i, Y_i) when the curve fit constants a and b are determined by the regression analysis. Schenck (1979) states that a +/-2(SEE) band will contain approximately 95% of the data points. Appendix C contains the SEE values for the direct and cross-coupled damping values. This statistic has the units of force over displacement, or in the case of the line from which damping is determined, N/mm (Damping has units of N-s/mm, which is the slope of the line).

Figure 10 compares the scatter in the direct and cross-coupled damping data. Cross-coupled damping SEE values are very high, which indicates that there is a large scatter in the data. The magnitudes of the Im(Fy/X) are low and very scattered in comparison. All cross-coupled damping data show this behavior; therefore none of the cross-coupled damping data is presented in graphical form. The graphs which represent the slope for direct damping show approximate magnitudes of Im(Fx/X) between 25 and 75 N/mm. The SEE value for the direct damping case is

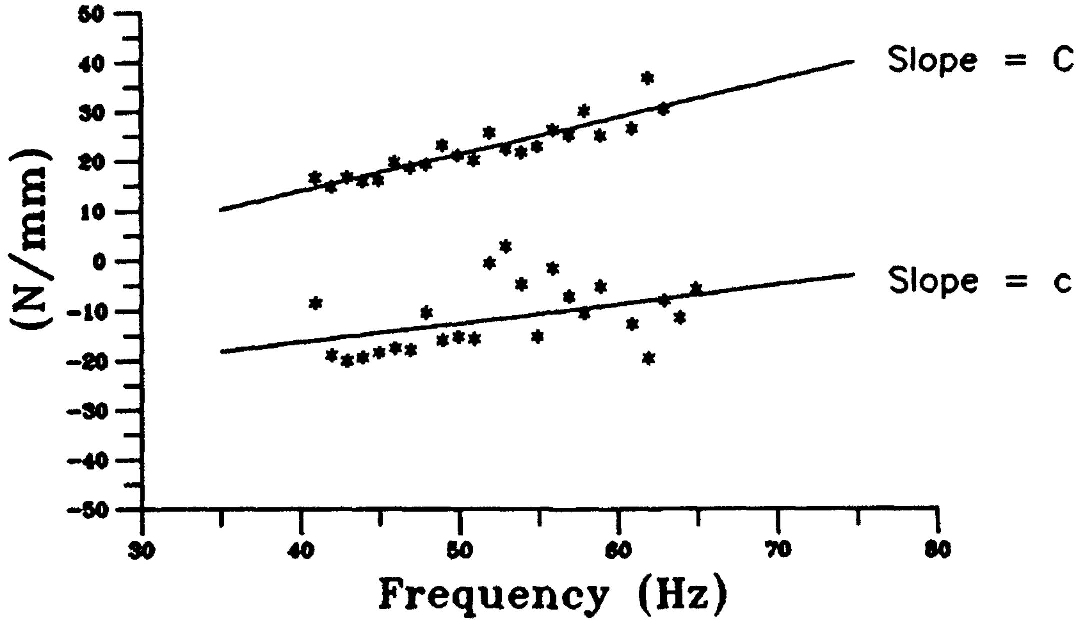

Figure 10 - Scatter comparison of direct and cross-coupled damping data.

approximately 20-30% of the Im(Fx/X) magnitude. Although this is rather high, the trend of the data can still be shown with some accuracy. Therefore, direct damping for all cases tested will be presented in graphical form.

CHAPTER III

TEST RESULTS

Test data were taken for three different seal spacings. As mentioned in Chapter II, four brush seals were used to obtain large enough forces for rotordynamic coefficient analysis. A listing of the data is tabulated in Appendices A and B.

The test program was carried out to determine the leakage and rotordynamic characteristics of brush seals and ascertain whether these characteristics are affected by *inlet swirl, inlet pressure, pressure ratio, rotor speed,* or seal spacing. Torque imposed on the rotor by friction of the bristles riding on the shaft surface is also investigated.

Test Parameters

Rotational speed, inlet pressure, pressure ratio, and fluid pre-rotation are the *four independent* test parameters varied on the test apparatus. Three seal configurations, each having a different inter-stage seal spacer, were tested separately. The order of testing was seal 2, seal 1, then seal 3. This order of testing will determine whether effects from one spacer configuration to the next are from wear or from the spacers placed between the seal stages. Figure 11 shows the seal configurations and defines the seal notation which will be used throughout the thesis.

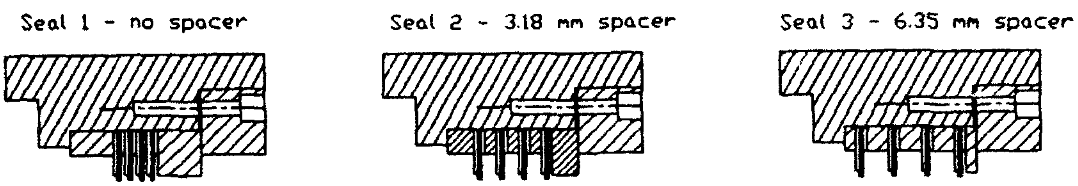

Figure 11 - Seal configurations.

Speed of the rotor is controlled by a 100 Hp electric variable speed motor and a synchronous belt drive system. The maximum speed of the test shaft is presently 16000 cpm. Inlet pressure is regulated by a control valve located upstream of the test section. The pressure ratio is defined by the exit pressure divided by the inlet pressure. The variation in the exit pressure, fluid pre-rotation, and inter-stage spacing have been discussed in Chapter II. The results are plotted as a function of the inlet circumferential velocity ratio, defined as the tangential velocity of the flow divided by the surface speed of the rotor. Values for the five test parameters are listed in Table 1.

Table 1 - Test parameters.

Speed (cpm)	P_O (bar)	P_{RATIO} (bar)	Swirl (-)
1 - 5,000	1 - 7.9	1 - 0.55	1 - None
2 - 12,000	2 - 13.1	2 - 0.40	2 - Int.
3 - 16,000	3 - 18.3	3 - 0.25	3 - High
		4 - 0.14	

The notation within Table 1 is used throughout the presentation of the data. The ceramic-coated test rotor is machined to the same specification as the internal diameter of the seal, simulating worn-in conditions. However, due to inertial and thermal effects, the rotor diameter increases as a function of speed. Table 2 shows the radial growth of the rotor with rotor speed.

Table 2 - Rotor growth as a function of speed.

Rotor Speed (cpm)	Radial Rotor Growth (mm)
5,000	0.0037
12,0[illegible]	0.0211
1[illegible]00	0.0396

Previous seal data obtained from this test apparatus has been normalized using the seal radial clearance for comparison purposes. Since the brush seals have zero radial clearances, no normalized coefficients are presented here.

<u>Inter-Stage Pressure Profiles</u>

For seals 2 and 3, pressure quills were inserted through the spacer to allow measurement of the cavity pressure by a pressure transducer. Figures 12 through 17 gives the inlet, exit, and cavity pressures as a function of the axial position, speed, inlet pressure, and pressure ratio. Figures 12, 13, and 14 show the pressure distribution for seal number 2 for the zero, intermediate, and high fluid pre-rotation

respectively, while Figures 15, 16, and 17 present the pressure distributions for seal 3. Appendix B contains the tabulated cavity pressure and related test conditions for seals 2 and 3. From these figures, the pressure distribution appears to be virtually the same for the three fluid pre-rotation cases tested. For the case of no fluid pre-rotation, seal 2 at 5000 cpm shows that most of the pressure drop is across the last stage of the seal. Note that this is the first point tested in the test program. Seal 3 also shows this trend, but not to the same degree; therefore, this trend could disappear as the seals wear into place. Figures 18, 19, and 20 are graphs of delta P across each stage versus speed, inlet pressure, and pressure ratio with no swirl, intermediate swirl, and high inlet swirl, respectively. The data shown is for seal 3, which is the last seal tested in the test program, and is, therefore, representative of the worn-in conditions. In general, the last stage of the seal group encounters a slightly higher pressure drop at the lower inlet pressures. As the speed and inlet pressure increases, the level of delta P across the seal stages become approximately the same. An explanation of this phenomena could be due to a formation of a shear layer of fluid between the rotor and bristles at higher speeds and densities. At higher inlet pressures, the bristles would tend to bend axially towards the low pressure side. This would cause a fluid film to easily develop. The film would also develop at higher rotational speeds. This hypothesis is supported by all of the rotordynamic and leakage data recorded; i.e., all of the data at the lowest inlet pressure and rotor speed is sporadic.

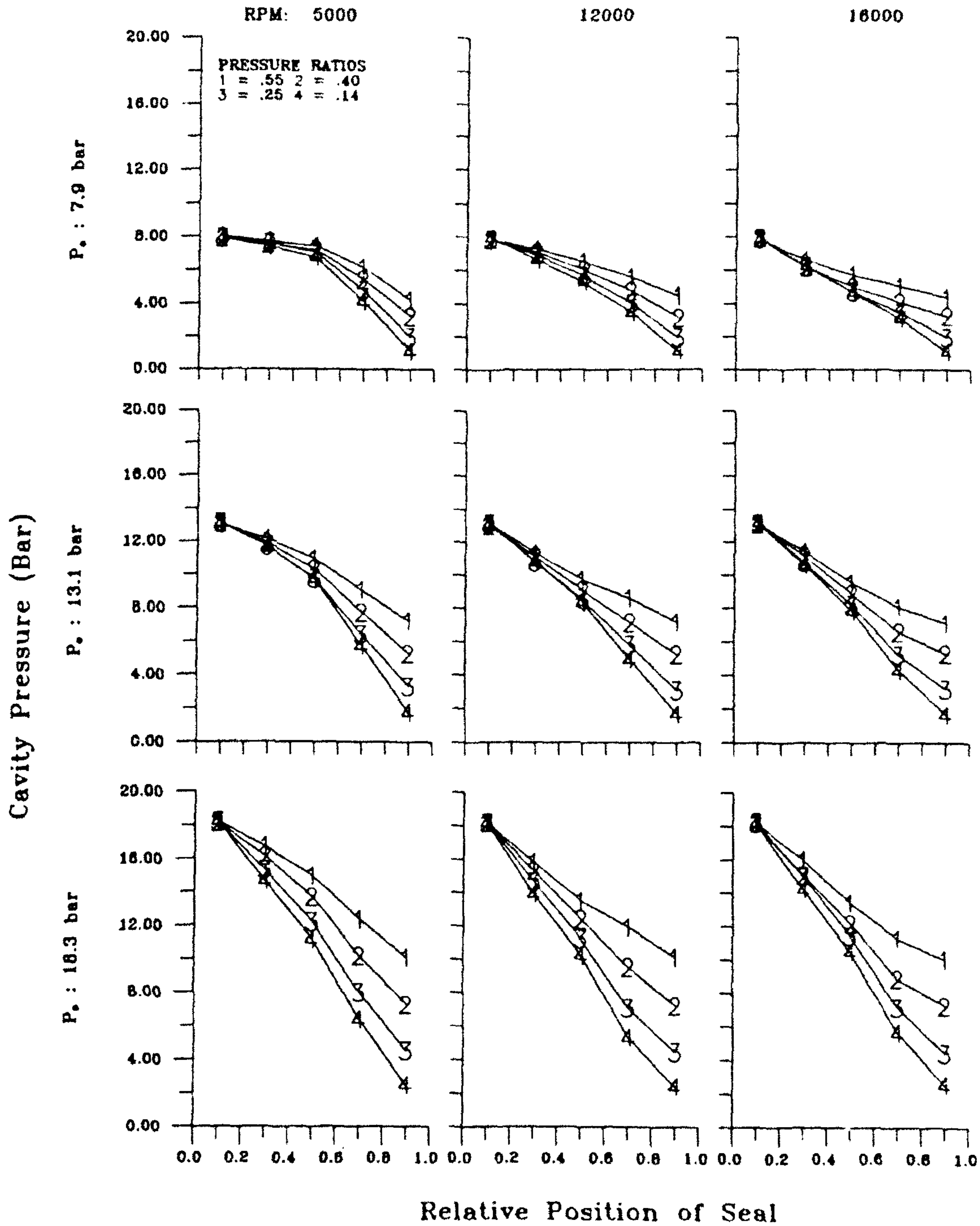

Figure 12 - Pressure distribution for seal 2 with no inlet swirl.

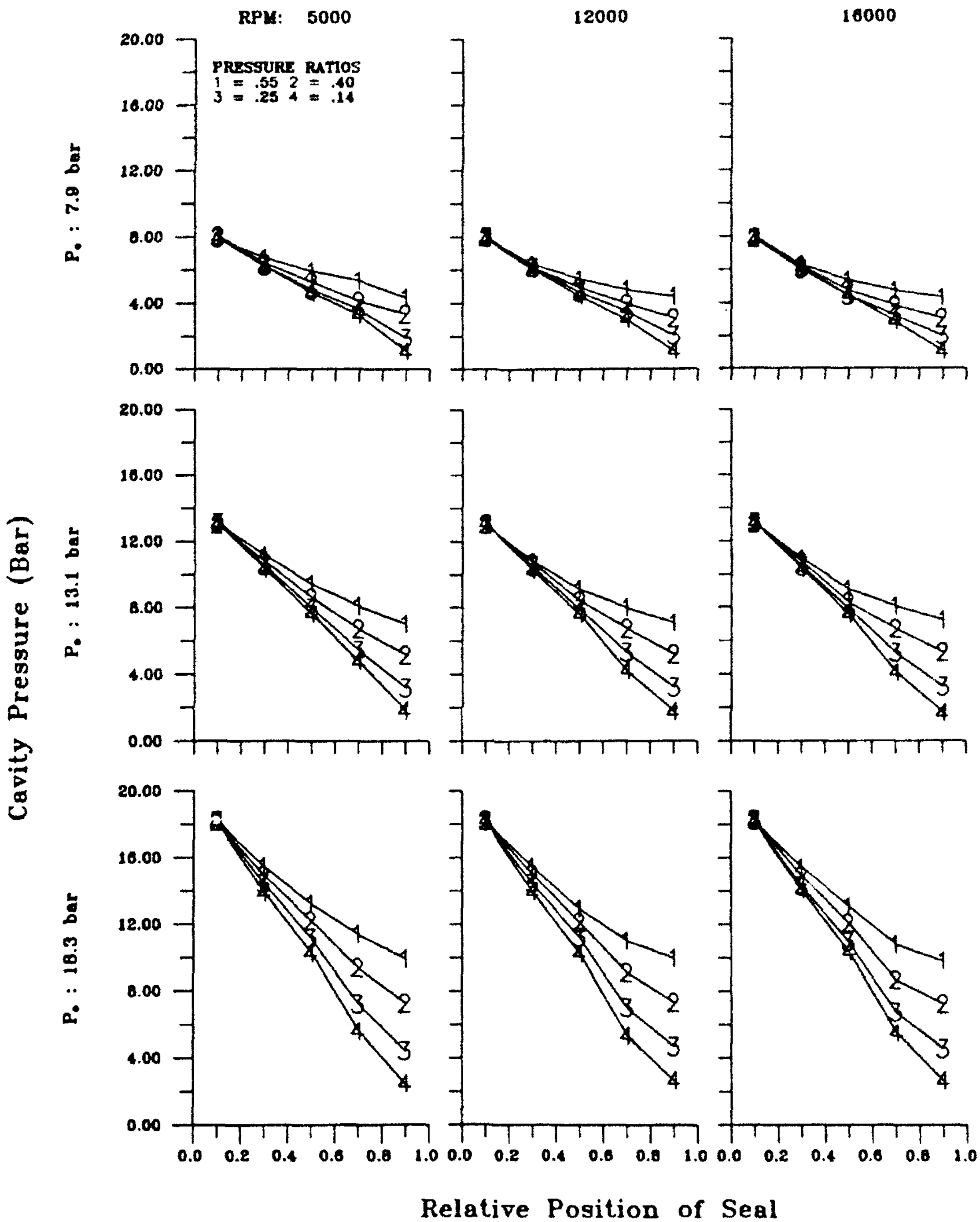

Figure 13 - Pressure distribution for seal 2 with intermediate swirl.

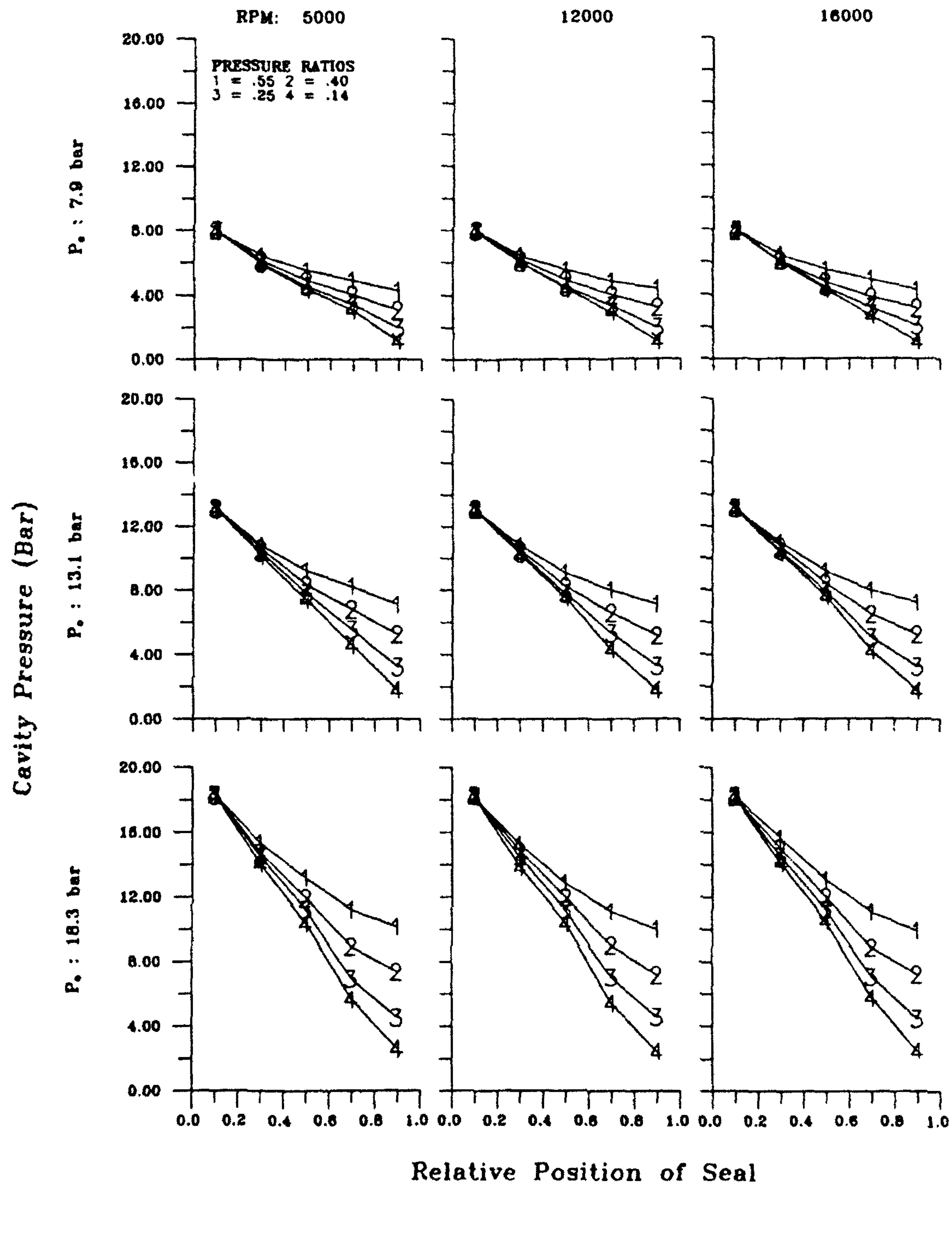

Figure 14 - Pressure distribution for seal 2 with high inlet swirl.

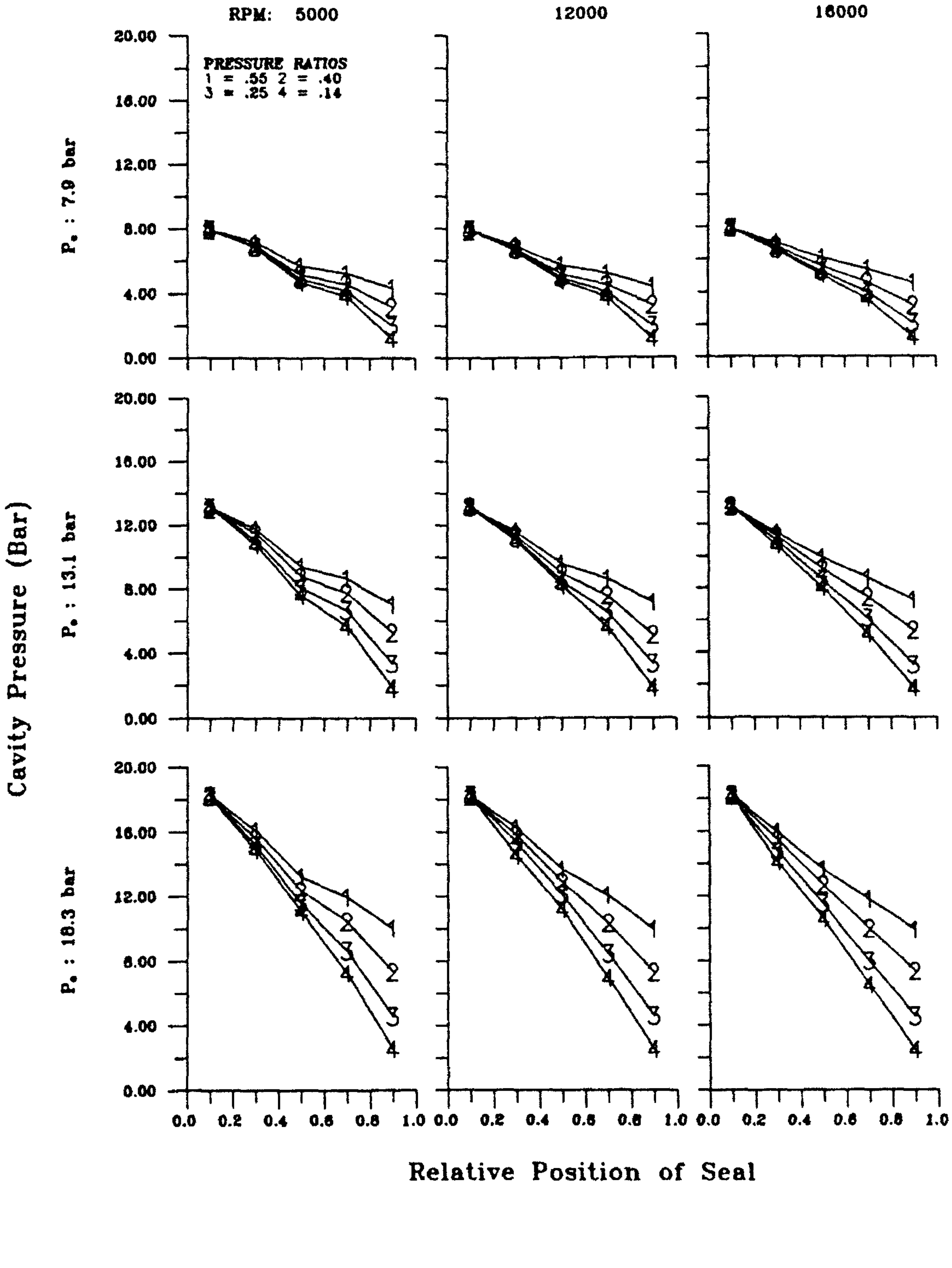

Figure 15 - Pressure distribution for seal 3 with no inlet swirl.

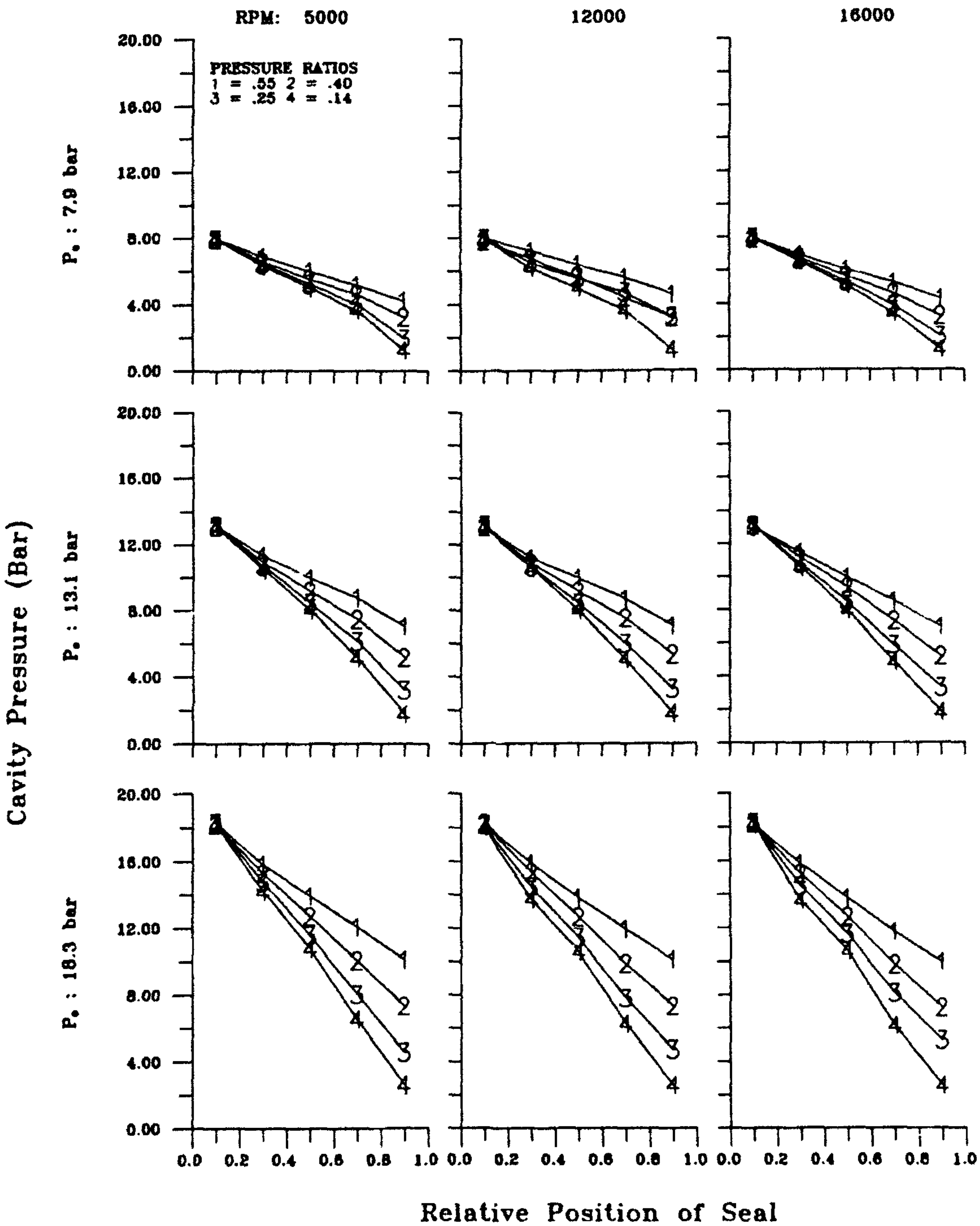

Figure 16 - Pressure distribution for seal 3 with intermediate swirl.

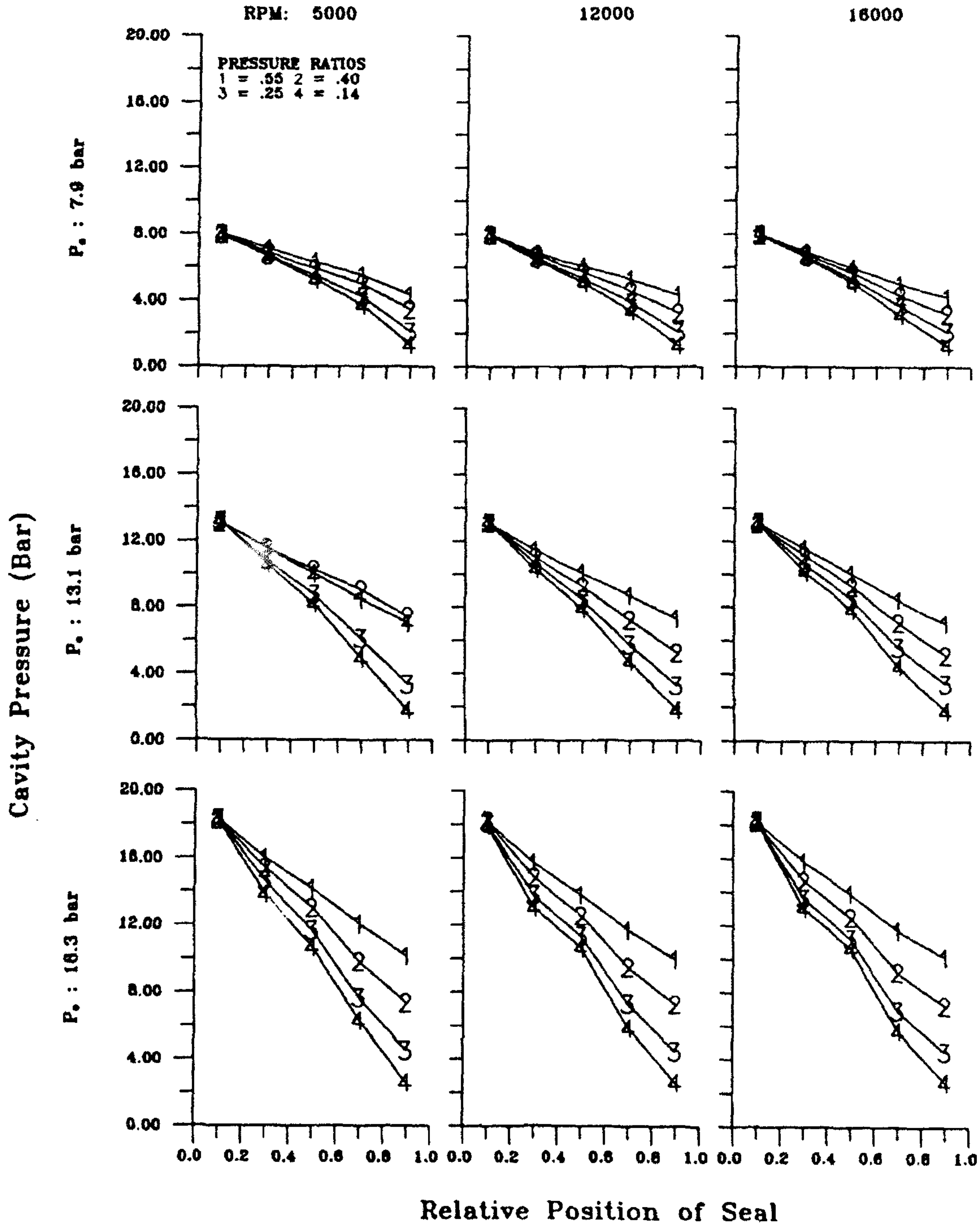

Figure 17 - Pressure distribution for seal 3 with high swirl.

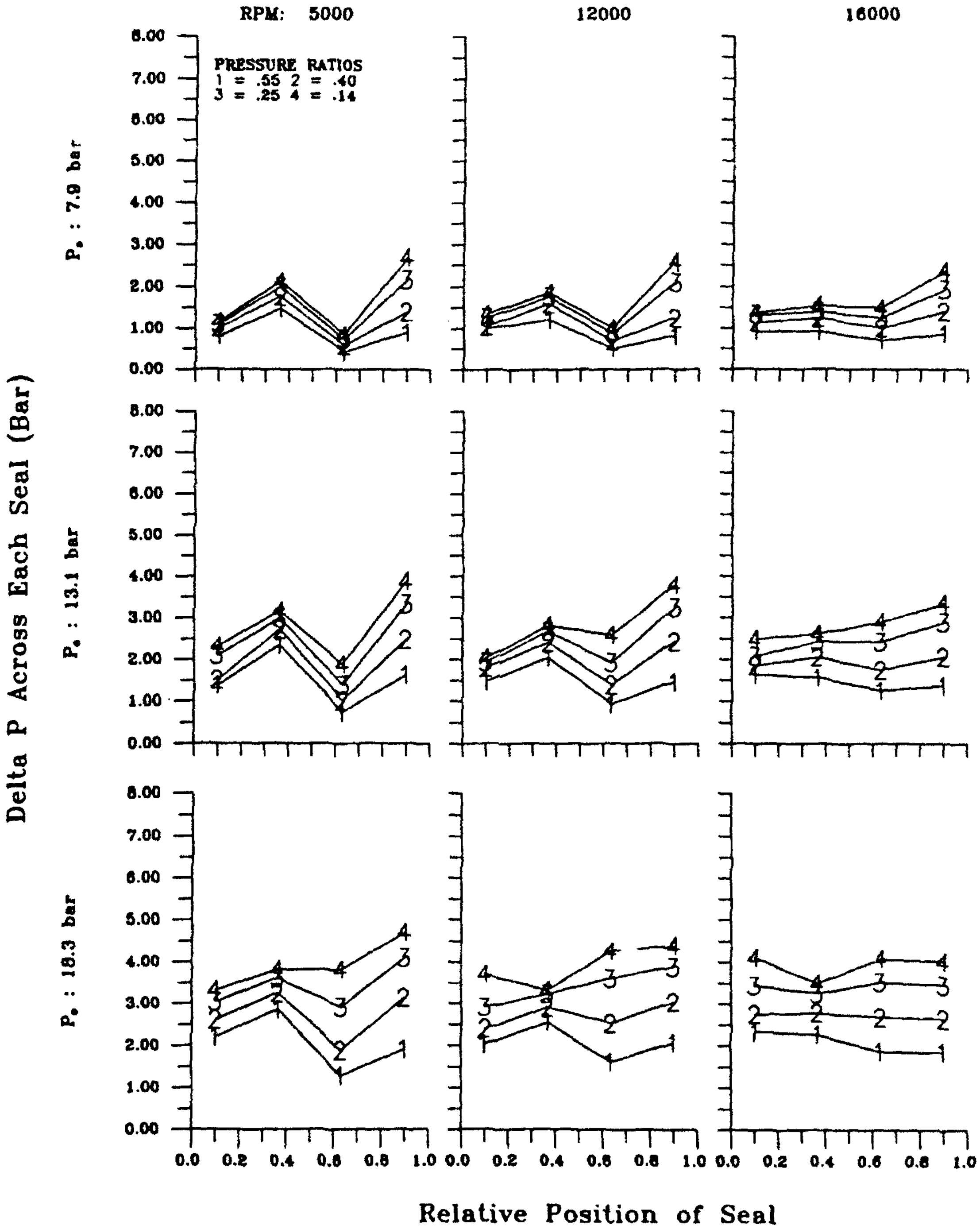

Figure 18 - Delta P across each stage with no inlet swirl for seal 3.

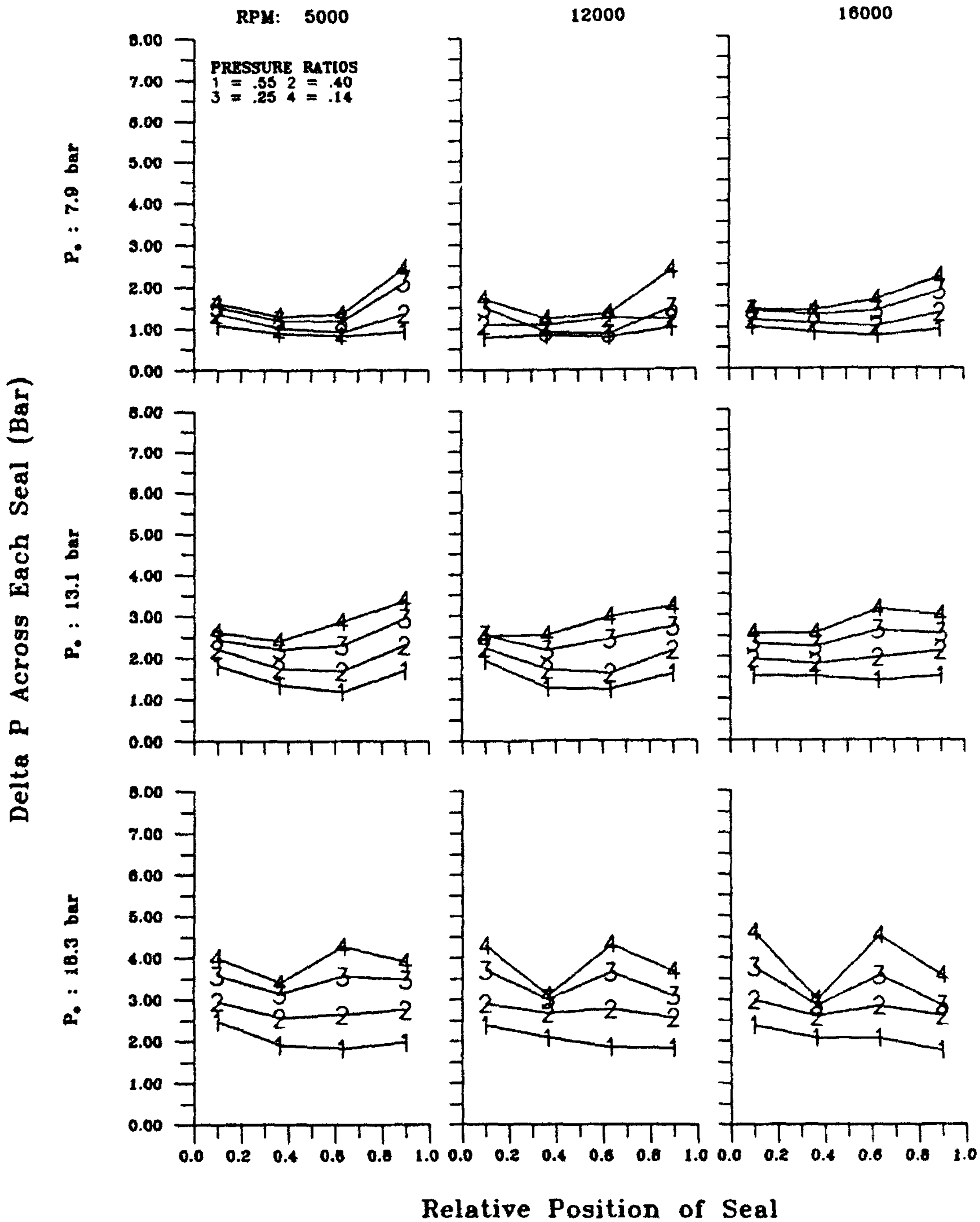

Figure 19 - Delta P across each stage with intermediate inlet swirl for seal 3.

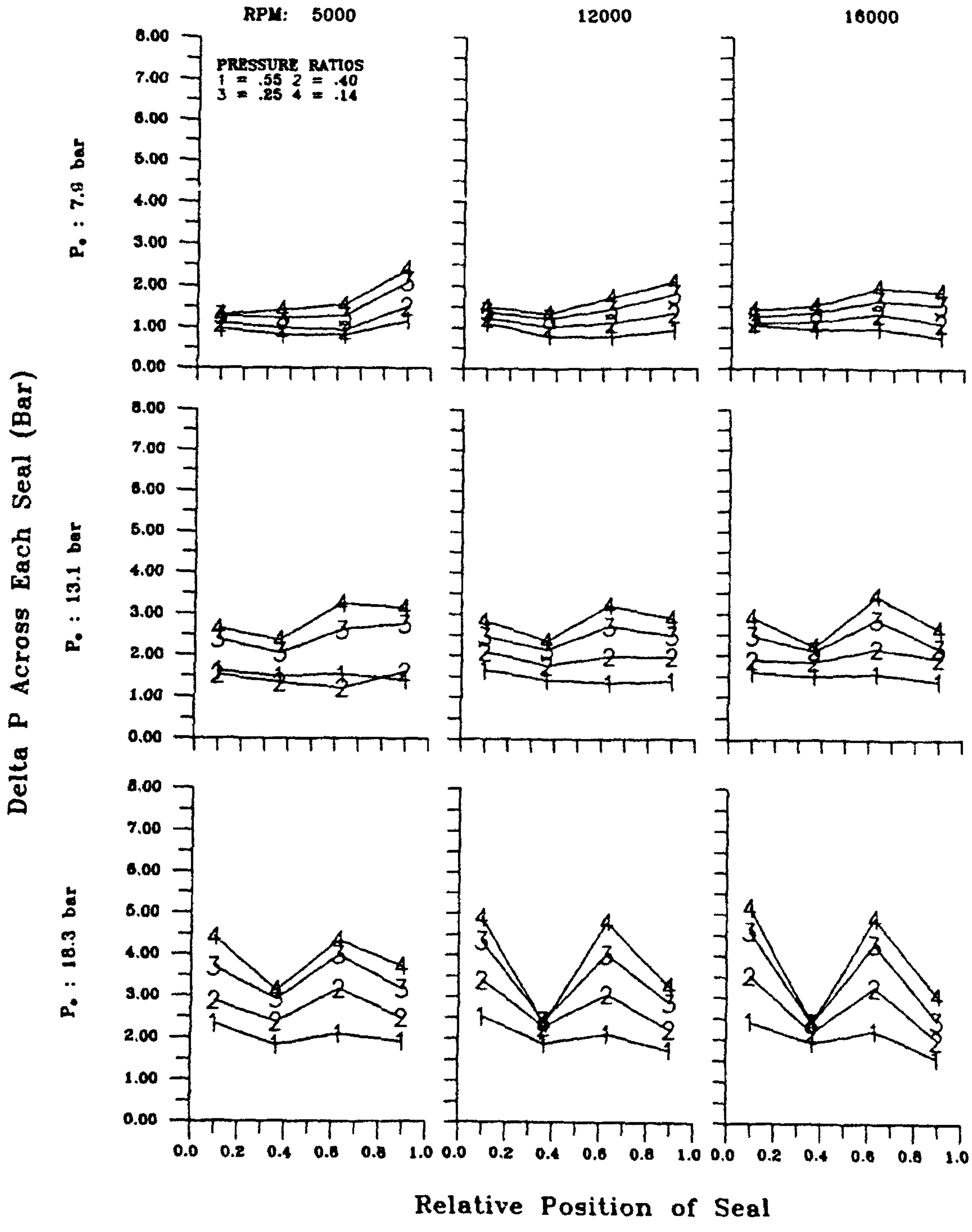

Figure 20 - Delta P across each stage with high inlet swirl for seal 3.

Leakage Characteristics

In the following sections, the mass flow rate and rotordynamic coefficients are plotted with respect to the inlet circumferential velocity ratio, $U_{\theta o}/r\omega$. The calculation of $U_{\theta o}$ is described in Chapter II. Figures 21, 22, and 23 show the tangential velocity as a function of both inlet pressure and rotor speed for seals 1, 2, and 3, respectively.

Figures 24, 25, and 26 show how the mass flow rate increases slightly as the inlet tangential velocity increases. This increase is more prevalent in seals 1 and 3, which were the second and last seal configurations tested. This suggests that this behavior occurs as the seals wear into place. The mass flow rate also increased in the order of testing (seal 2, 3, then 1), supporting the arguments made by Chupp and Nelson [3], and Holle and Krishnan [4]; viz., brush seals require a wear-in period. Inlet pressure and pressure ratio both influence the mass flow rate. At an inlet pressure of 7.9 bar, pressure ratio does not have much effect on the flow rate. However, as inlet pressure increases, the pressure ratio has a greater effect, again suggesting that the bristles lift off the rotor due to a presence of a shear layer gap at higher inlet pressures. Figure 27 shows that there is a definite increase of flow rate with an increase in inlet pressure for all pressure ratios. This is true for all seal configurations. Rotor speed has no influence on the mass flow rate.

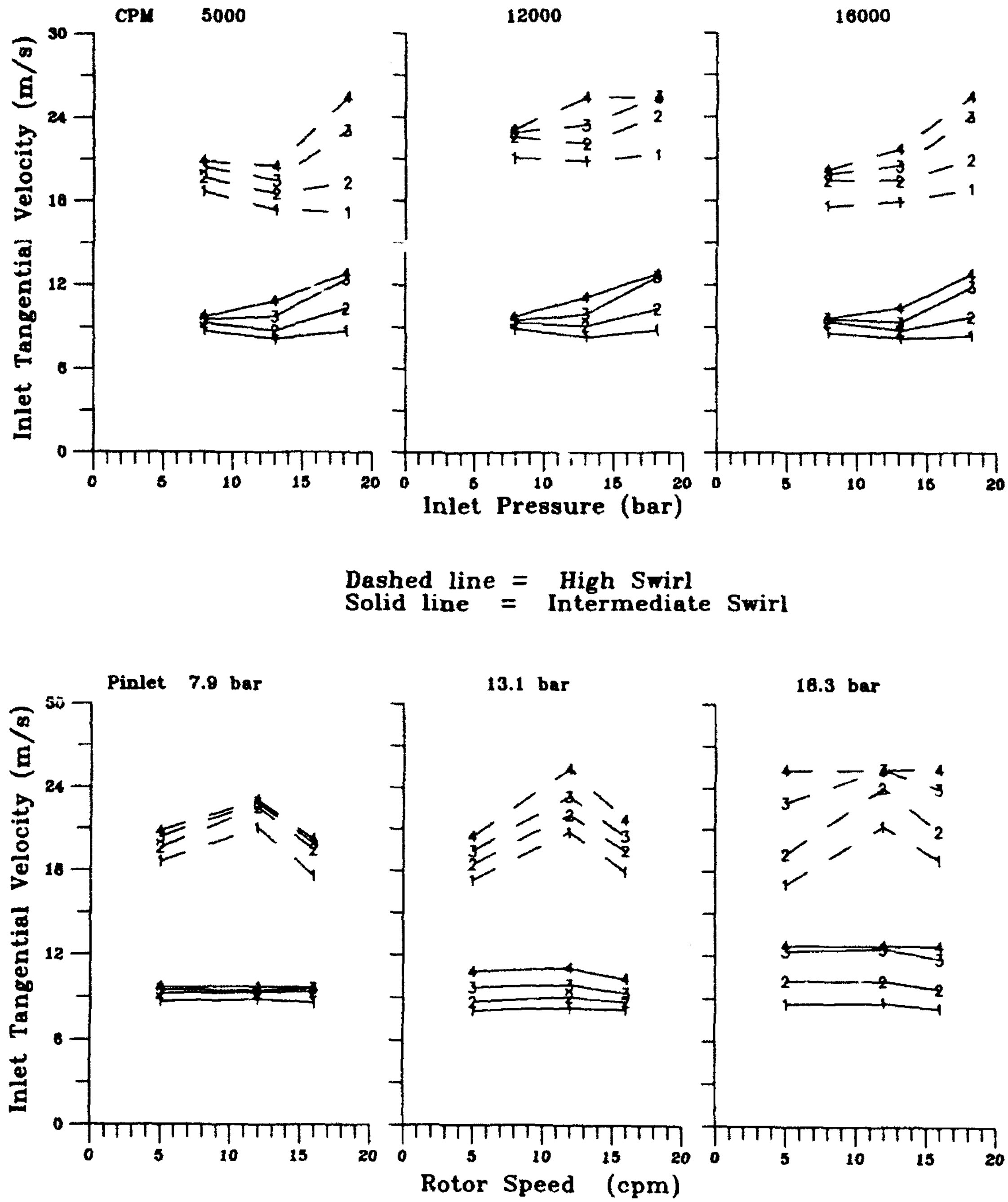

Figure 21 - Inlet tangential velocity vs. inlet pressure and rotor speed for seal 1.

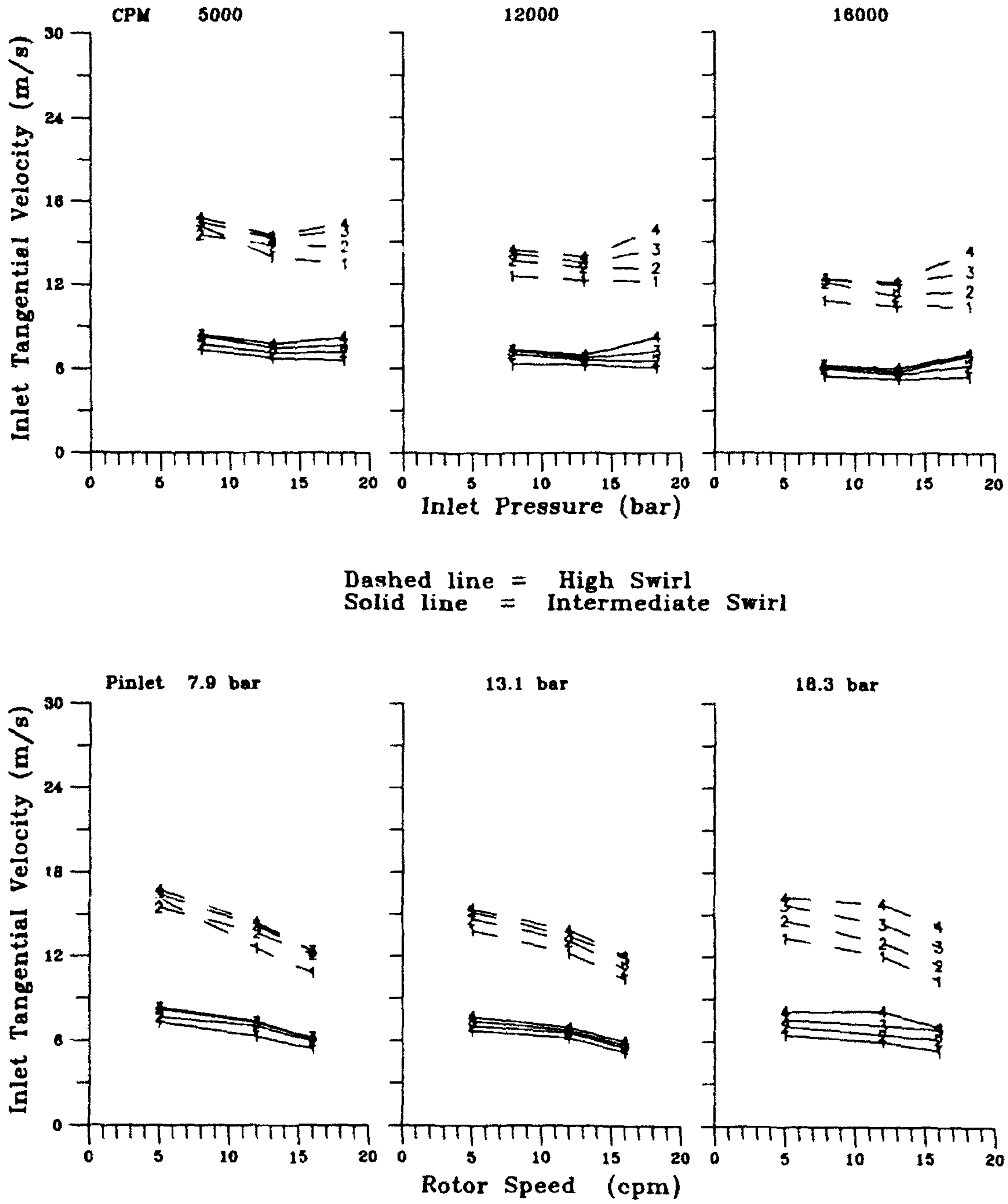

Figure 22 - Inlet tangential velocity vs. inlet pressure and rotor speed for seal 2.

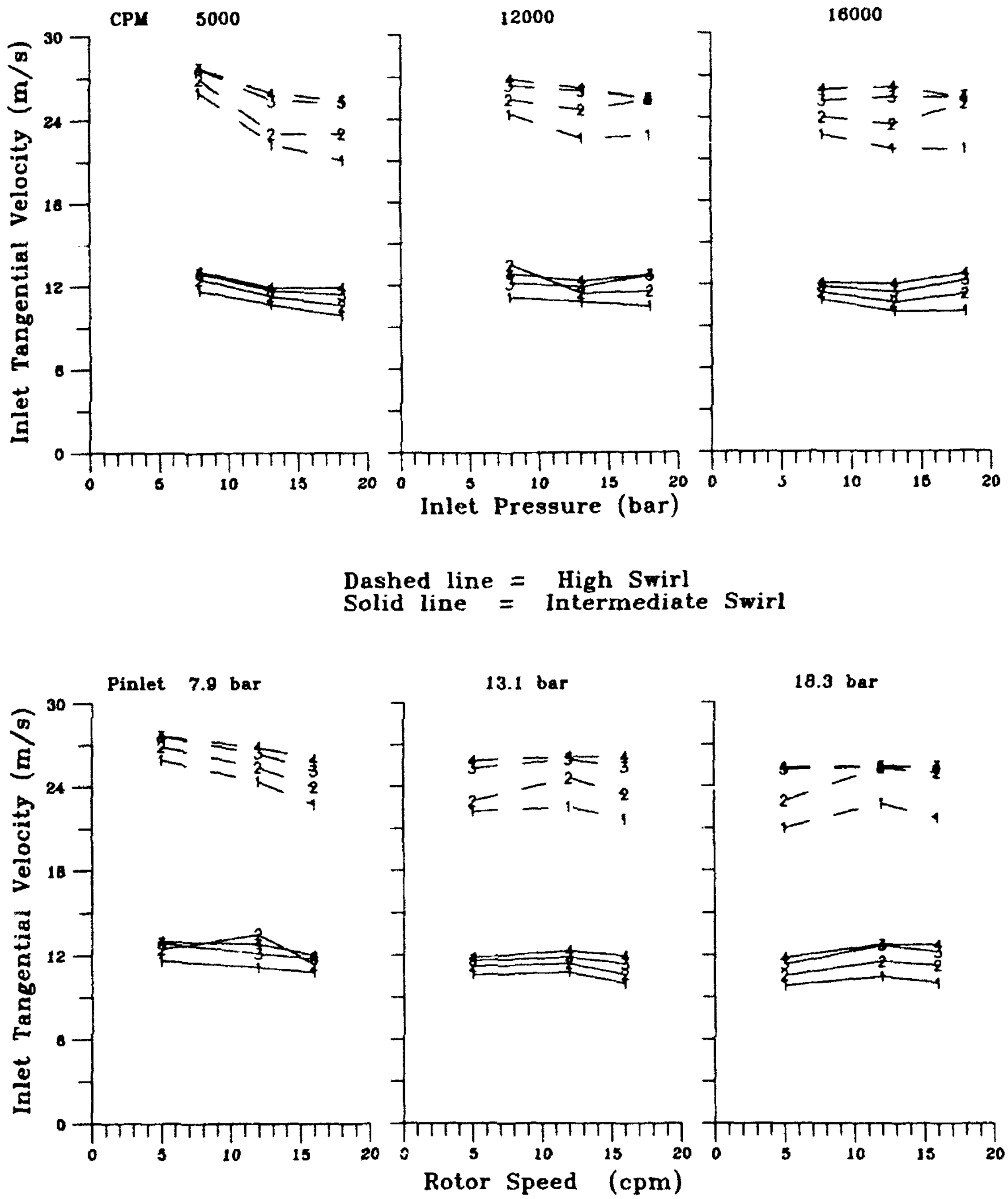

Figure 23 - Inlet tangential velocity vs. inlet pressure and rotor speed for seal 3.

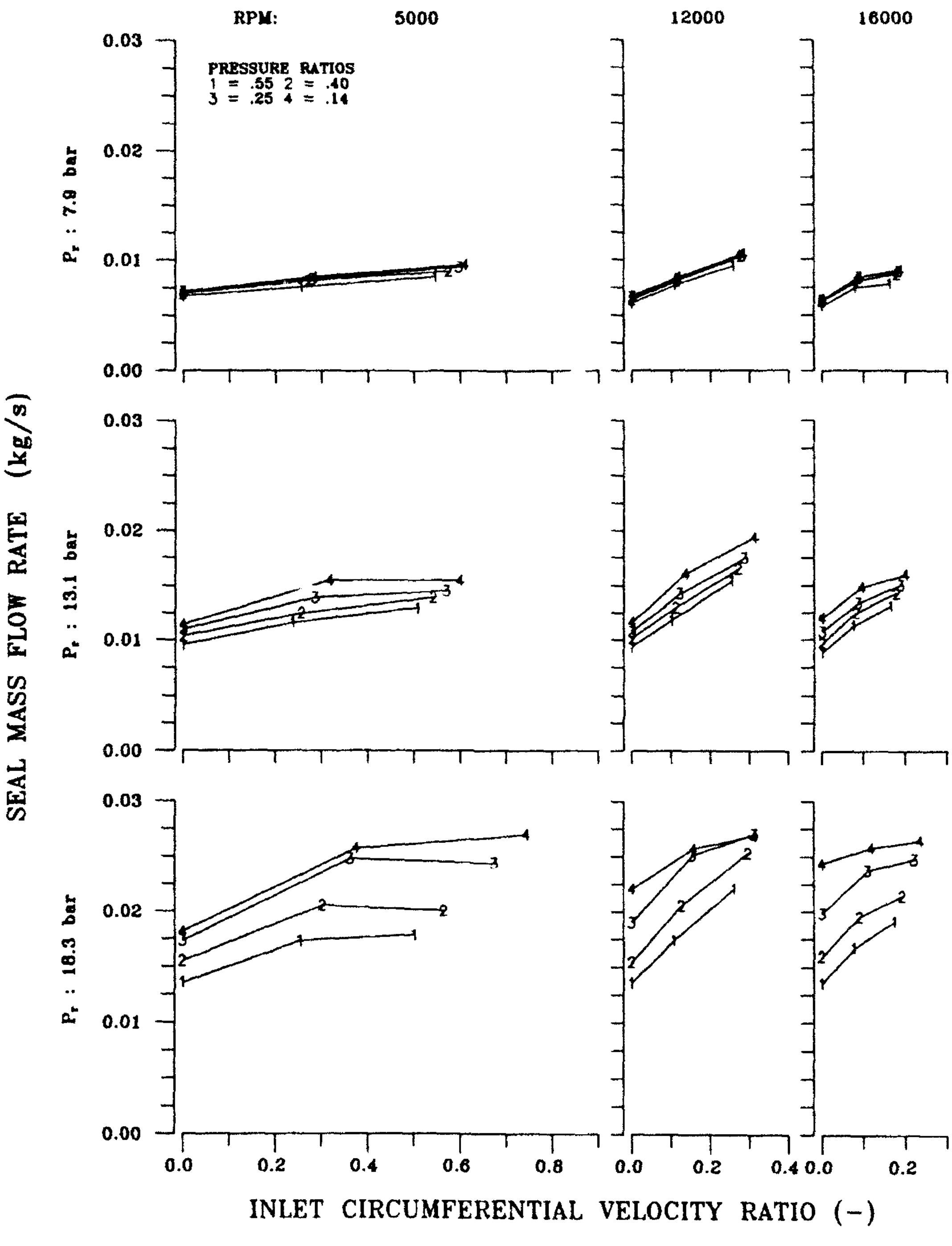

Figure 24 - Mass flow rate vs. inlet circumferential velocity ratio for seal 1.

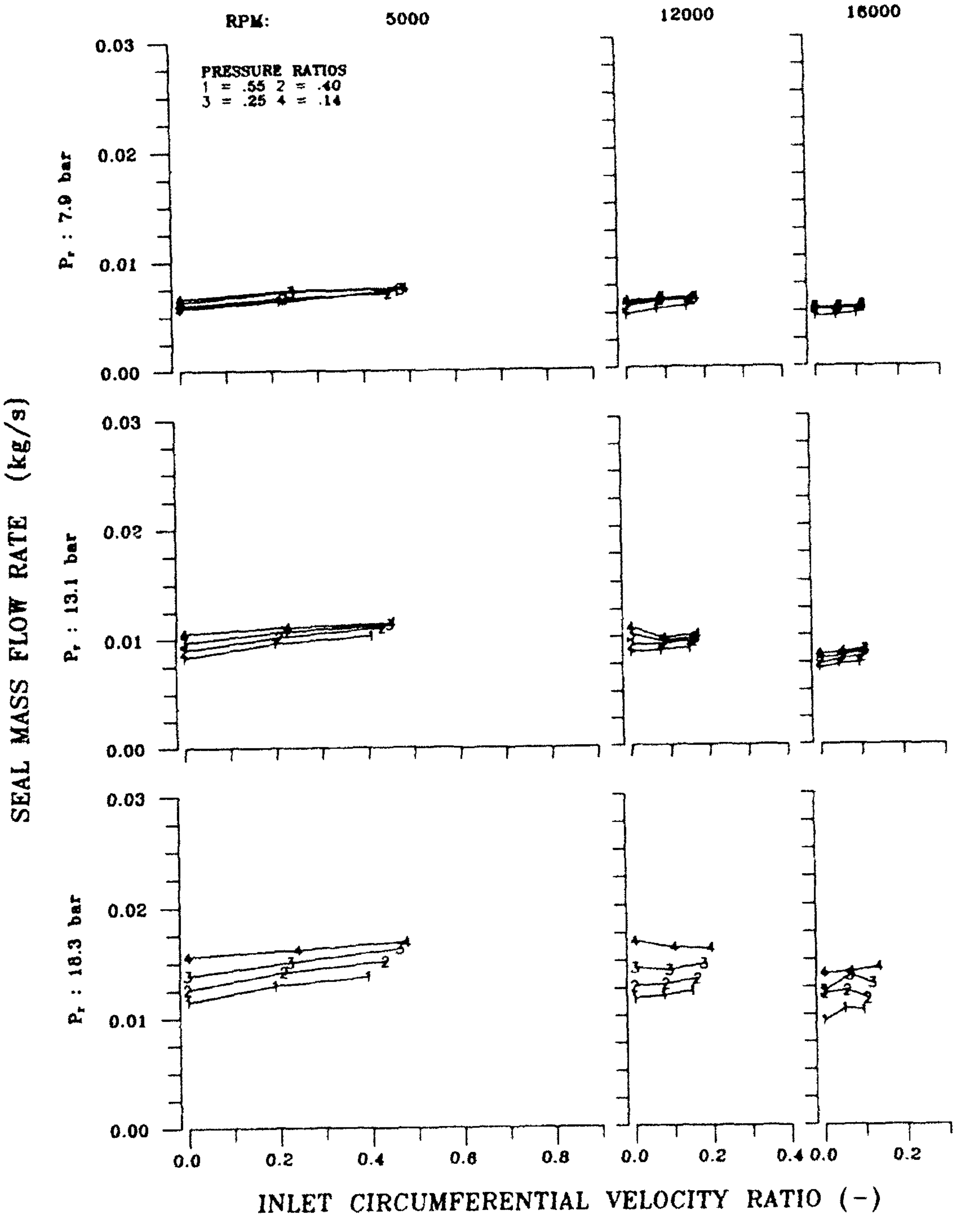

Figure 25 - Mass Flow rate vs. inlet circumferential velocity ratio for seal 2.

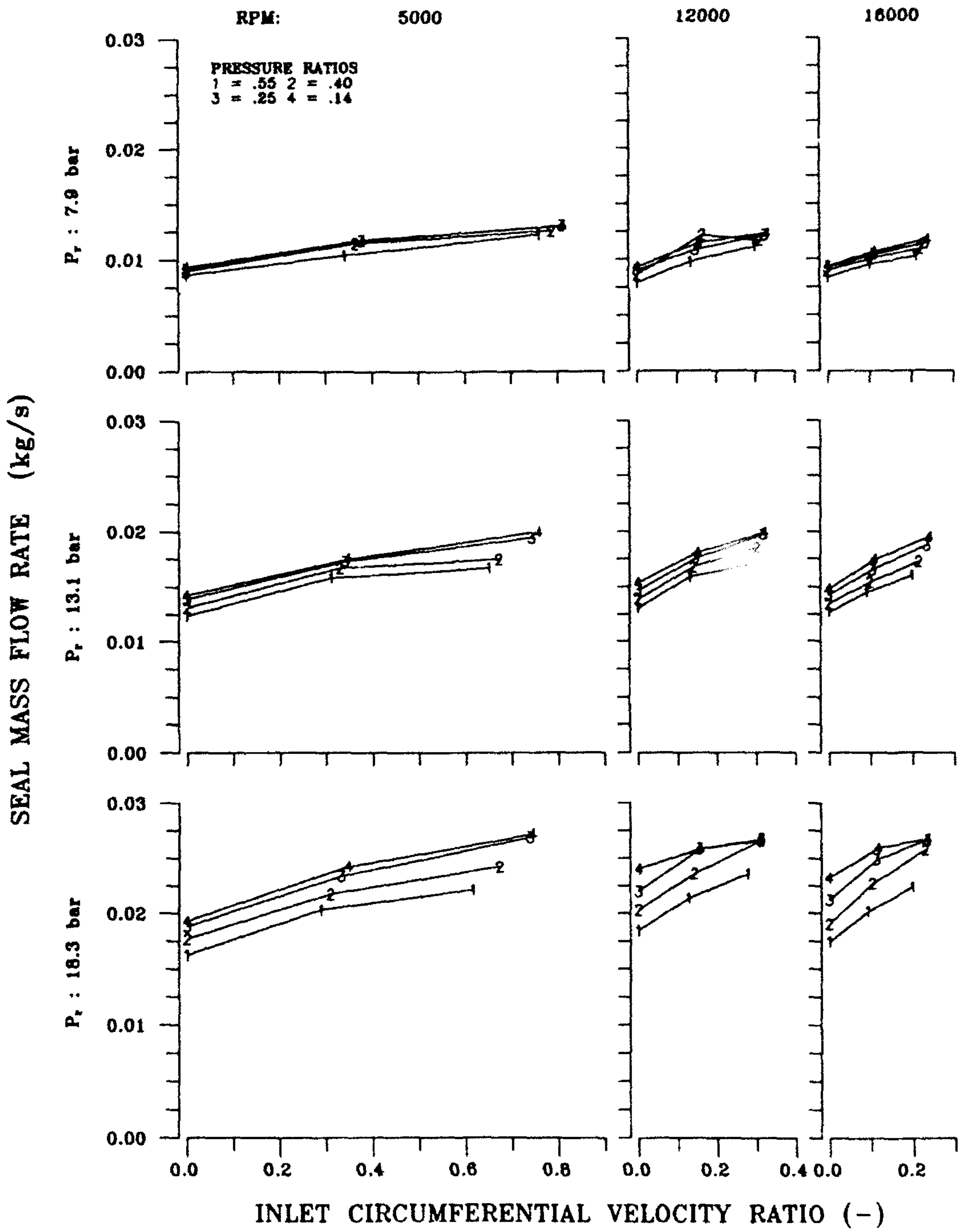

Figure 26 - Mass flow rate vs. inlet circumferential velocity ratio for seal 3.

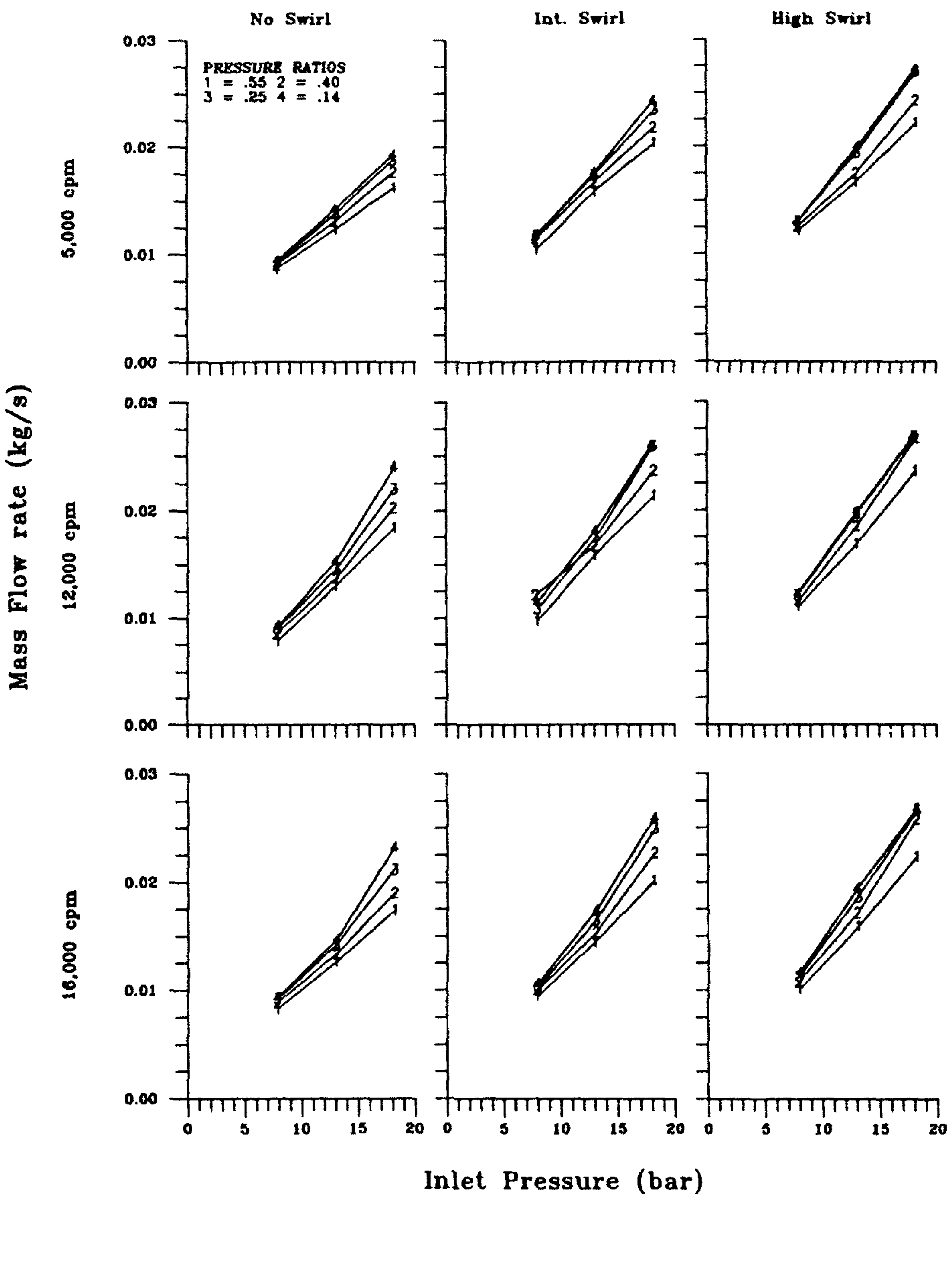

Figure 27 - Mass flow rate vs. inlet pressure.

Direct Stiffness

The model of equation 4 applies for annular, non-contacting gas seals. How well this model would apply to brush seals was a question to be resolved in the present study. The mathematical rotordynamic model shown in equation 4 assume that the stiffness and damping coefficients are independent of excitation frequency, as is the case for traditional annular seals. However, experimental test results show that this is not the case for the direct stiffness, K.

Figure 28 is an example of direct stiffness versus excitation frequency. All of the seal configurations show a direct stiffness which varies linearly with frequency. Although the slope of this linear relationship remained relatively constant for the two highest rotor speeds, Figure 29 illustrates the slight drop in the value of the intercept at $\omega = 0$ as the rotor speed increases. This drop is more prevalent and less sporadic with an increase in inlet pressure. Figures 30, 31, and 32 are the mean values of K as a function of the inlet velocity ratio. In general, these figures show that as speed and inlet pressure increase, the dependence of K on pressure ratio decreases, again suggesting the presence of a shear layer at high surface speeds and inlet pressures. Seal 3, the last seal tested, showed a slight decrease in K as inlet swirl increases. This trend is not as prevalent in the data for seals 1 and 2.

The reader is reminded that the direct stiffness times radial displacement is a force in the radial direction, as shown in Figure 2. If the net force in the radial direction is highly positive or negative, only the natural frequency of the shaft will be affected, not the rotordynamic stability. The experimental results show that the direct stiffness force in all cases is positive and relatively small in comparison to bearing stiffness.

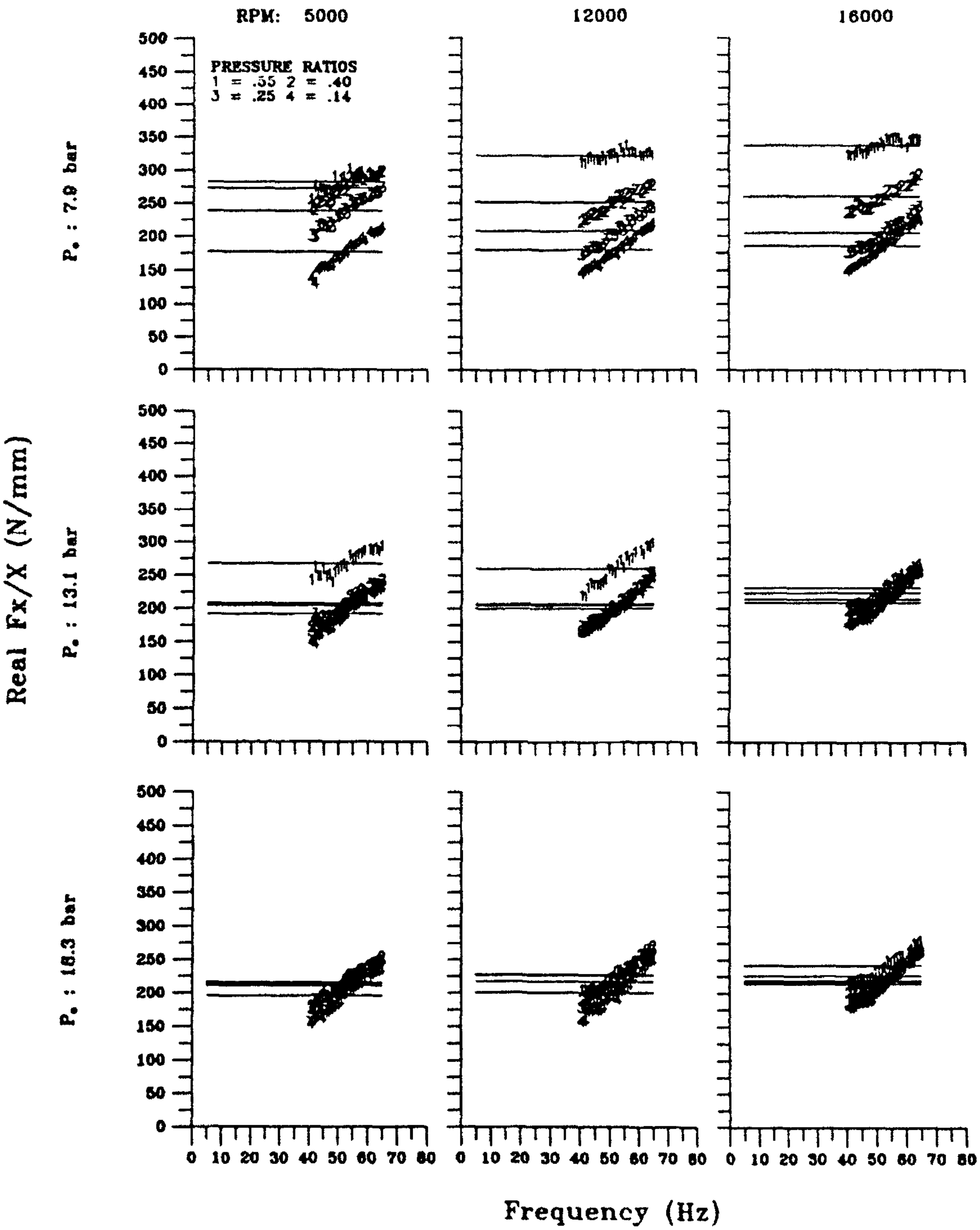

Figure 28 - Direct stiffness as a function of frequency.

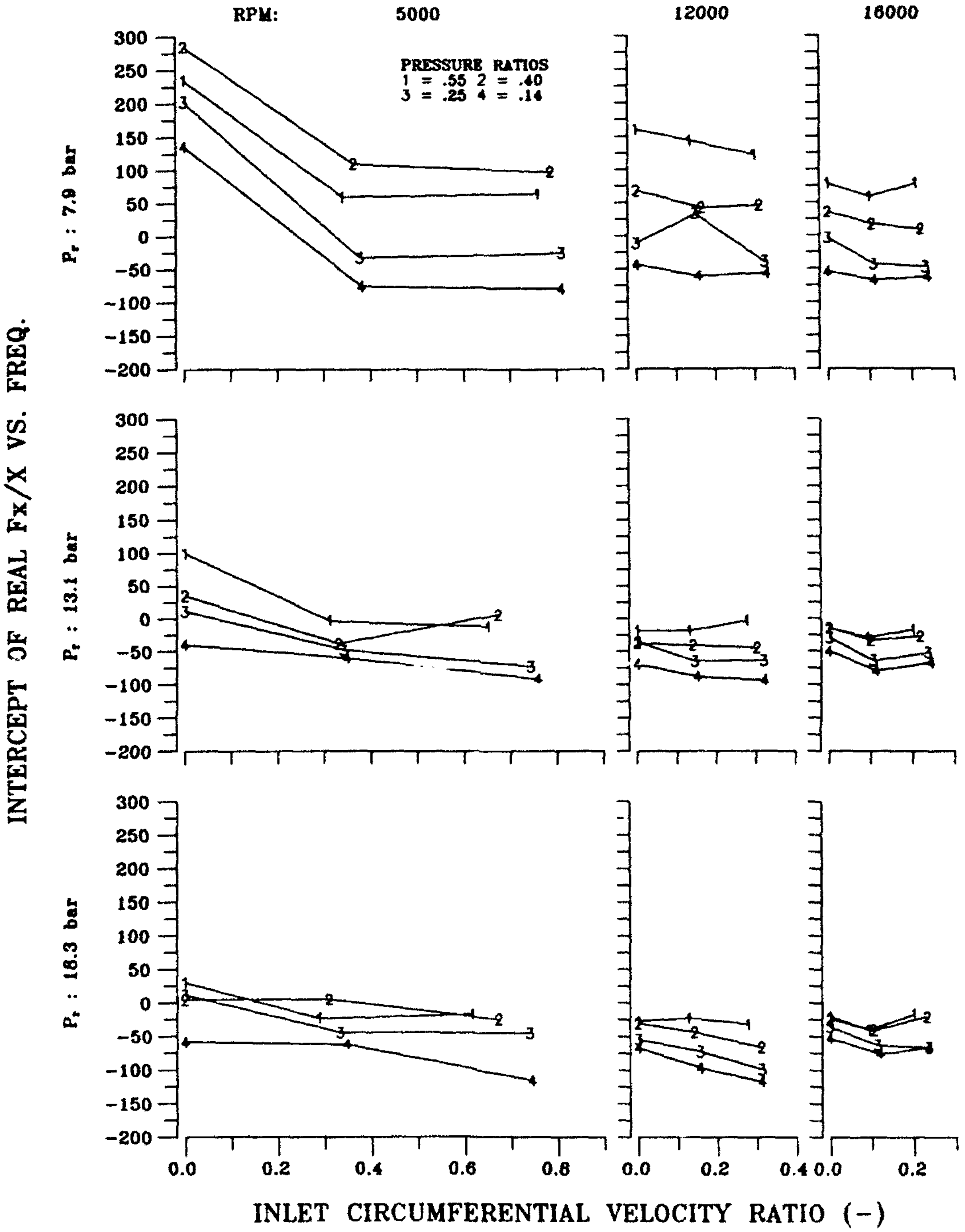

Figure 29 - Intercept of Re($\hat{F}/\hat{X}$) vs. inlet velocity ratio.

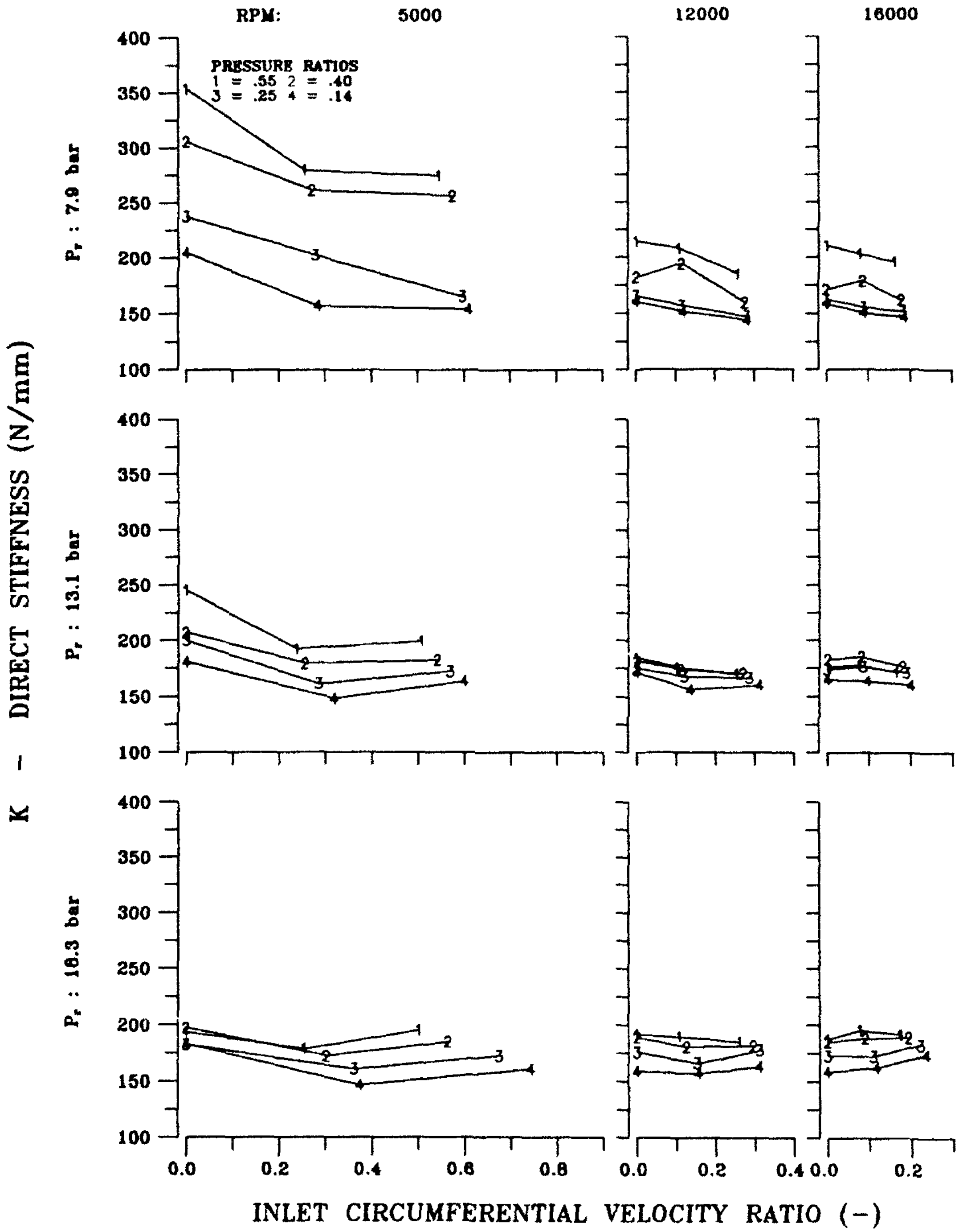

Figure 30 - Mean value of K vs. inlet circumferential velocity ratio for seal 1.

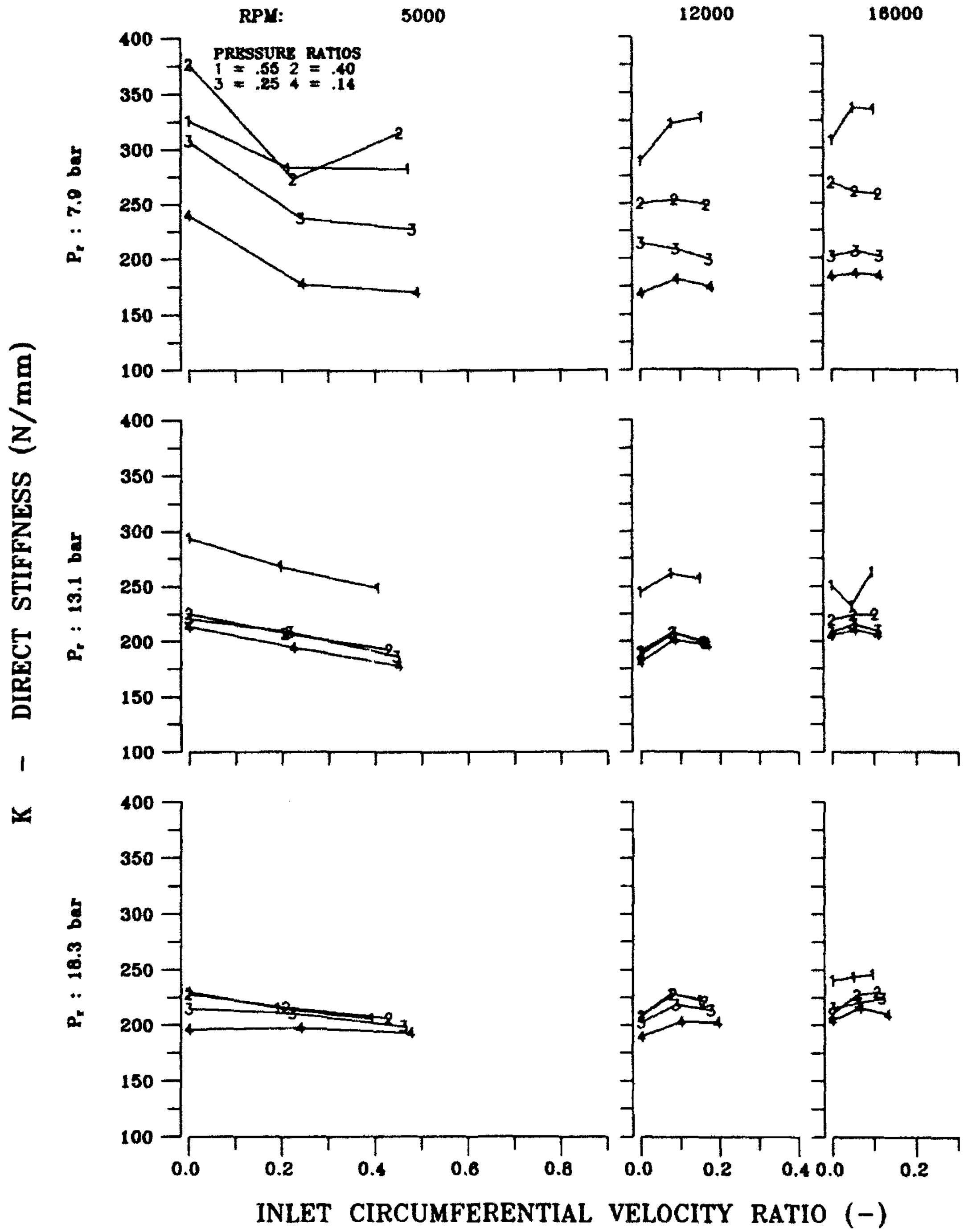

Figure 31 - Mean value of K vs. inlet circumferential velocity ratio for seal 2.

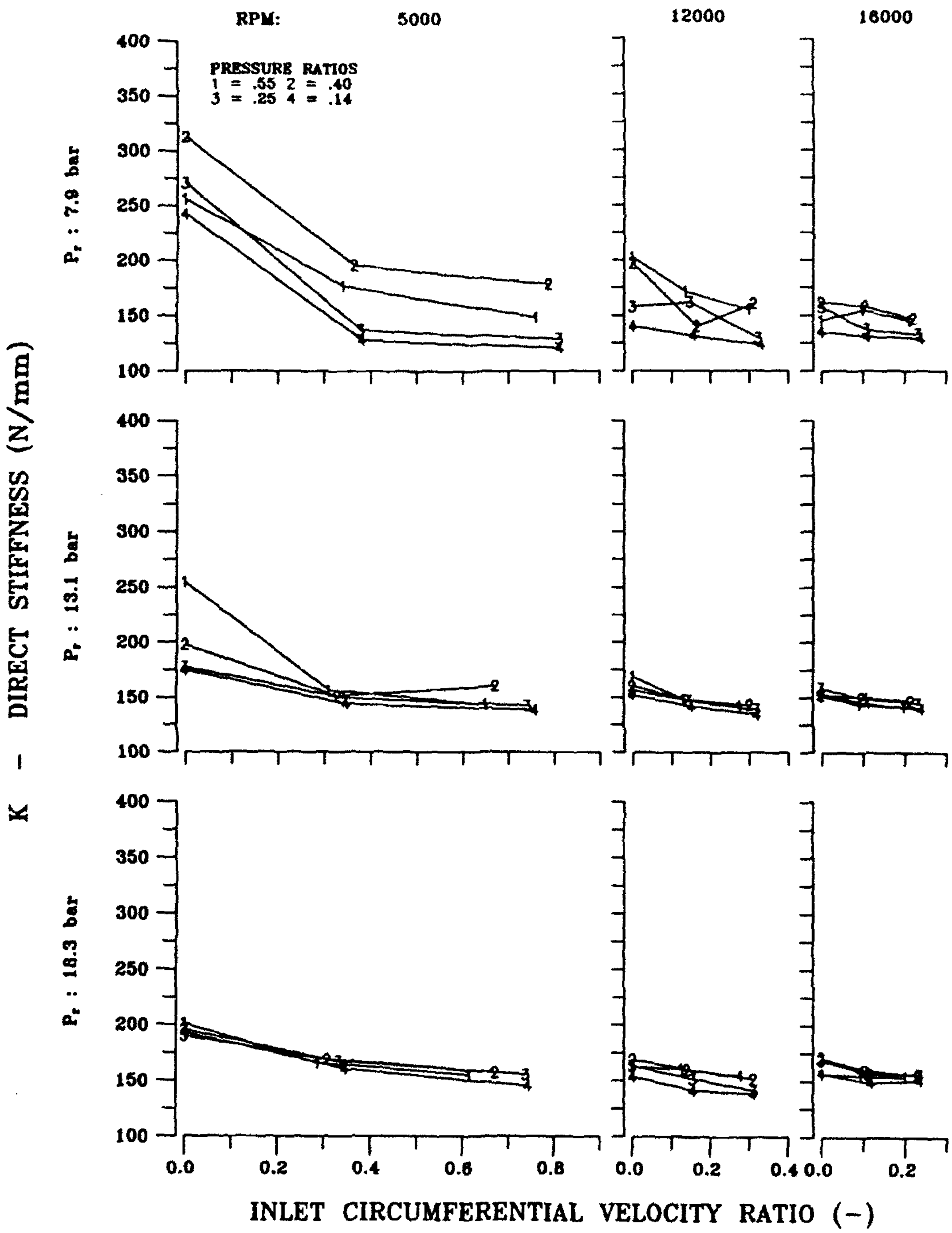

Figure 32 - Mean value of K vs. inlet circumferential velocity ratio for seal 3.

Cross-Coupled Stiffness

Rotordynamic stability is most heavily influenced by the tangential force on the rotor, which arise due to the cross-coupled stiffness coefficient k and direct damping coefficient C (see Figure 2). A positive net tangential force is destabilizing because it tends to drive the rotor into forward whirl. If negative, this force is stabilizing because it tends to prevent forward whirl. Therefore, C should be maximized and k should be minimized, or negative if possible, for the greatest stability.

Dependence of k is not as pronounced as for K; however, the $Re(\hat{F}_Y/\hat{X})$ versus frequency plots (see Appendix A) show that k increases slightly with frequency in most cases. Figures 33, 34, and 35 show the mean value of cross-coupled stiffness versus inlet circumferential velocity ratio for three inlet pressures and three speeds with pressure ratio as the parameter for seals 1, 2, and 3, respectively. All of the values for k are very low, and generally negative, therefore stabilizing. Seals 1 and 3, at the lowest supply pressure and speed case, show a small increase in k with increasing $U_{\theta o}$. This trend is not evident in seal 2; therefore, the trend could be sporadic and possibly caused by the lack of the fluid film between the bristles and rotor. At the middle and highest inlet pressures, k is relatively constant and not dependent on inlet swirl. Hence, the seal reduces or eliminates the destabilizing effect of inlet tangential velocity. For seals 2 and 3, as speed increases, the effect of pressure ratio on k becomes more prevalent.

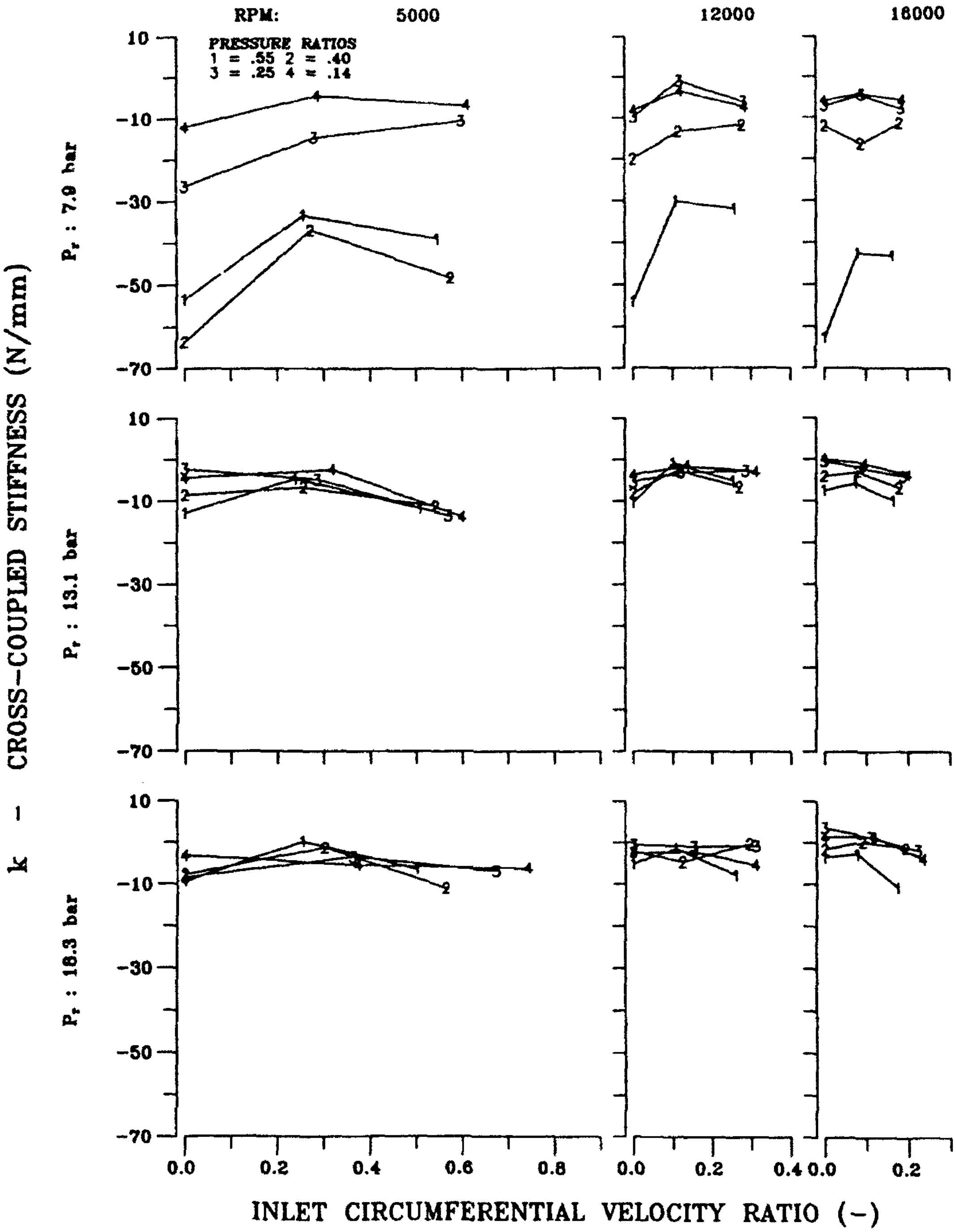

Figure 33 - Cross-coupled stiffness versus inlet circumferential velocity ratio for seal 1.

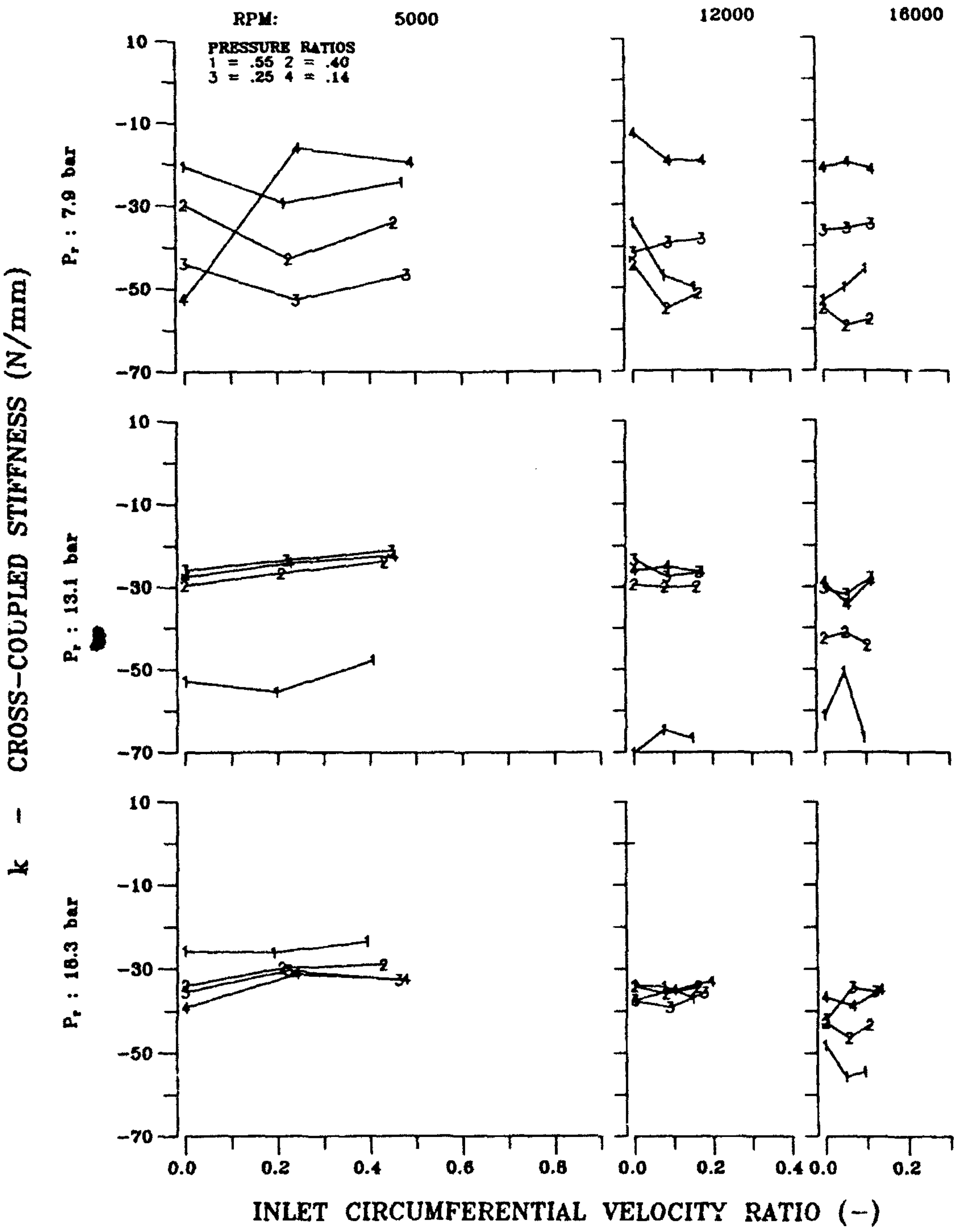

Figure 34 - Cross-coupled stiffness versus inlet circumferential velocity ratio for seal 2.

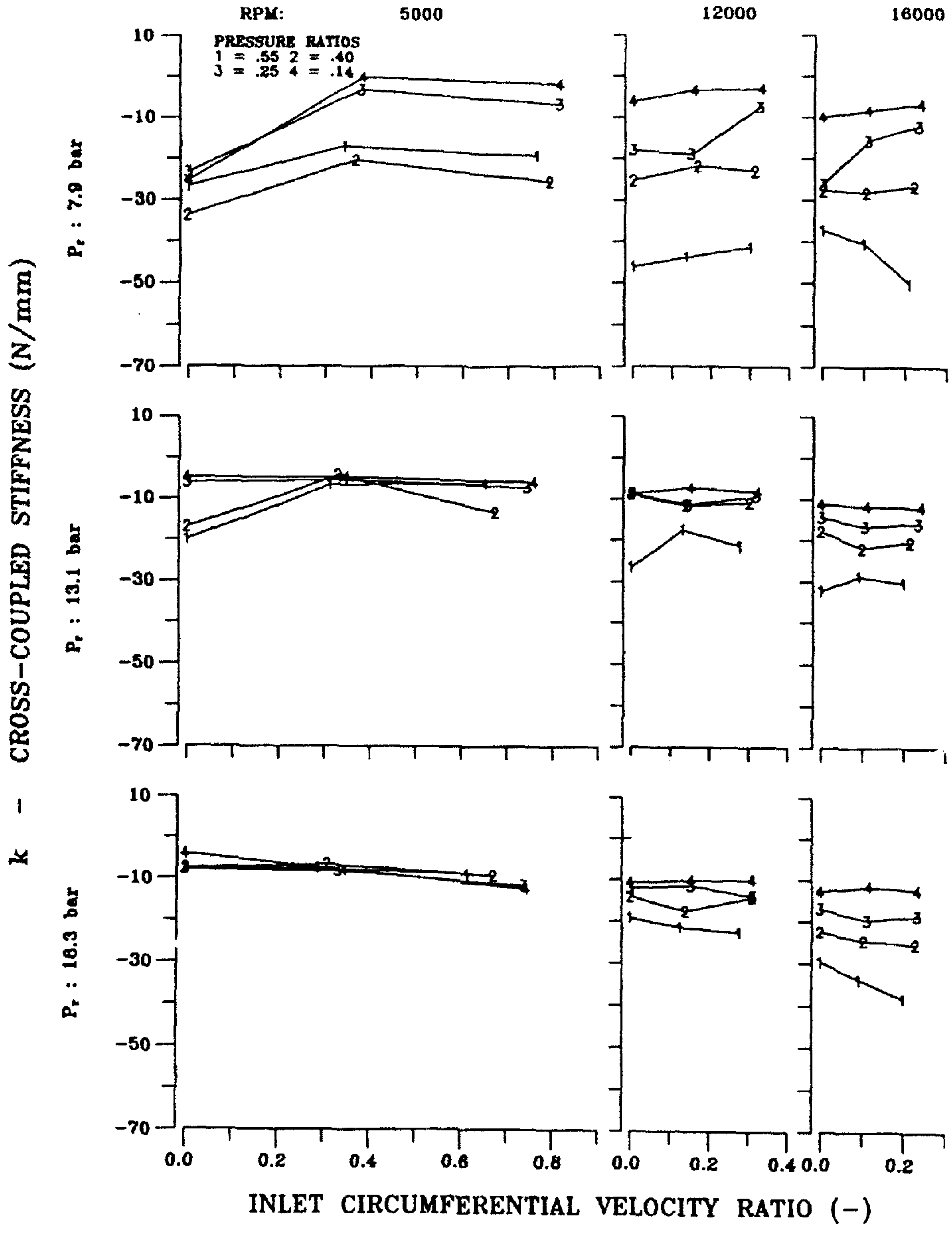

Figure 35 - Cross-coupled stiffness versus inlet circumferential velocity ratio for seal 3.

Direct Damping

Figures 36, 37, and 38 show the direct damping coefficient versus inlet circumferential velocity ratio for three inlet pressures and three speeds with pressure ratio as the parameter for seals 1, 2, and 3, respectively. Although there is no discernable trend with respect to pressure ratio or inlet swirl, direct damping does increase with increasing speed and inlet pressure. Dependence of direct damping on inter-seal spacing is sporadic and inconclusive.

According to the simplified model outlined in equation 4, the intercept of the $Im(\hat{F}_X/\hat{X})$ vs. frequency line at $\omega=0$ should be zero. Note that the intercept is not zero and does follow a trend. Figures 39, 40, and 41 show how the intercept decreases with increasing speed and inlet pressure.

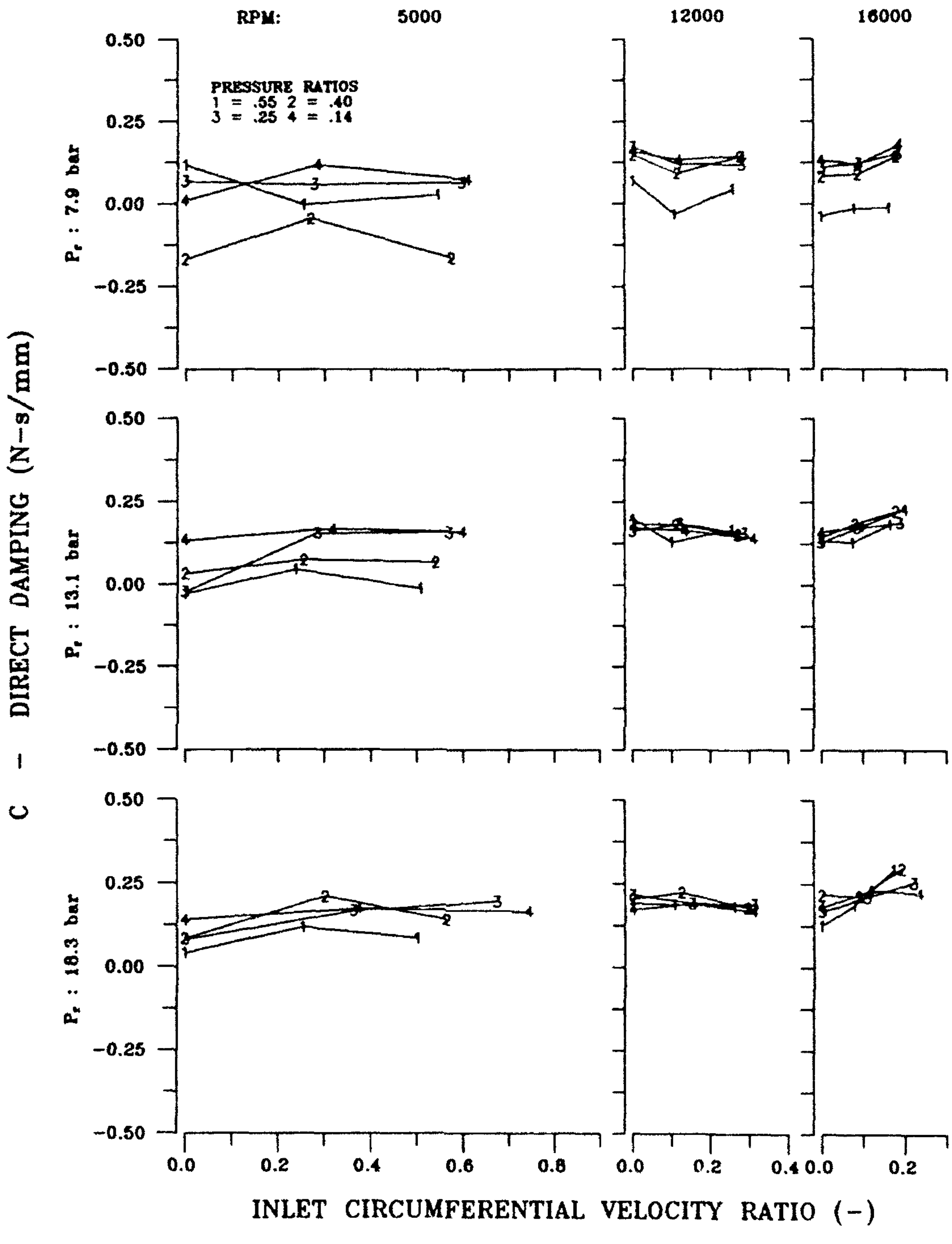

Figure 36 - Direct damping versus inlet circumferential velocity ratio for seal 1.

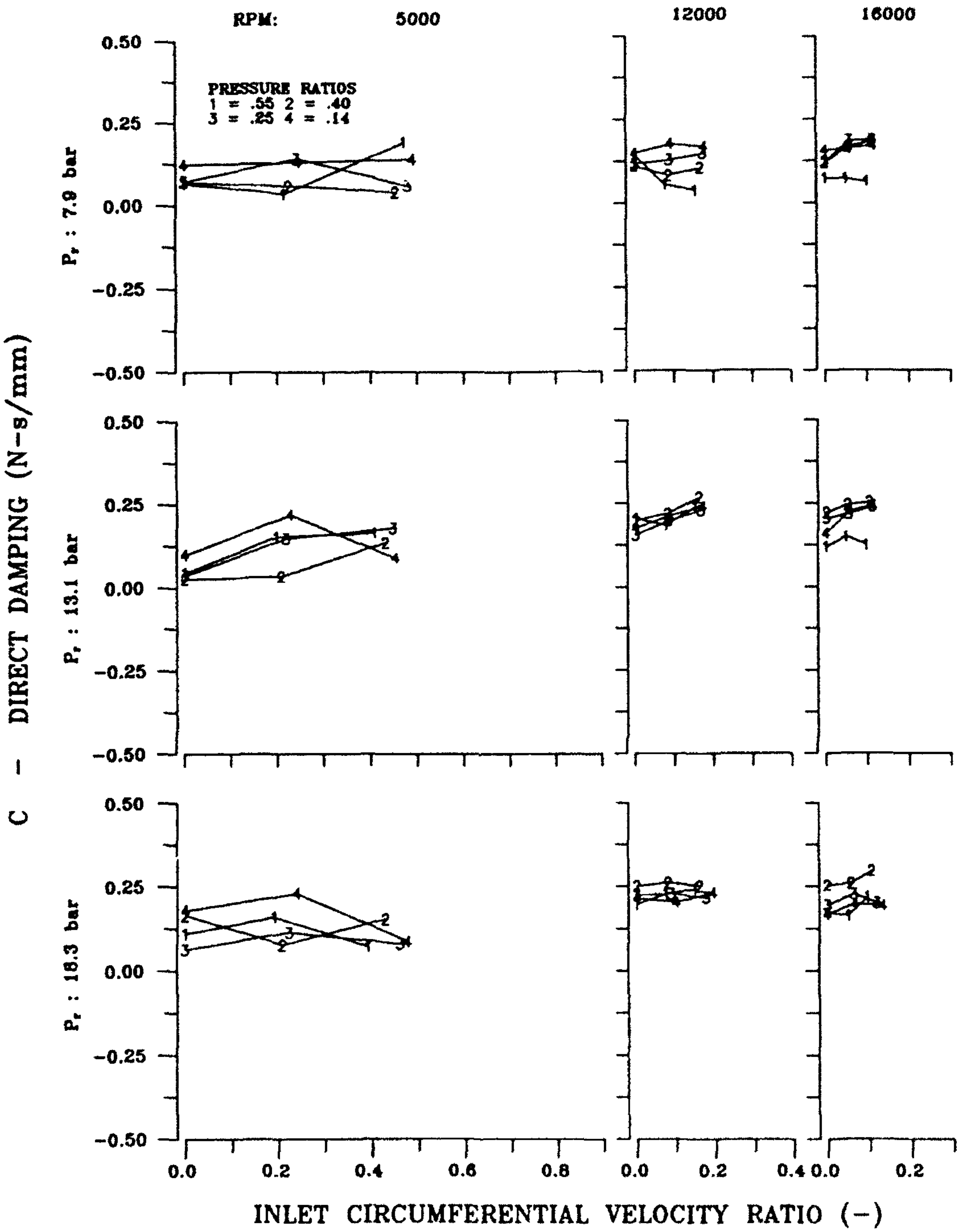

Figure 37 - Direct damping versus inlet circumferential velocity ratio for seal 2.

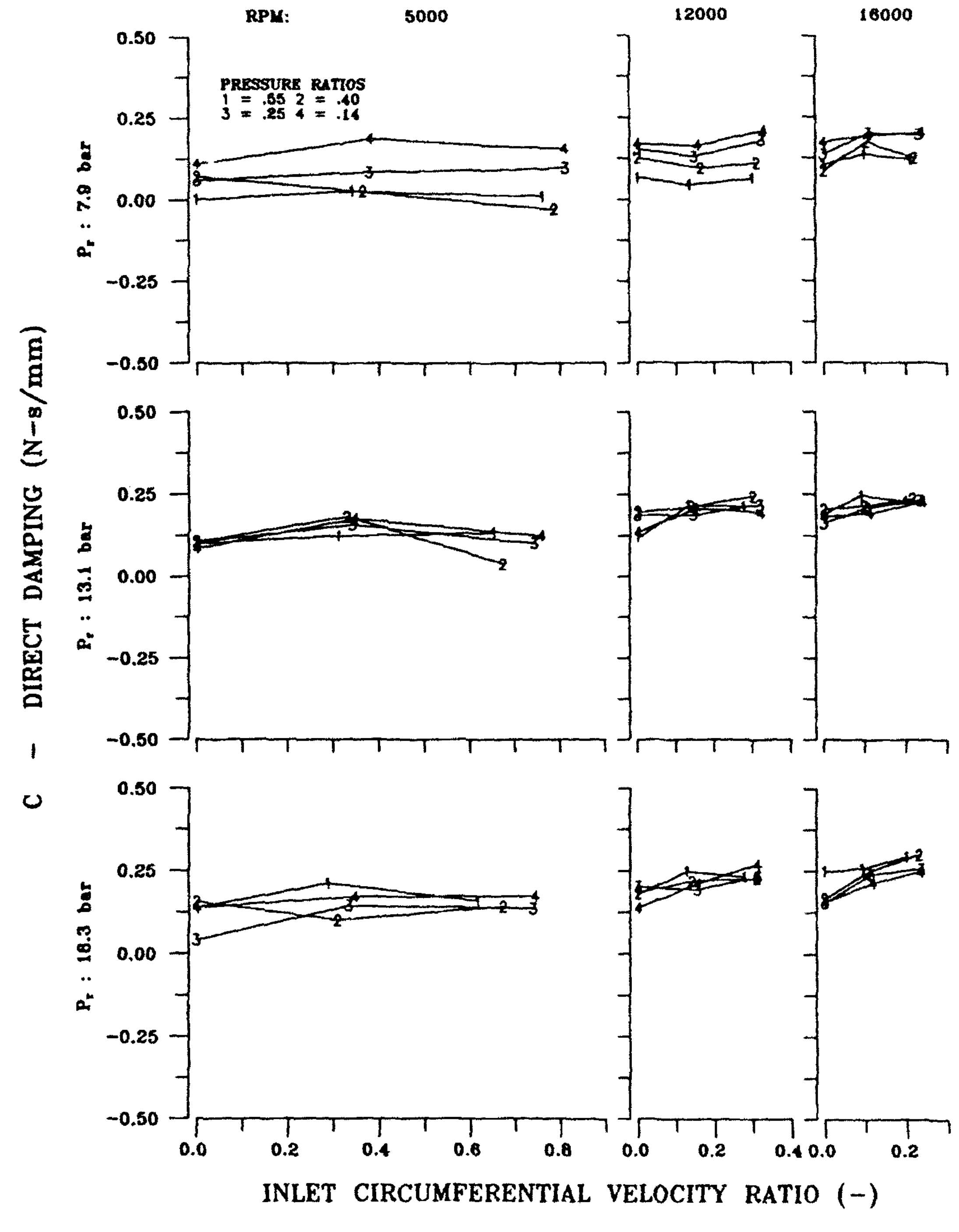

Figure 38 - Direct damping versus inlet circumferential velocity ratio for seal 3.

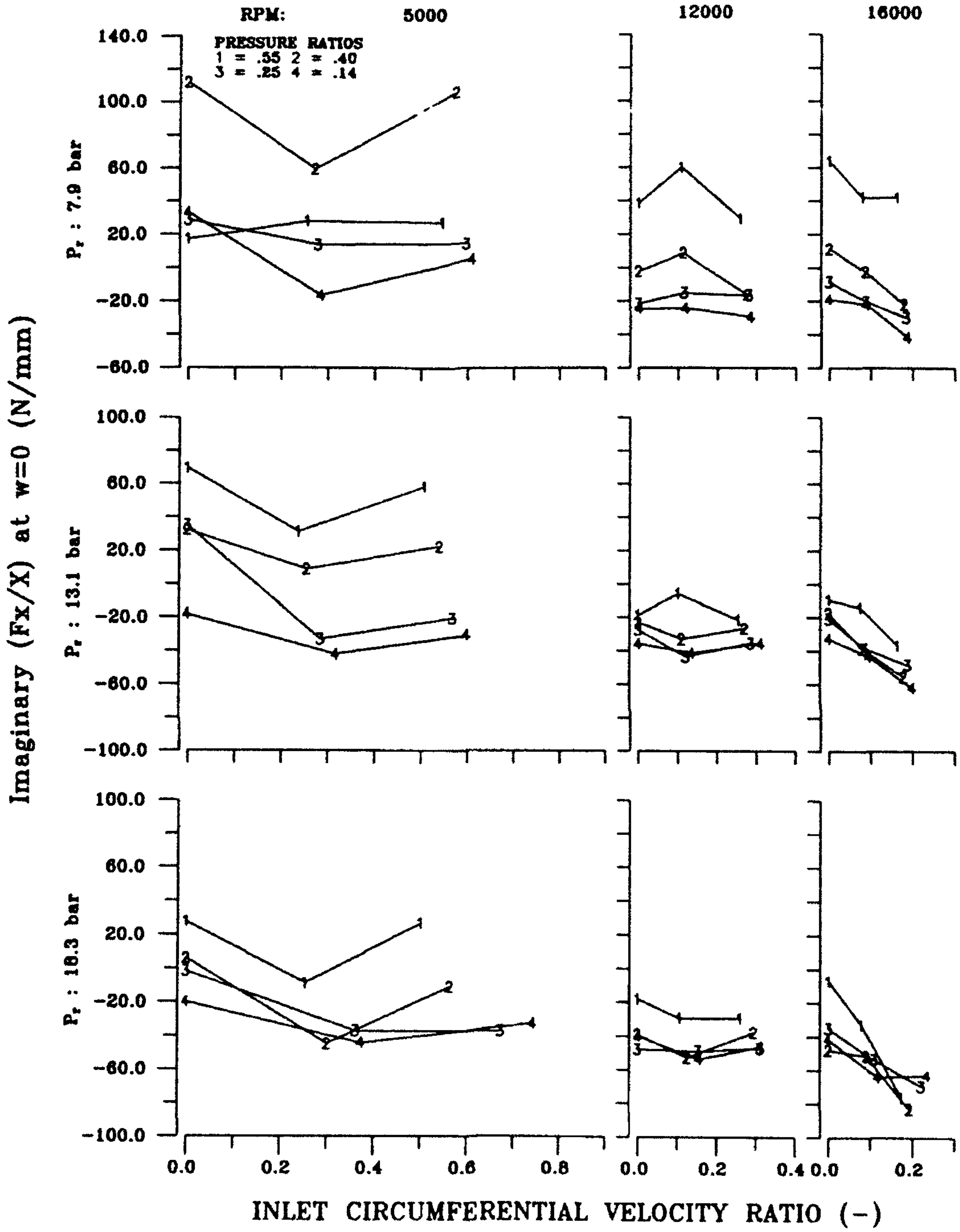

Figure 39 - $\mathrm{Im}(\hat{F}_X/\hat{X})$ intercept at $\omega=0$ versus inlet circumferential velocity ratio for seal 1.

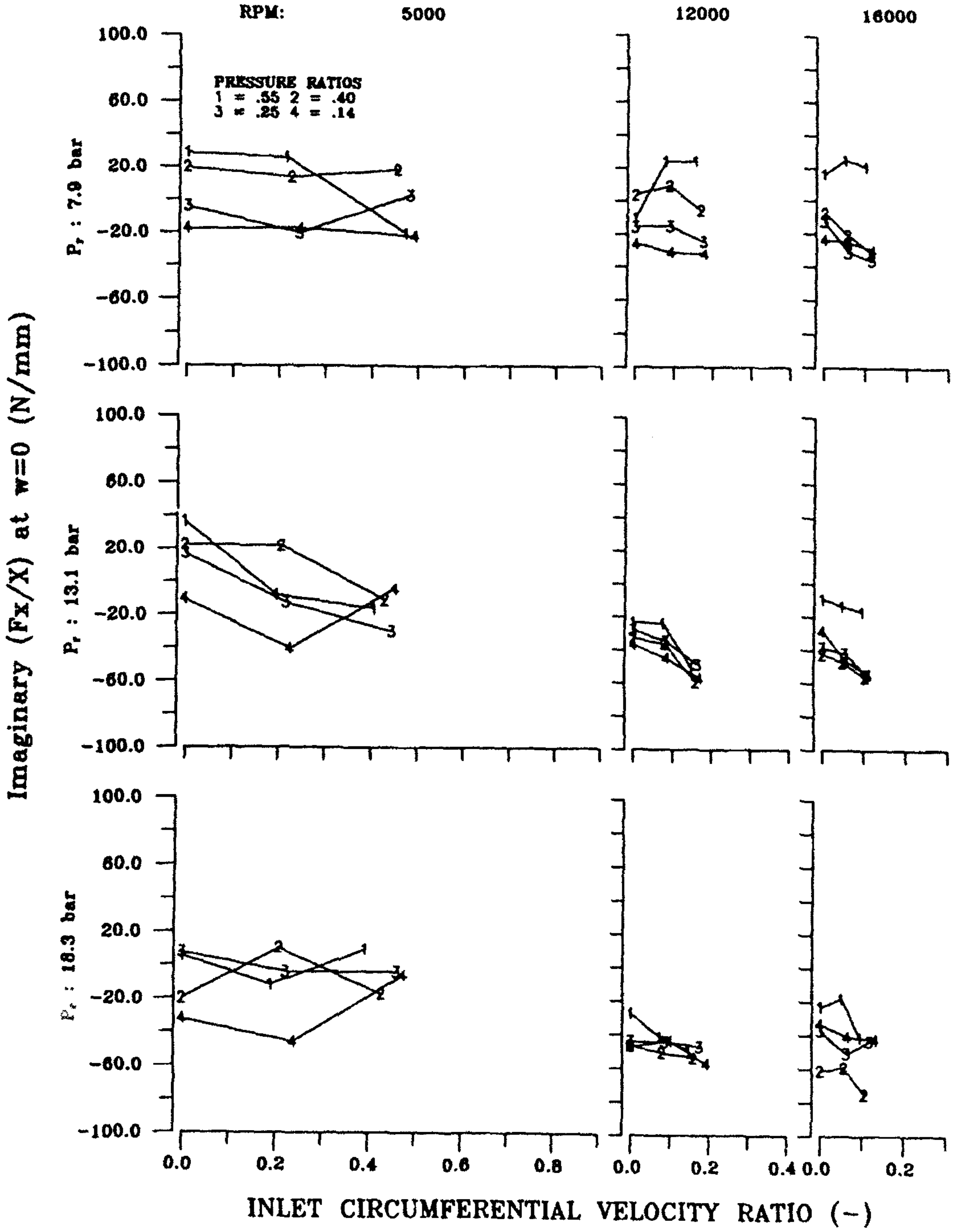

Figure 40 - Im($\hat{F}_X/\hat{X}$) intercept at ω=0 versus inlet circumferential velocity ratio for seal 2.

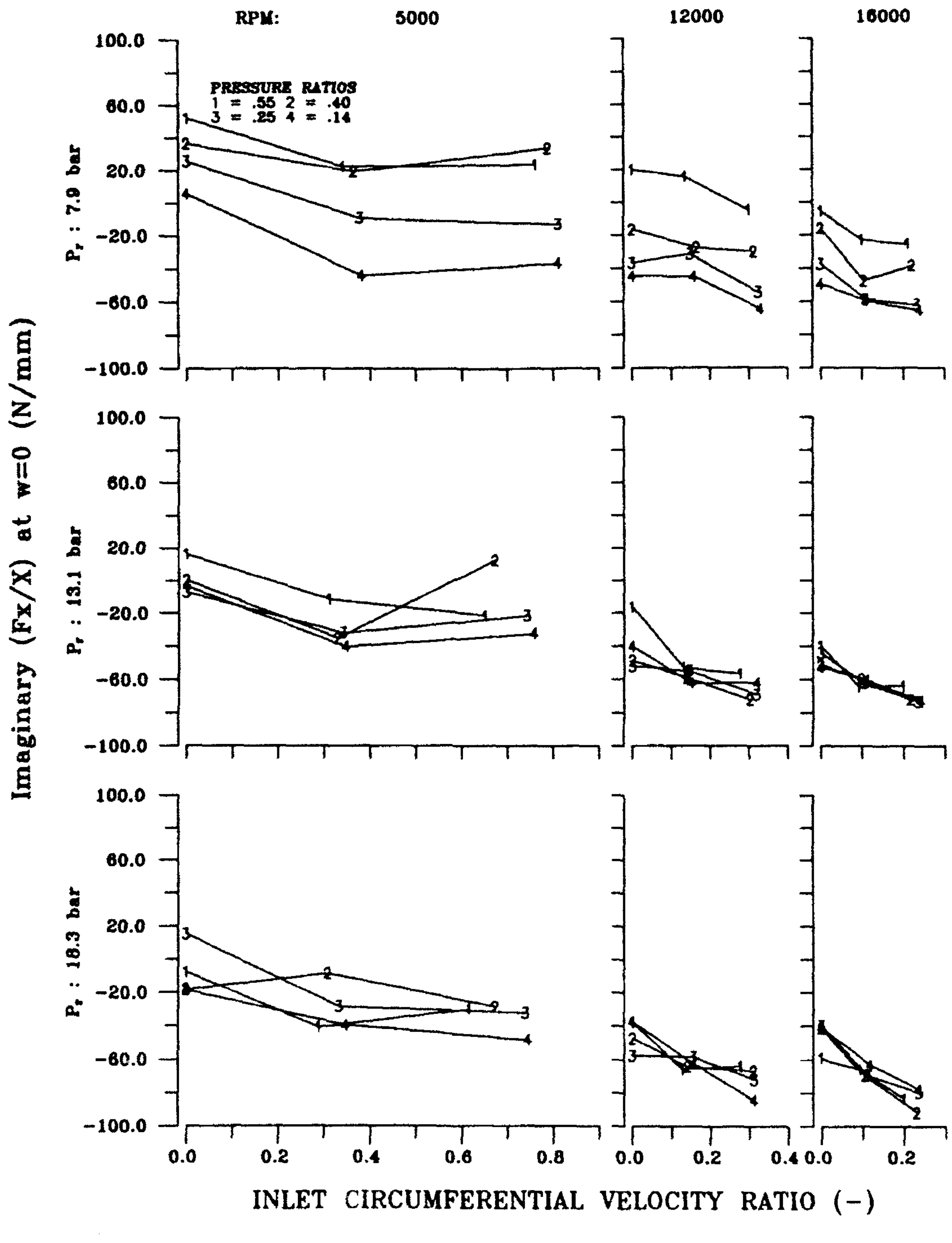

Figure 41 - $\mathrm{Im}(\hat{F}_X/\hat{X})$ intercept at $\omega=0$ versus inlet circumferential velocity ratio for seal 3.

Whirl-Frequency Ratio

The whirl frequency ratio, $f = k/C\omega$, where ω is the running speed, is a useful measure of the stability of a seal. This ratio for brush seals is very small and usually negative, which is an indication of a stable seal.

Figures 42, 43, and 44 show the whirl frequency ratio for the three inlet pressures and three speeds with pressure ratio as the parameter for seals 1, 2, and 3, respectively. In general, the data show sporadic behavior at 5000 cpm. This is more prevalent at the two lowest inlet pressures. However, at 12,000 and 16,000 cpm, the whirl frequency ratio is extremely close to zero and independent of any test parameters, including spacing. This indicates that the brush seal is generally stabilizing under any combination of the test parameters varied in this study.

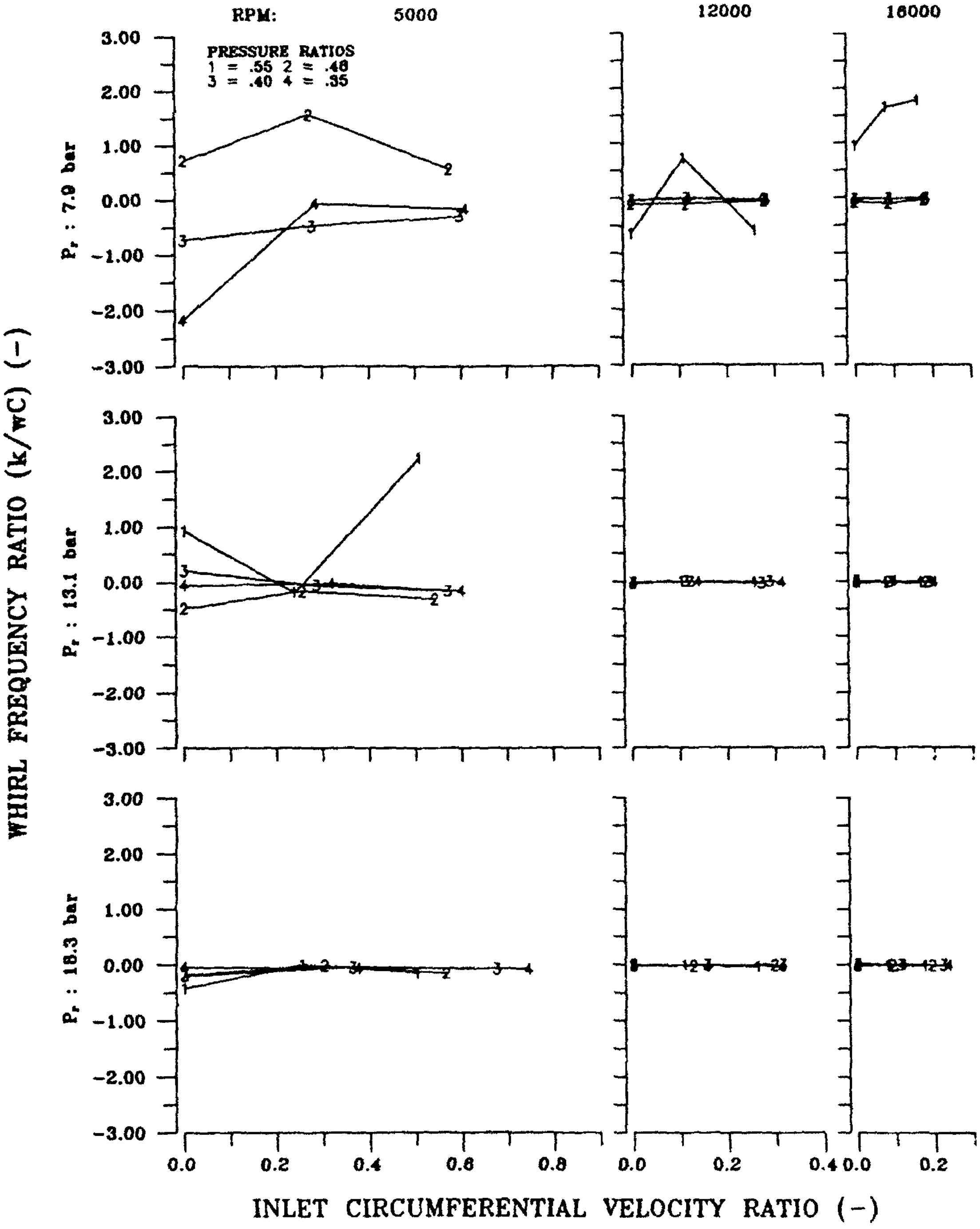

Figure 42 - Whirl frequency ratio versus inlet circumferential velocity ratio for seal 1.

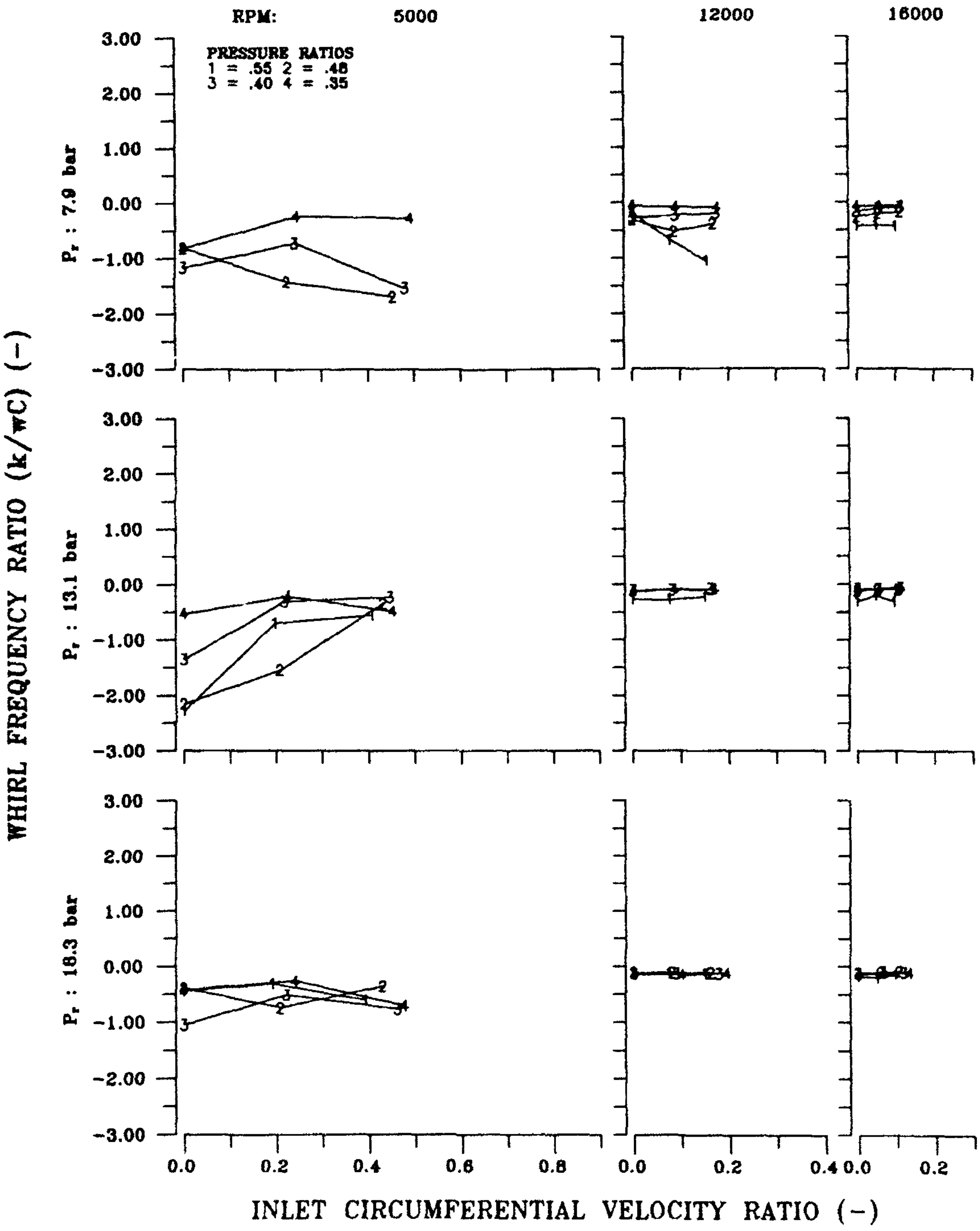

Figure 43 - Whirl frequency ratio versus inlet circumferential velocity ratio for seal 2.

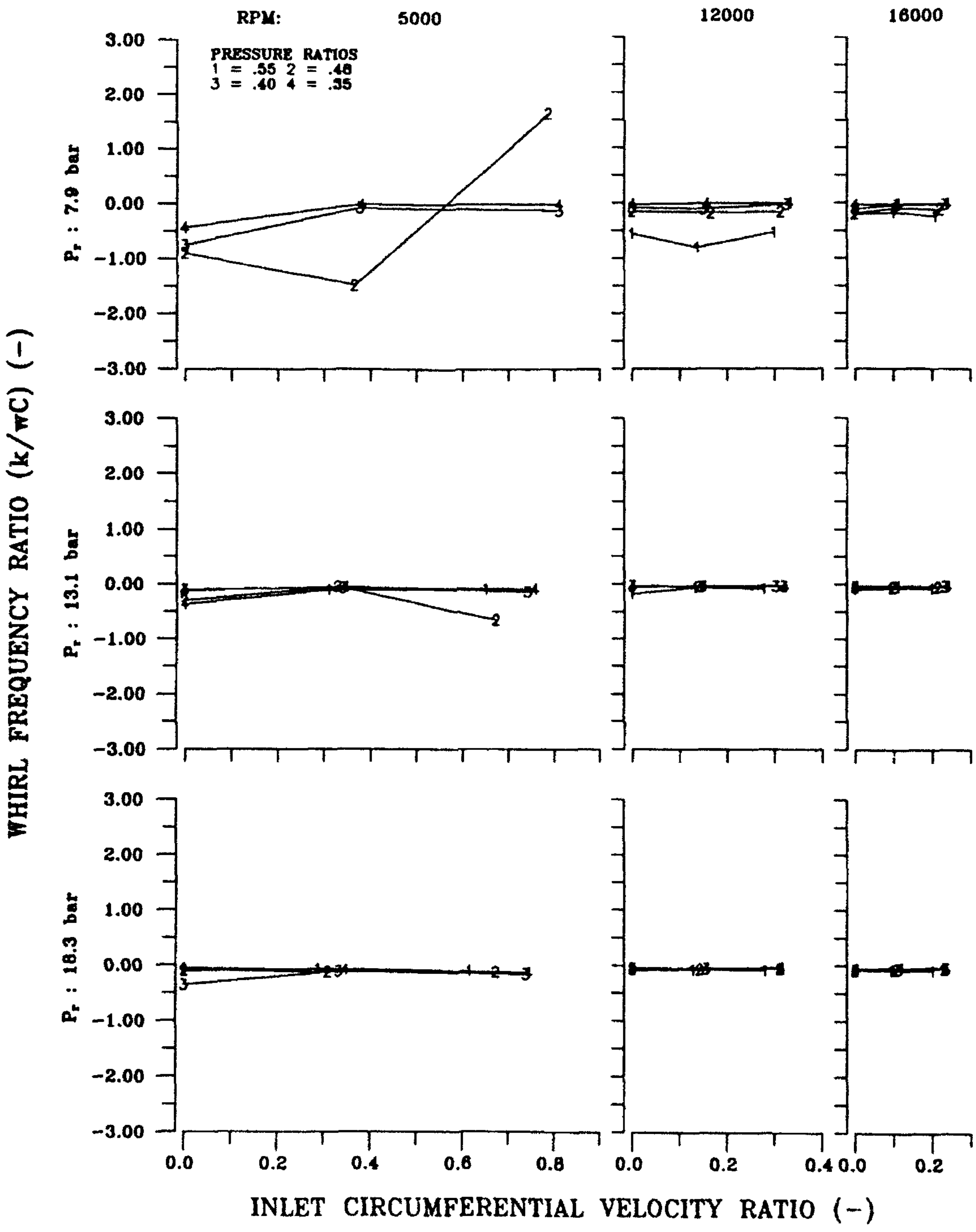

Figure 44 - Whirl frequency ratio versus inlet circumferential velocity ratio for seal 3.

Comparison to a Tooth-on-Rotor Labyrinth Seal

It is difficult to define a "comparable" seal to the brush seal due to the nature of the design of the brush stage; therefore, the shortest tooth-on-rotor seal for which rotordynamic test data are available was chosen. The labyrinth seal used for comparison has a rotor diameter of 151.36 mm and a clearance of 0.24 mm. Cavity width and tooth height are both 3.18 mm. This seal was tested on the same test apparatus by Pelletti (1990). Data for the rotordynamic coefficients labyrinth seals are compared to seal 1 using the common pressure ratio of 0.55 at an inlet pressure of 18.3 bar.

Figure 45 is a comparison of the flow rate for the 4-stage brush seal and the labyrinth seal described above. The leakage rate for the brush seal is an order of magnitude lower than the labyrinth seal, which is consistent with all reported leakage data for brush seals.

As shown in Figure 46, direct stiffness values for the labyrinth seal are generally negative; whereas, K for the brush seal is always positive. Figure 47 shows that the cross-coupled stiffness k of the labyrinth seal is always positive, therefore destabilizing. The magnitude of k for the labyrinth seal increases dramatically as the inlet swirl increases. Figure 47 also shows that k for the brush seal is low and generally negative, and does not depend on speed or inlet swirl.

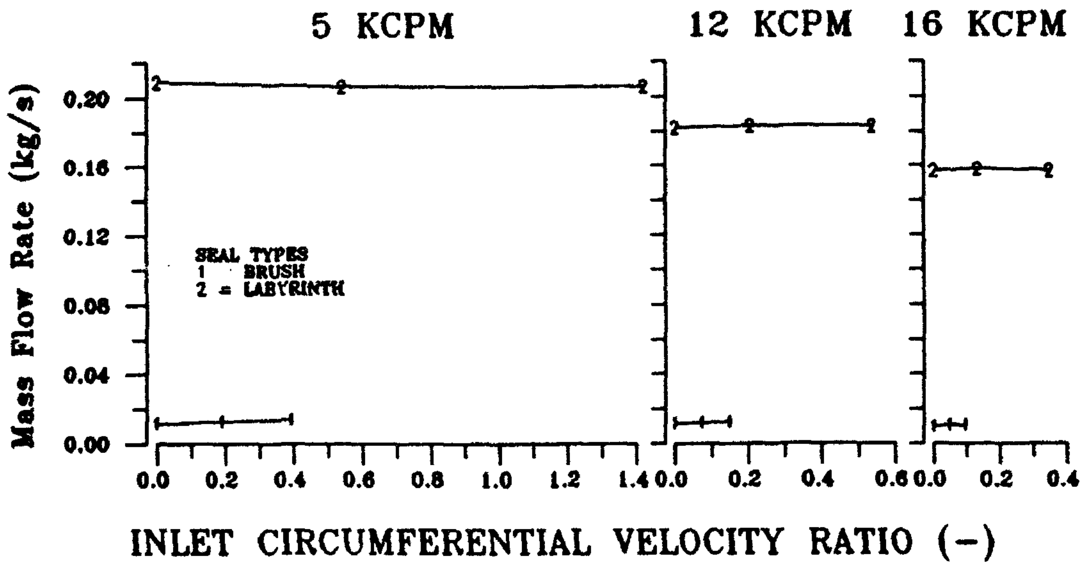

Figure 45 - Leakage rate comparison between a 4-stage brush seal and a 9-cavity tooth-on-rotor labyrinth seal.

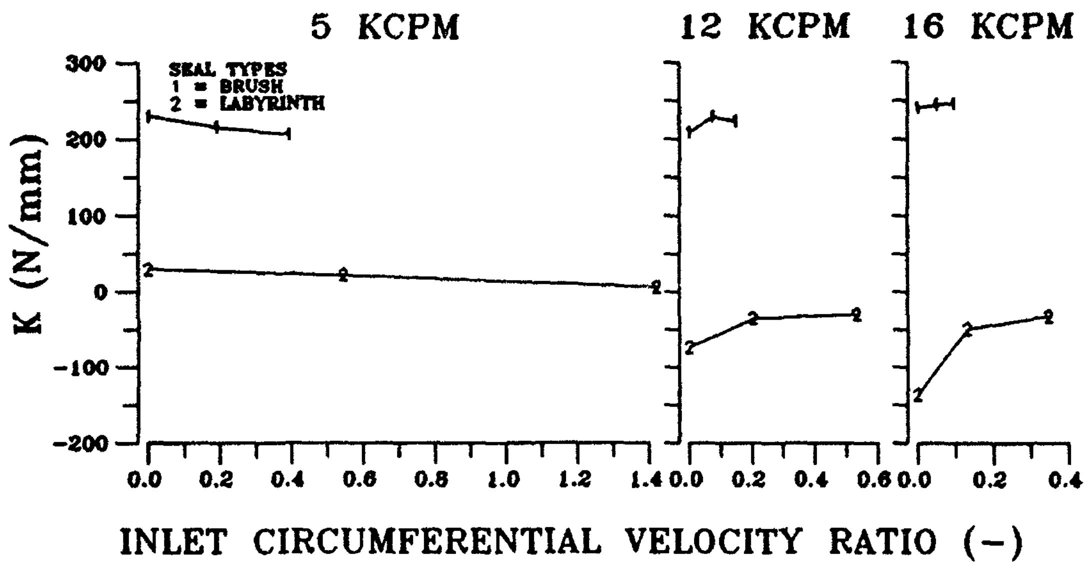

Figure 46 - Direct stiffness comparison between labyrinth and brush seals.

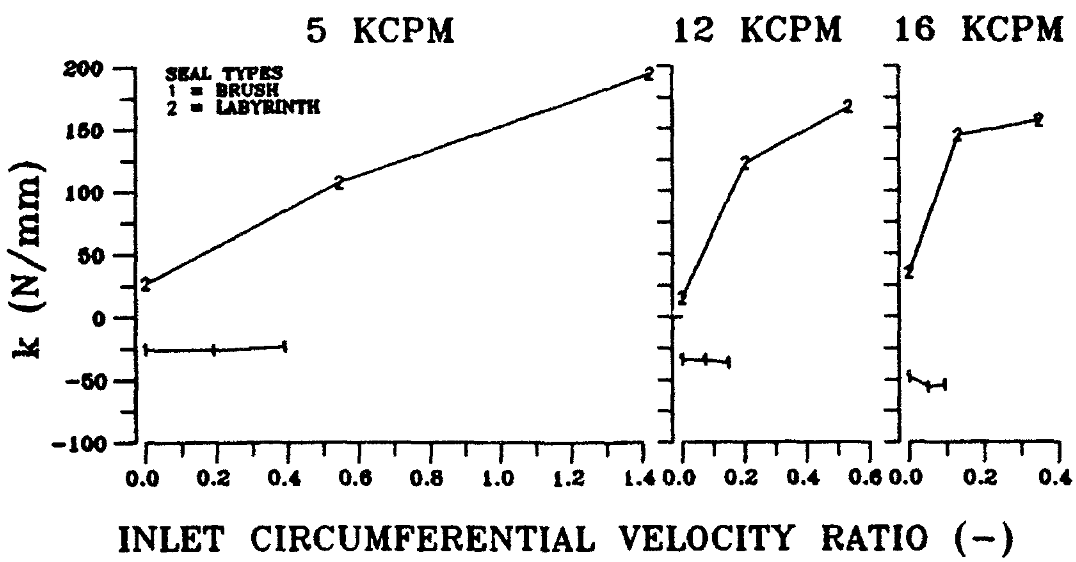

Figure 47 - Cross-coupled stiffness comparison for labyrinth and brush seals.

As shown in Figure 48, direct damping values for the labyrinth seal are higher than the brush seal. For the brush seal, C increases with an increase in rotor speed, whereas it is relatively constant for the labyrinth seal.

The whirl frequency ratio, $f = k/C\omega$, where ω is the running speed, is a useful measure of the stability of a seal. This ratio for brush seals is very small and usually negative, which indicates a stable seal, and does not depend on any of the parameters tested. Figure 49 shows that the whirl frequency ratio for the labyrinth seal becomes destablizing at high inlet tangential velocities. The ratio for a long labyrinth seal is approximately 0.5. This ratio for brush seals does not depend on any of the test parameters, indicating that the seal is very stable at all of the tested conditions.

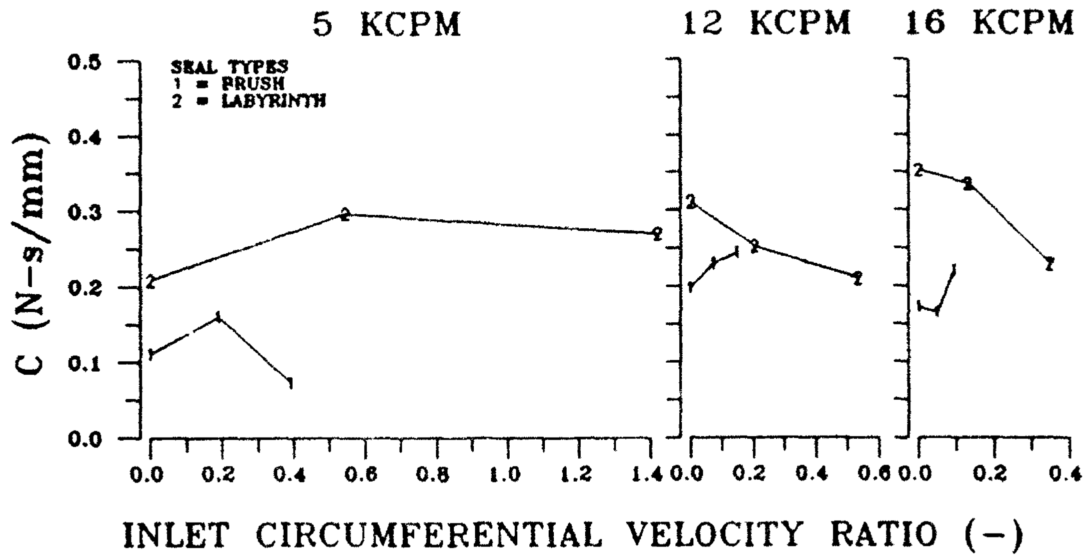

Figure 48 - Direct damping comparison for labyrinth and brush seals.

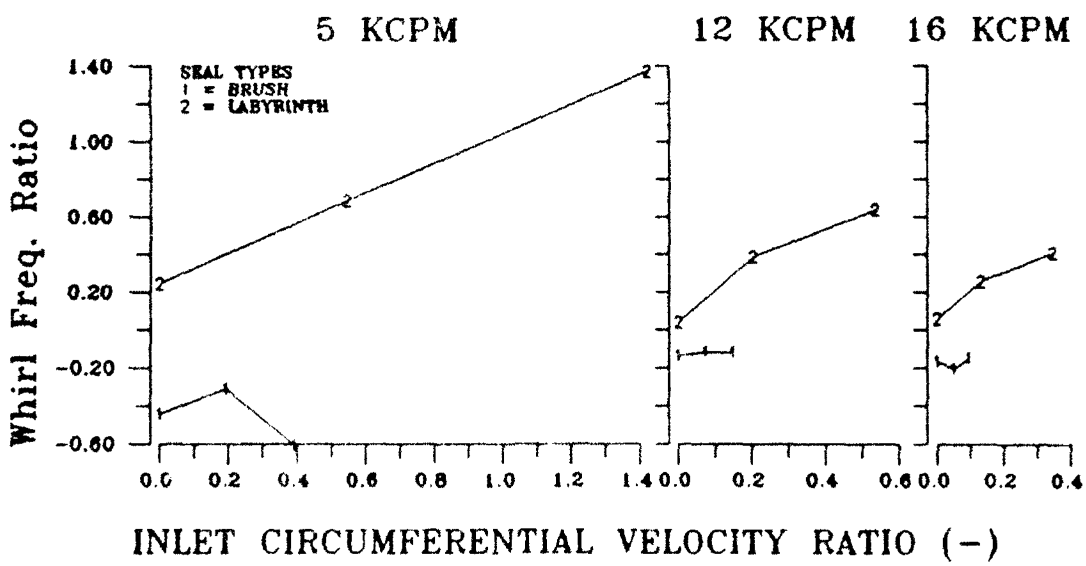

Figure 49 - Whirl frequency comparison for labyrinth and brush seals.

Torque Imposed on the Shaft Due to Friction

In order to get an accurate measurement for an uncertainty value, four time traces of the voltage output from each load cell were recorded at set conditions. The voltage output from each load cell corresponds to a force imposed on the load cell. This force in turn can be converted to torque. An uncertainty value in this voltage would ultimately lead to a torque uncertainty.

The four graphs shown in figure 50 correspond to inlet pressure of 7.9 bar, pressure ratio of 0.14, and rotor speed of 12,000 cpm. Other test conditions were tested; however, they generated the same type of results. Generally, the voltage has a resolution of 0.2 volts, which corresponds to a static torque of 74 in-lbs. Intuitively, this uncertainty is well above any reasonable expected torque imposed by the bristles. Therefore, measurement of the torque was not possible.

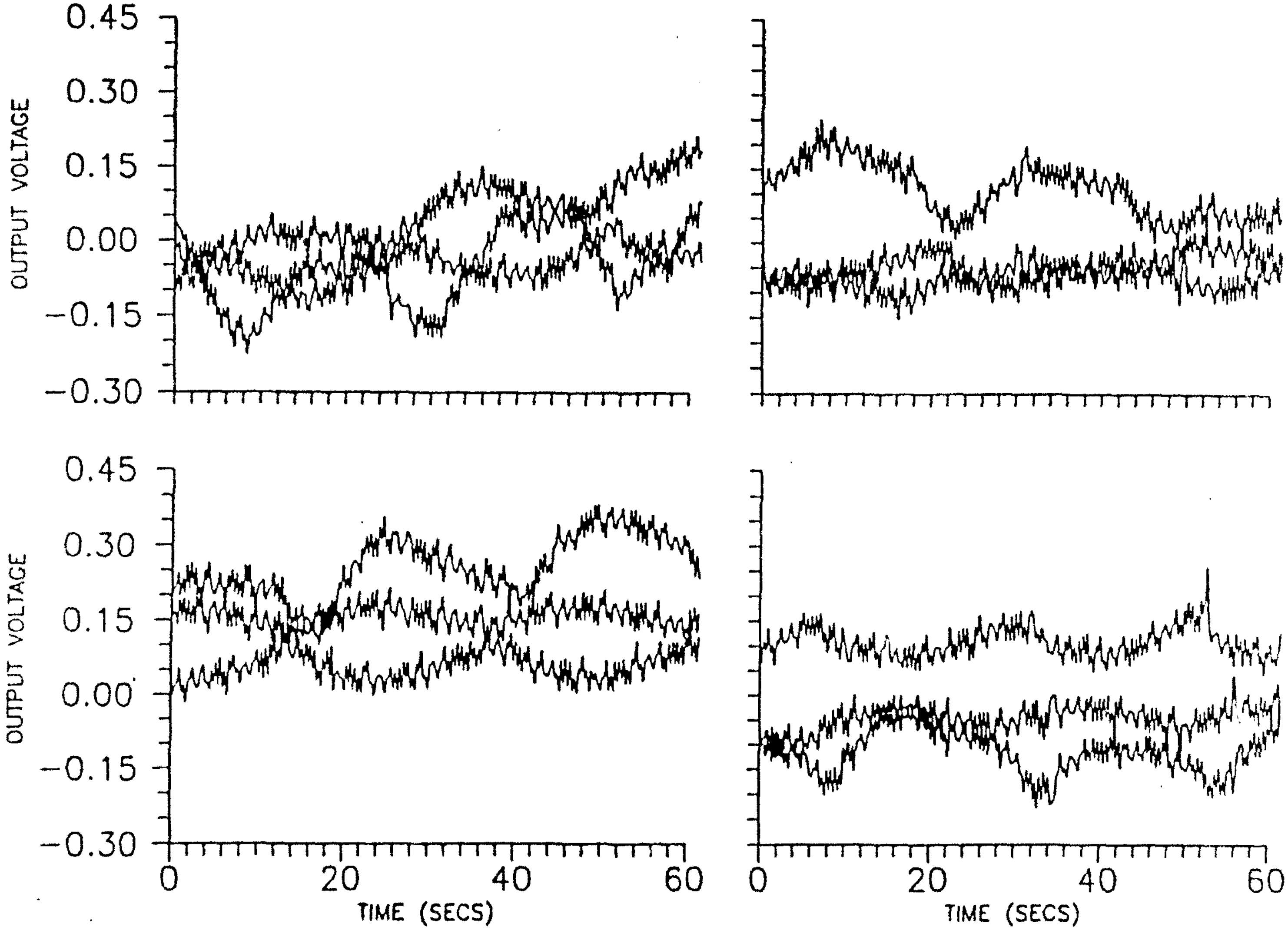

Figure 50 - Time traces of the load cell output in volts.

CHAPTER IV

CONCLUSIONS

Repeatable data for the rotordynamic coefficients and leakage characteristics of a 4-stage brush seal were obtained. This work was primarily undertaken to determine the rotordynamic coefficients of the brush seal. The experimental test results support the following conclusions:

(A) The last stage of the seal group generally develops a slightly higher pressure drop than the previous stages. The delta P levels across the stages become approximately equal as the rotor speed and inlet pressure are increased.

(B) At high shaft speeds and high inlet pressures, a fluid film seems to develop between the bristles and the surface of the rotor. This conclusion is supported by the "leveling out" of all of the rotordynamic coefficients with increasing running speed and delta P and the very sporadic behavior of the coefficients at the lowest rotor speed and lowest inlet pressure.

(C) The leakage flow rate increased with the order of testing; i.e., seal 3 leaked more than seal 1, which leaked more than seal 2. This suggests that even with a line-to-line fit, i.e., no interference between the bristles and rotor, wear does have an effect on the mass flow rate.

(D) Increasing the inlet tangential velocity causes a slight increase in leakage. This trend is most prevalent on the second and last seal tested, suggesting that this behavior occurs due to worn-in conditions.

(E) As the rotor speed and inlet pressure increase, leakage becomes more dependent on the pressure ratio, again suggesting the formation of the fluid shear layer.

(F) The rotordynamic coefficients, K, k, C, and c, do not depend on seal spacing or inlet tangential velocity.

(G) The direct stiffness coefficient is frequency dependent and always positive. The mean value of K is positive, yet not large in magnitude, for all conditions tested. K increased slightly with an increase in pressure ratio, and did not depend on the other test parameters.

(H) The cross-coupled stiffness coefficient is very low and generally negative, therefore stabilizing. k is generally independent of all test parameters, particularly the inlet pre-swirl.

(I) The direct damping coefficient increases with an increase in the rotor speed and inlet pressure. The intercept of the $Im(\hat{F}_X/\hat{X})$ versus frequency at $\omega = 0$ is not zero. This could be attributed to coulomb friction caused by the bristles on the shaft.

(J) The whirl frequency ratio indicates that the brush seal is extremely stable. This ratio did not vary with any of the test parameters.

The reader should bear in mind that rotordynamic coefficient results are compared for an 8-cavity labyrinth seal and a 4-stage brush seal. A 4-stage brush seal was tested in order to create large enough forces to measure. The 8-cavity labyrinth was the shortest seal for which rotordynamic coefficient data were available. Data for those seals indicate that replacement of a standard labyrinth seal with a multi-stage brush seal will generally improve the rotordynamic characteristics if the labyrinth seal is destabilizing,the rotor due to fluid preswirl. This conclusion follows from the low or negative cross-coupled stiffness value for brush seals, independent of fluid preswirl. However, given that brush seals have lower damping values than labyrinth seals direct replacement might, in some cases, cause a slight degradation of rotor response. a careful rotordynamics analysis to consider the influence of replacing a labyrinth seal by a brush seal is advised.

REFERENCES

Bolleter, U., Wyss, A., Welte, I. and Sturchler, R., "Measurement of Hydrodynamic Interaction Matrices of Boiler Feed Pump Impellers", ASME Journal of Vibrations, Stress and Reliability in Design, Vol.109, 1987, pp. 144-151.

Braun, M.J., Hendricks, R.C., and Canacci, V., "Flow Visualization in a Simulated Brush Seal", ASME Paper No. 90-GT-217, ASME Gas Turbine Conference, Brussels, Belgium, June 1990.

Childs, D.W., Baskharone, E., and Ramsey, C., "Test Results for Rotordynamic Coefficients of the SSME HPOTP Turbine Interstage Seal with Two Swirl Brakes", Accepted for presentation at the ASME-ASLE Tribology Conference, 7-10 October 1990.

Childs, D.W., and Ramsey, C., "seal Rotordynamic Coefficient Test Results for a Model SSME ATD-HPFTP Turbine Interstage Seal With and Without a Swirl Brake", Accepted for presentation at the ASME ASLE Tribology Conference, 7-10 October 1990.

Childs, D. W., and Scharrer, J.K., "Experimental Rotordynamic Coefficient Results for Teeth-on-Rotor and Teeth-on-Stator Gas Seals", ASME Transactions, Journal of engineering for Gas Turbine and Power, Vol. 108, October 1986.

Chupp, R.E., and Nelson, P., "Evaluation of Brush Seals for Limited-life Engines", AIAA Paper No. 90-2140, AIAA Conference, Orlando, Florida, July 1990.

Coleman, H.W., and Steele, G.W., Experimentation and Uncertainty Analysis for Engineers, Wiley-Interscience Publication, 1989, pp. 173-174.

Ewins, D.J., Modal Testing: Theory and Practice, Research Studies Press Ltd., Letchworth, Hertfordshire, England, 1986.

Ferguson, J.G., "Brushes as High Performance Gas Turbine Seals", ASME Paper No. 88-GT-182, ASME Gas Turbine Conference, Amsterdam, The Netherlands June 1988.

Flower, R., "Brush Seal Development System", AIAA Paper No. 90-2143, AIAA Conference, Orlando, Florida, July 1990.

Holle, G.F., and Krishnan, M.R., "Gas Turbine Engine Brush Seal Applications", AIAA Paper No. 90-2142, AIAA Conference, Orlando, Florida, July 1990.

Holman, J.P., Experimental Methods of Engineers, McGraw-Hill, 1978, p. 45.

Pelletti, J.M., "A Comparison of Experimental Results and Theoretical Predictions for the Rotordynamic Coefficients of Short (L/D = 1/6) Labyrinth Seals", Master's Thesis, Texas A&M University, College Station, Texas, 1990.

Scharrer, J.K., "A Comparison of Experimental and Theoretical Results for Labyrinth Gas Seals", Doctoral Dissertation, Texas A&M University, College Station, Texas, 1987.

Schenck, H., Theories of Engineering Experimentation, 3rd Ed., McGraw-Hill, New York, 1979.

White, R.G., and Pennington, R.J., "Practical Application of the Rapid Frequency Sweep Technique for Structural Frequency Response Measurement", Aeronautical Journal, Paper No. 961, May 1982, pp. 179-200.

APPENDIX A

IMPEDANCE FUNCTION PLOTS

The following 36 figures are the impedance plots which graphically show the data from which the rotordynamic coefficients are determined.

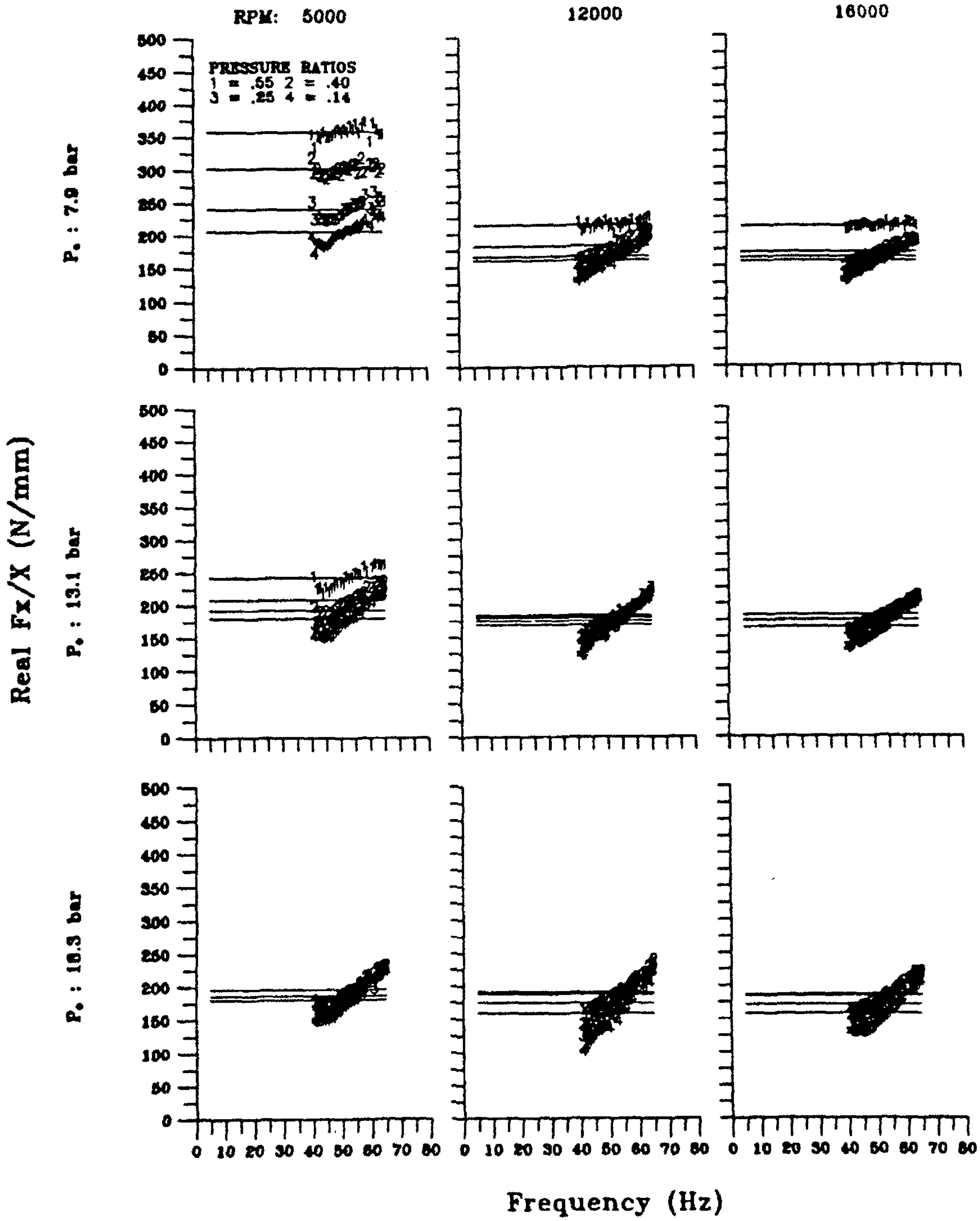

Figure 51 - Direct stiffness impedance graph for seal 1 with no fluid pre-rotation.

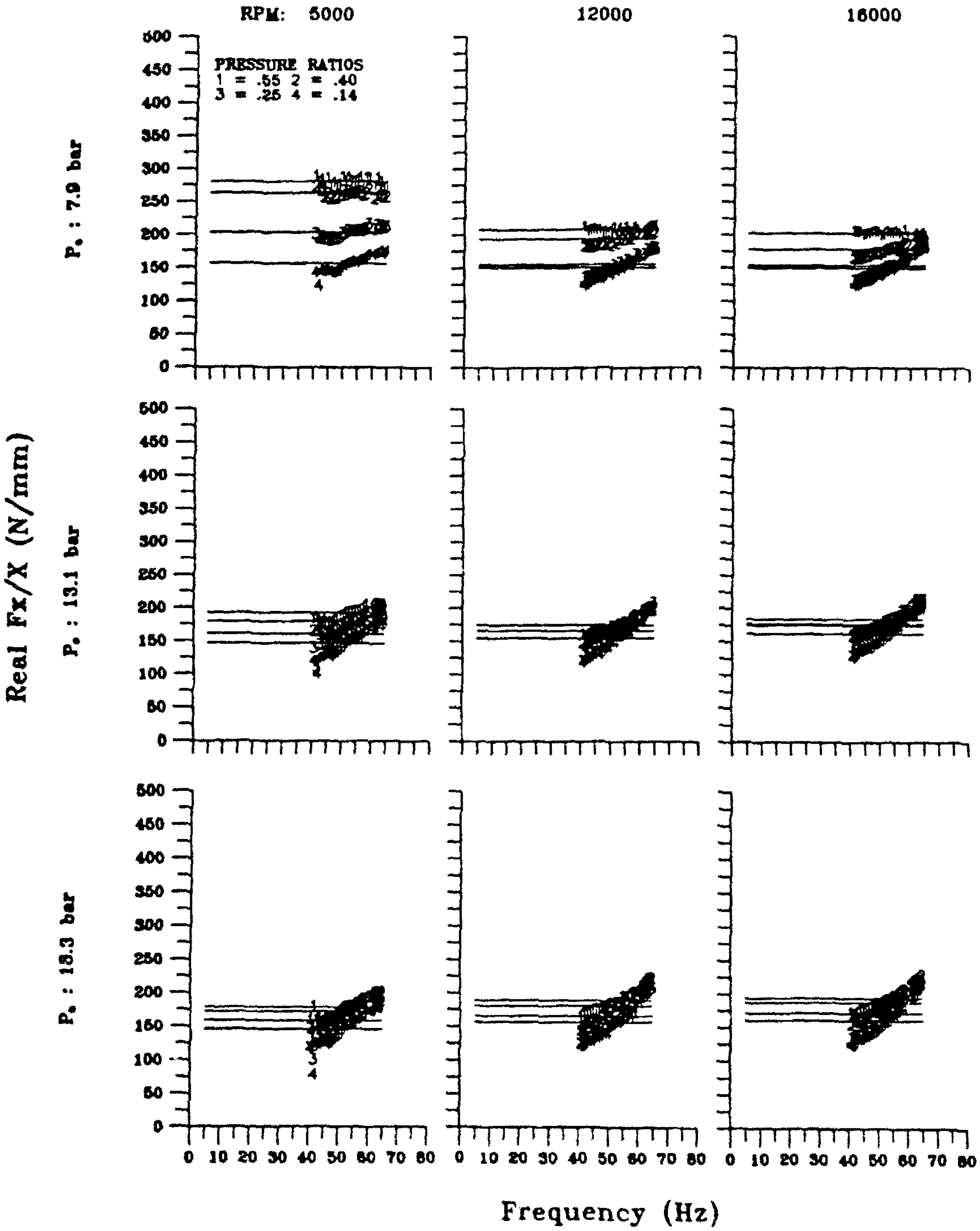

Figure 52 - Direct stiffness impedance graph for seal 1 with intermediate fluid pre-rotation.

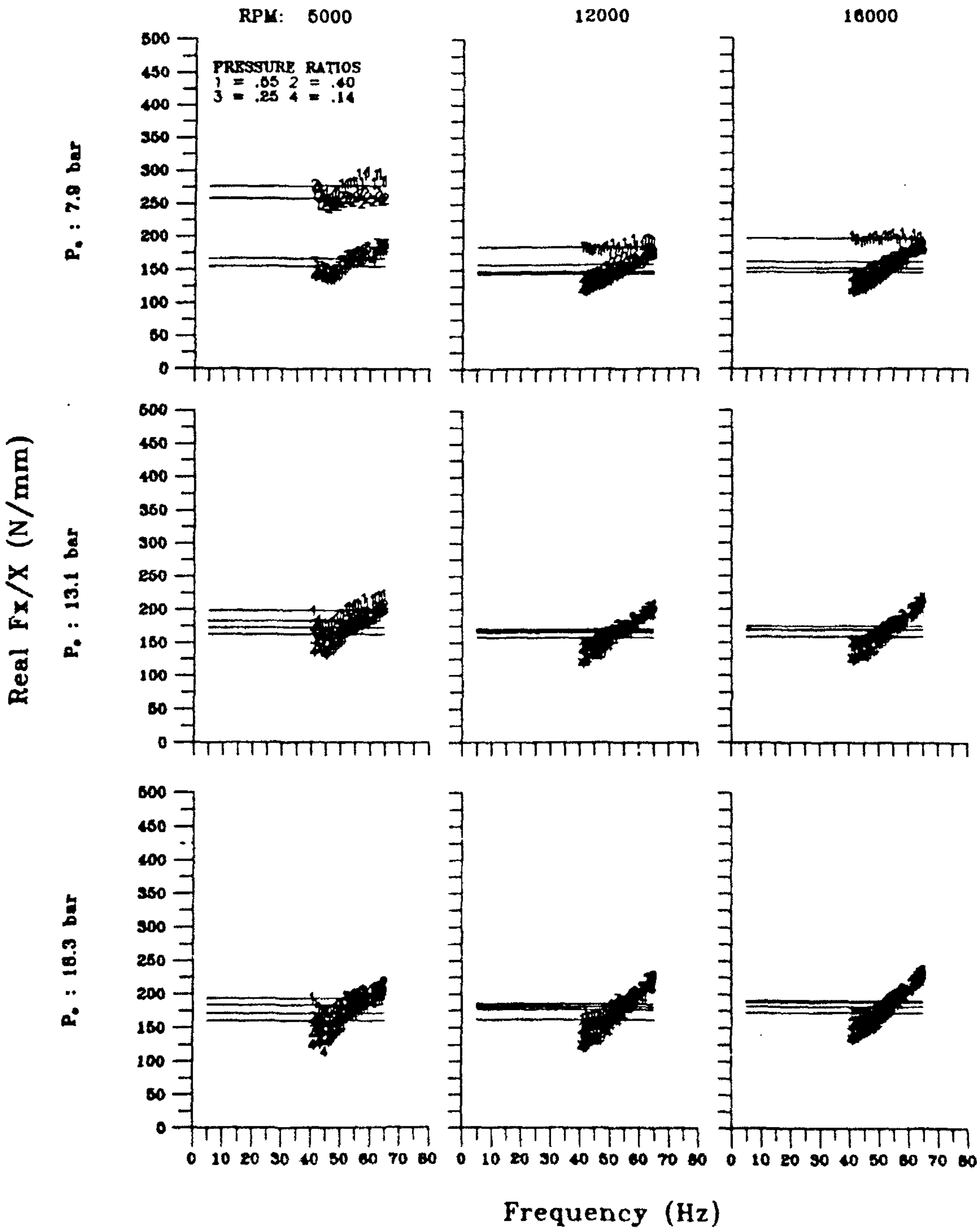

Figure 53 - Direct stiffness impedance graph for seal 1 with high fluid pre-rotation.

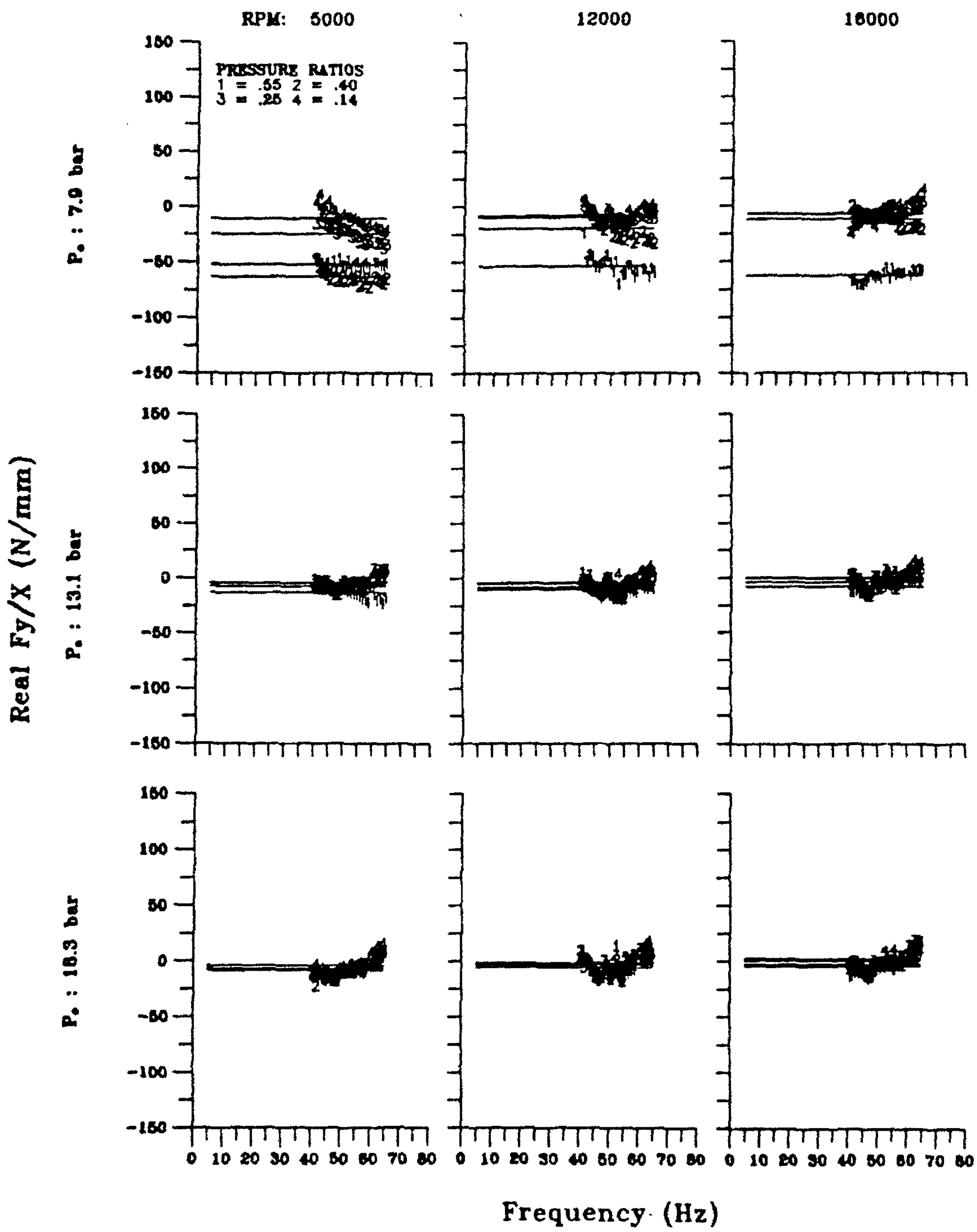

Figure 54 - Cross-coupled stiffness impedance graph for seal 1 with no fluid pre-rotation.

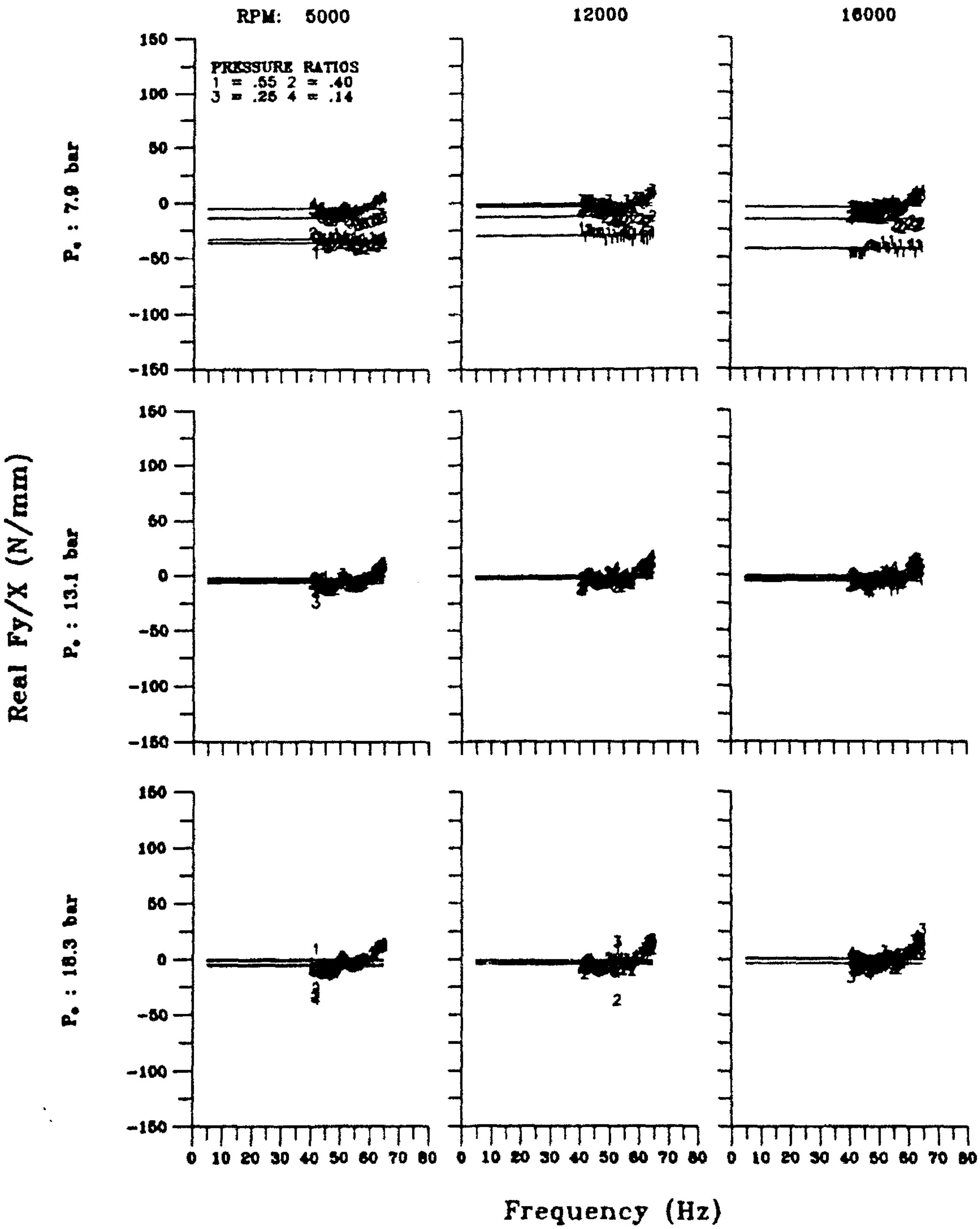

Figure 55 - Cross-coupled stiffness impedance graph for seal 1 with intermediate fluid pre-rotation.

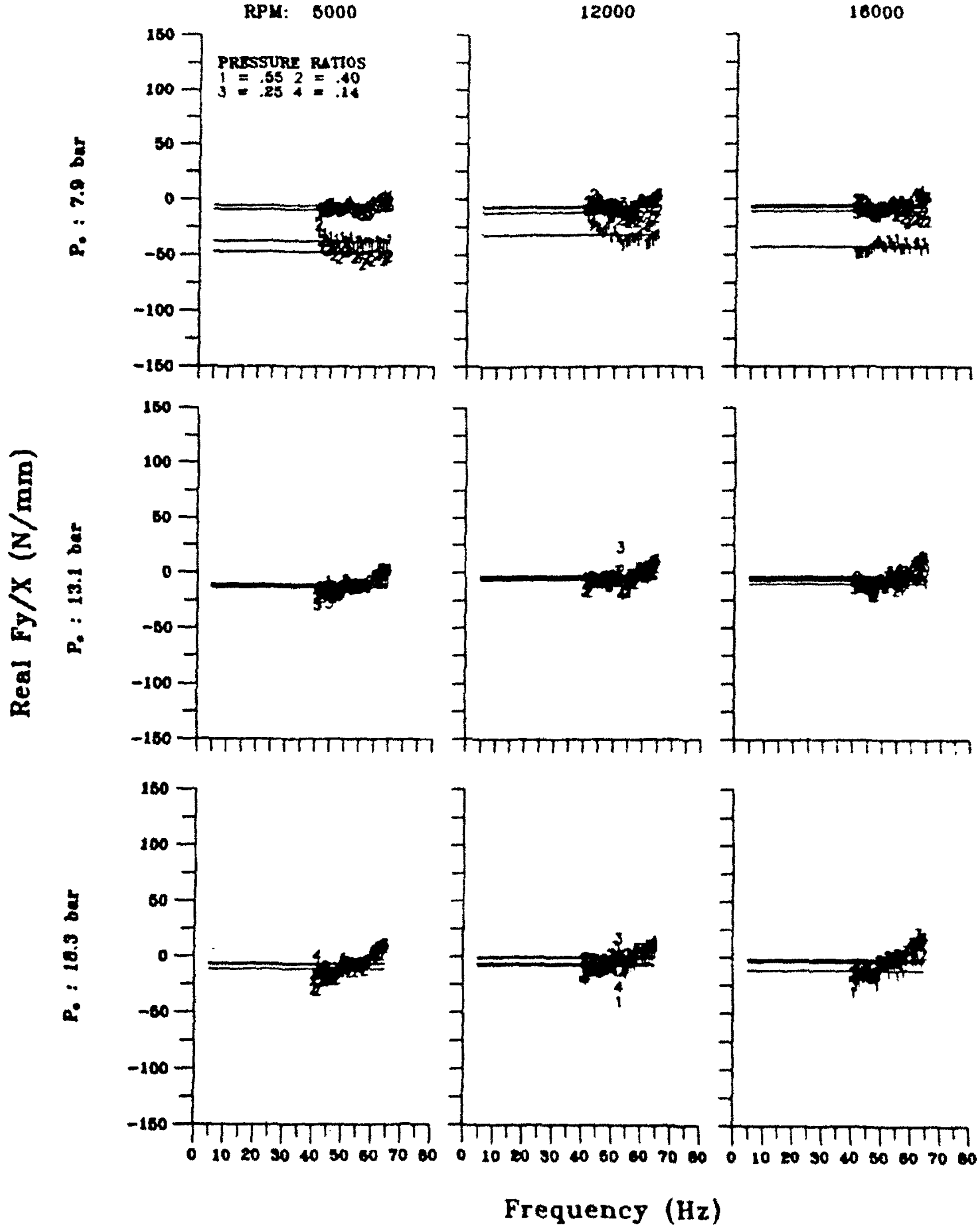

Figure 56 - Cross-coupled stiffness impedance graph for seal 1 with high fluid pre-rotation.

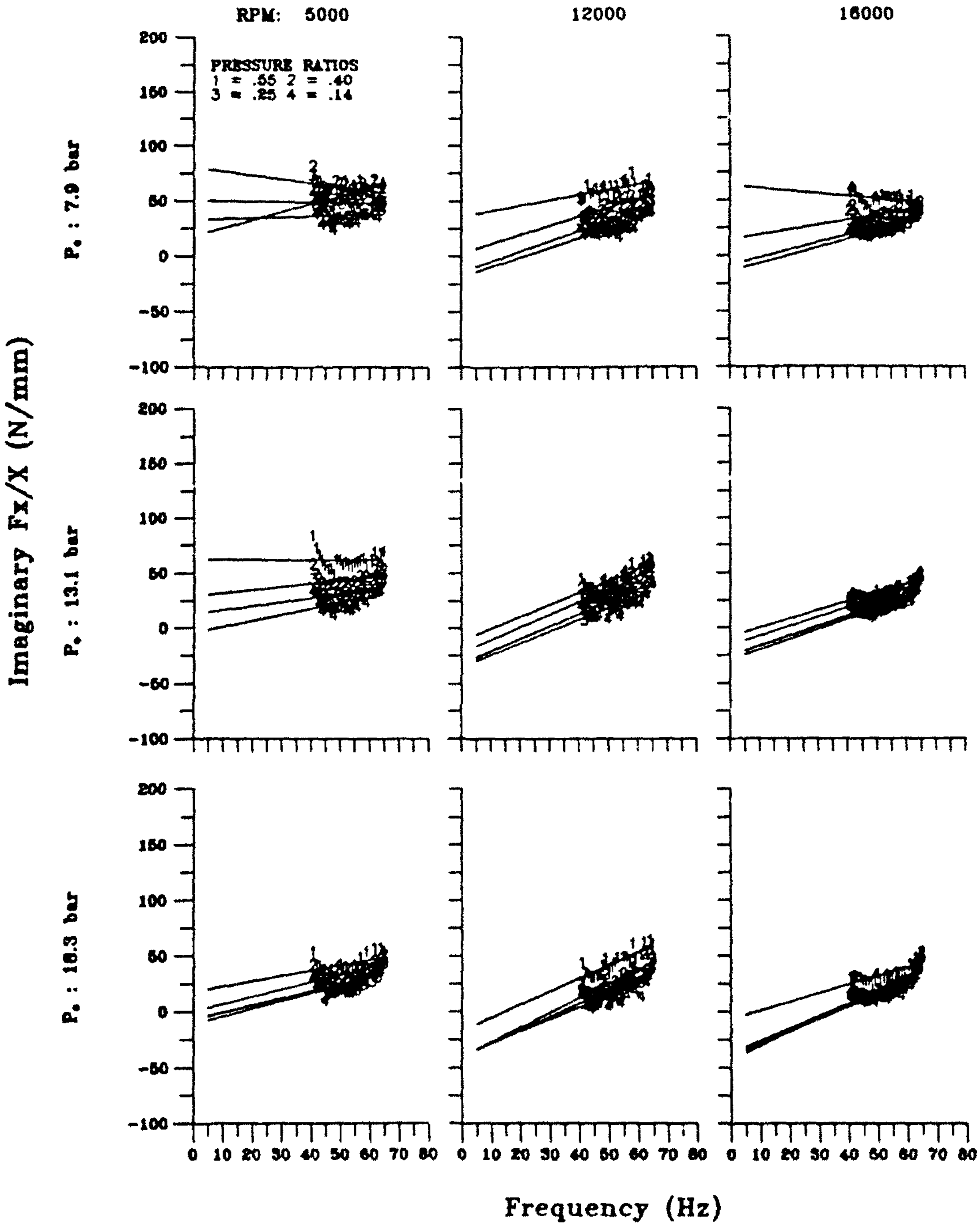

Figure 57 - Direct damping impedance graph for seal 1 with no fluid pre-rotation.

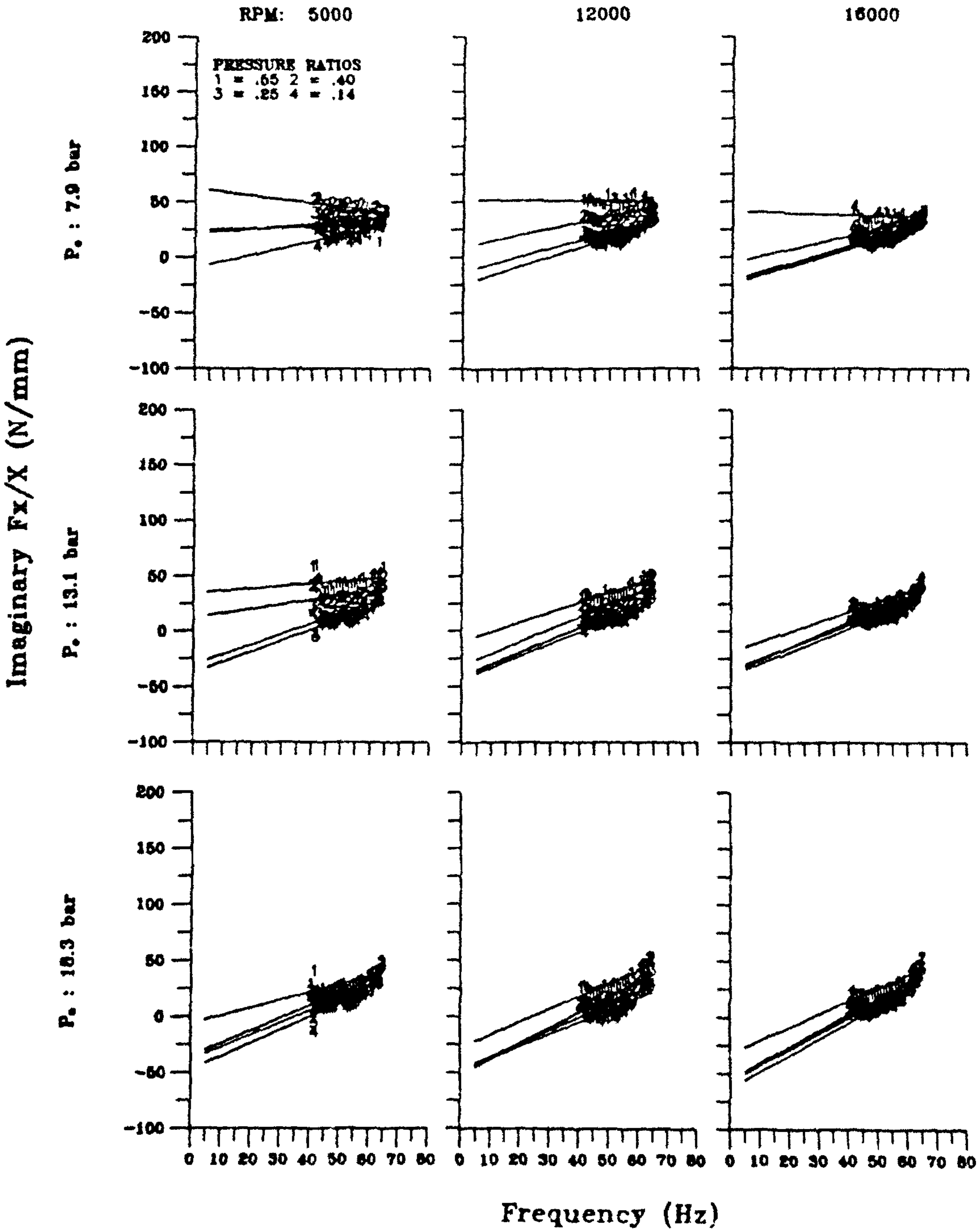

Figure 58 - Direct damping impedance graph for seal 1 with intermediate fluid pre-rotation.

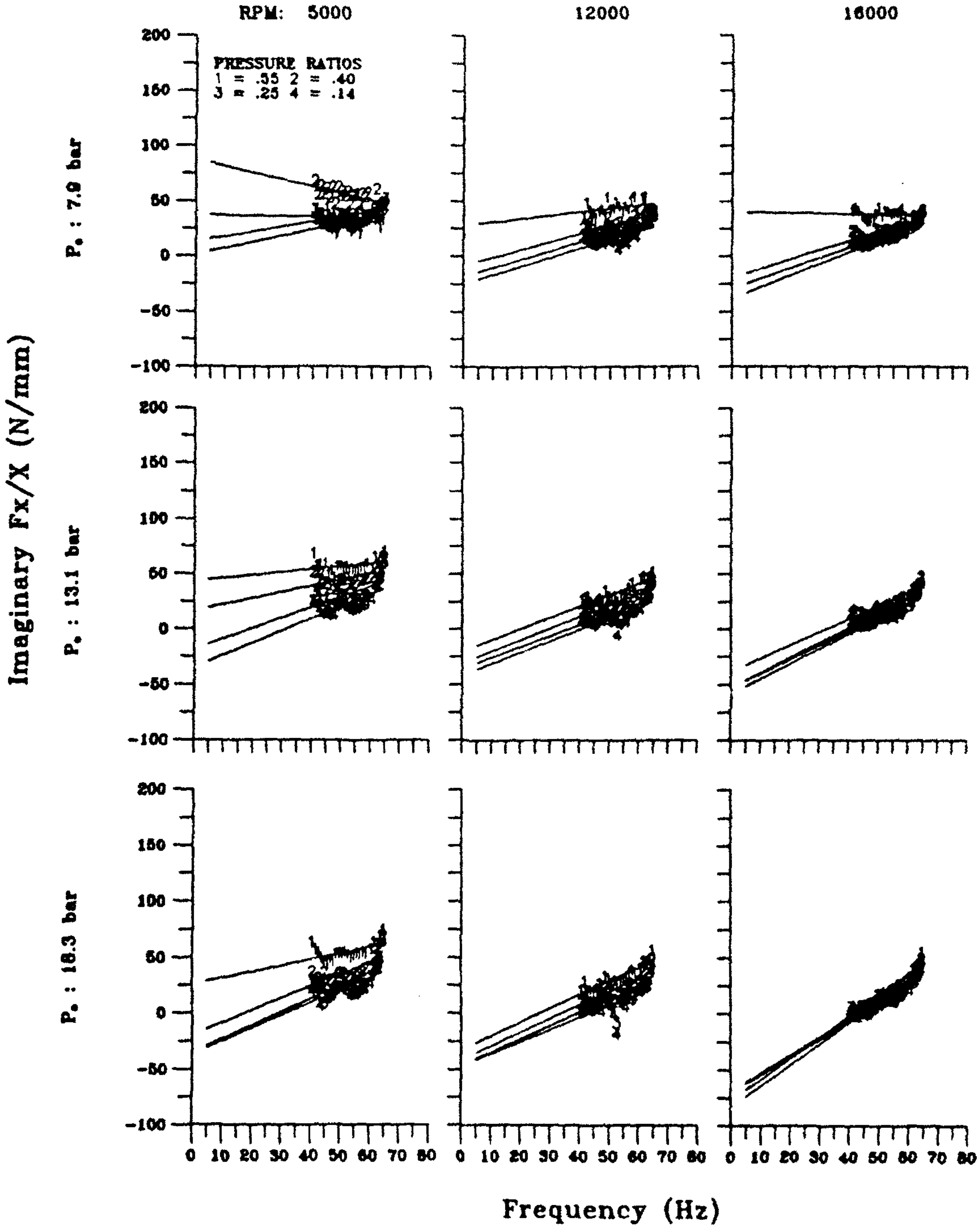

Figure 59 - Direct damping impedance graph for seal 1 with high fluid pre-rotation.

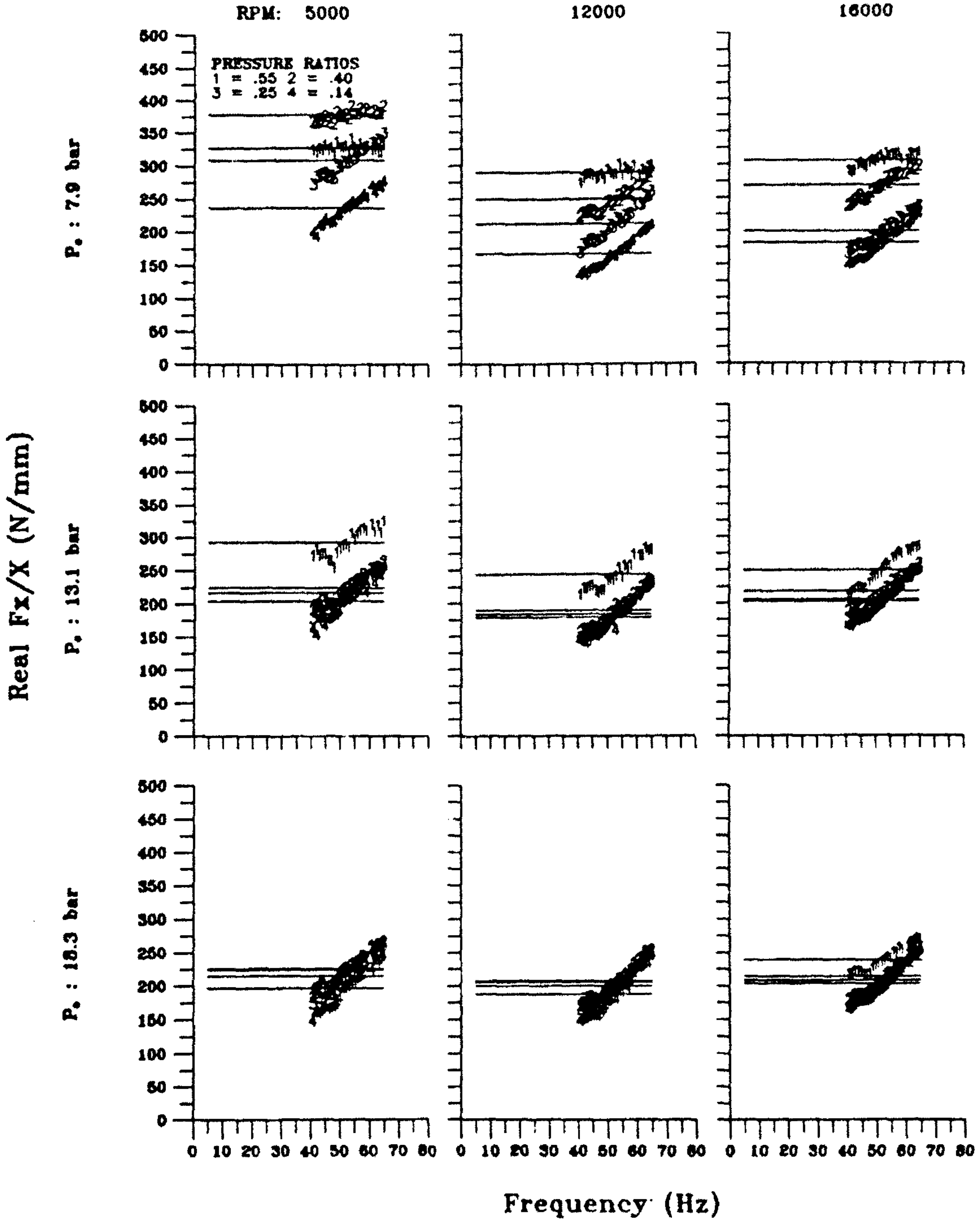

Figure 60 - Direct stiffness impedance graph for seal 2 with no fluid pre-rotation.

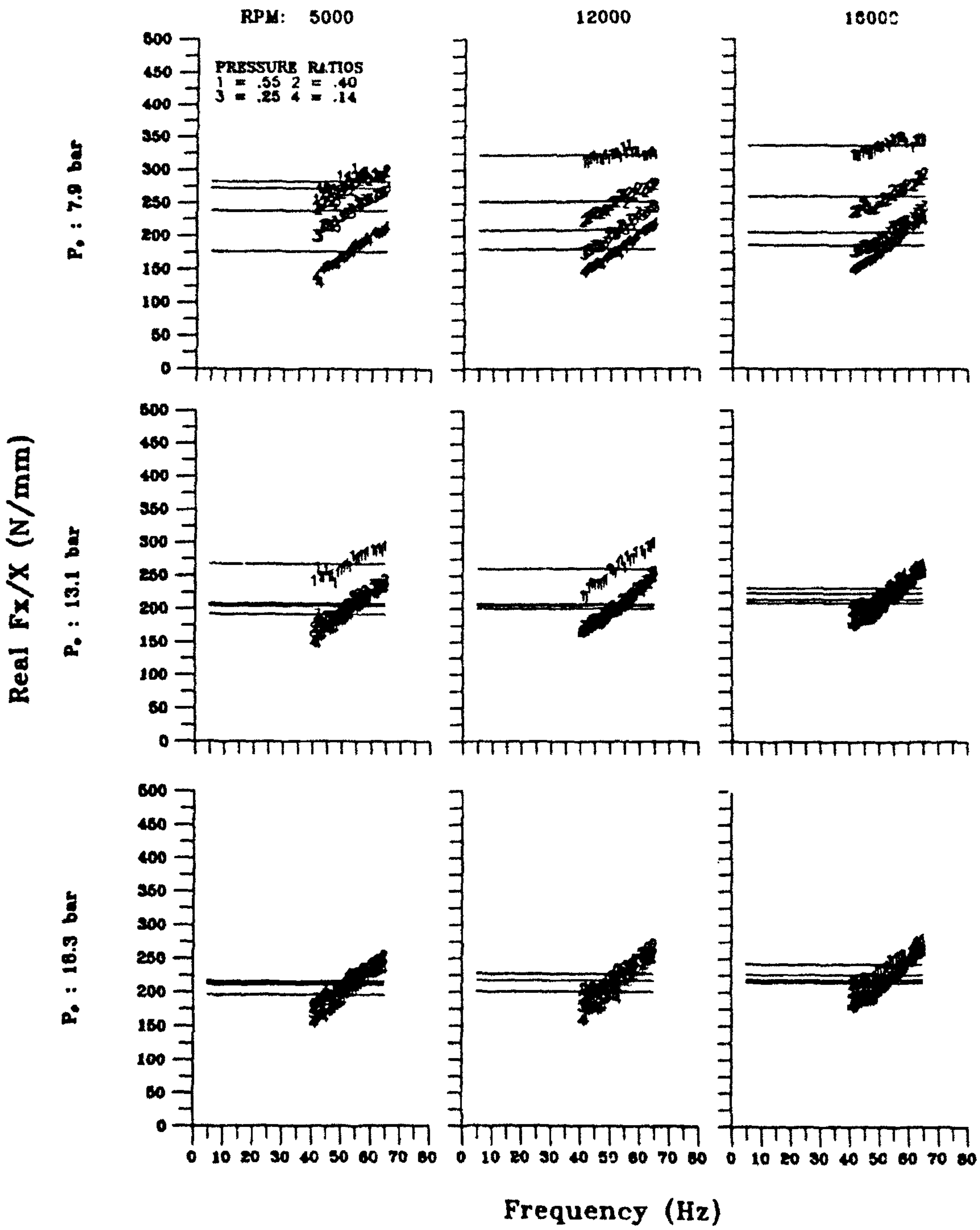

Figure 61 - Direct stiffness impedance graph for seal 2 with intermediate fluid pre-rotation.

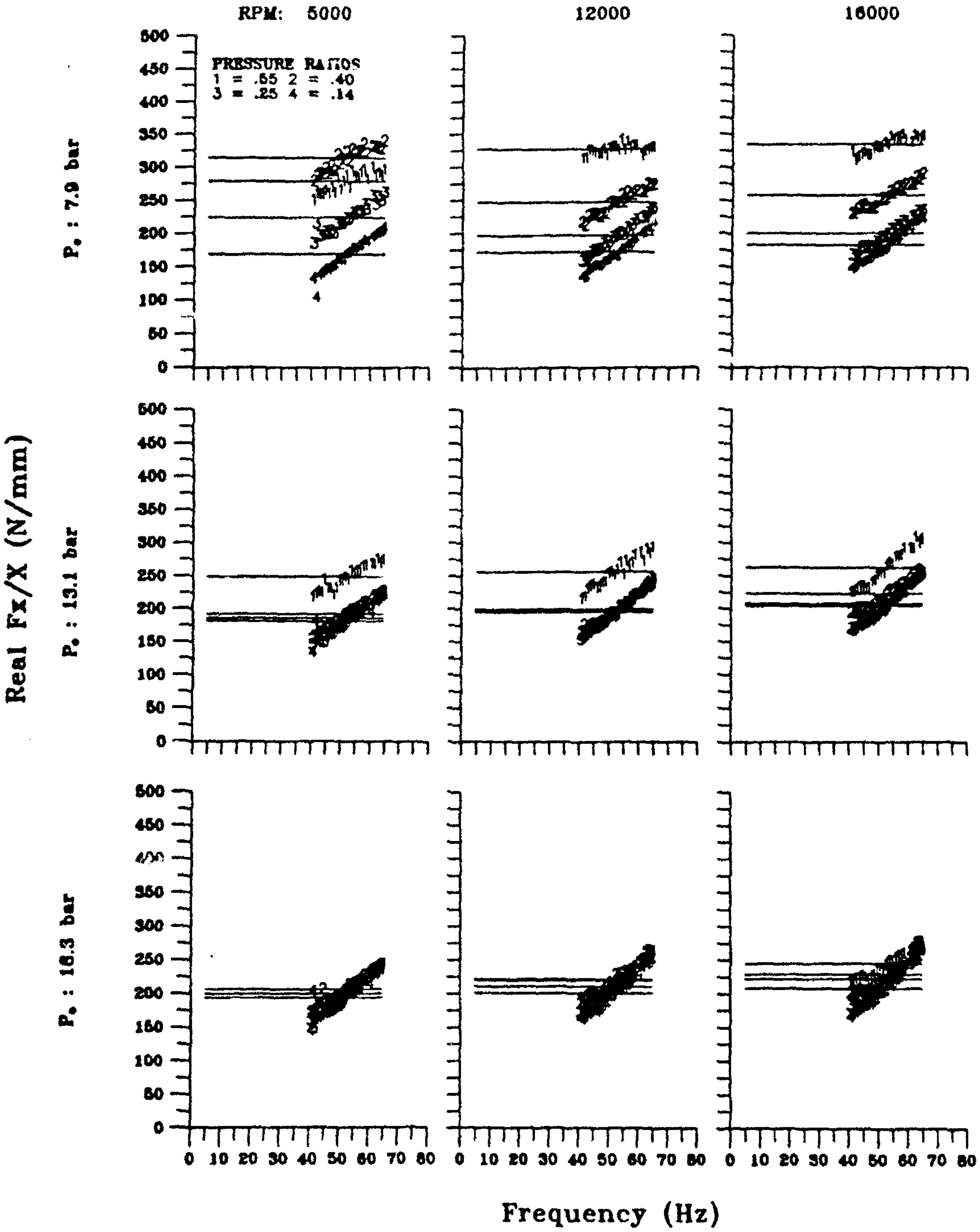

Figure 62 - Direct stiffness impedance graph for seal 2 with high fluid pre-rotation.

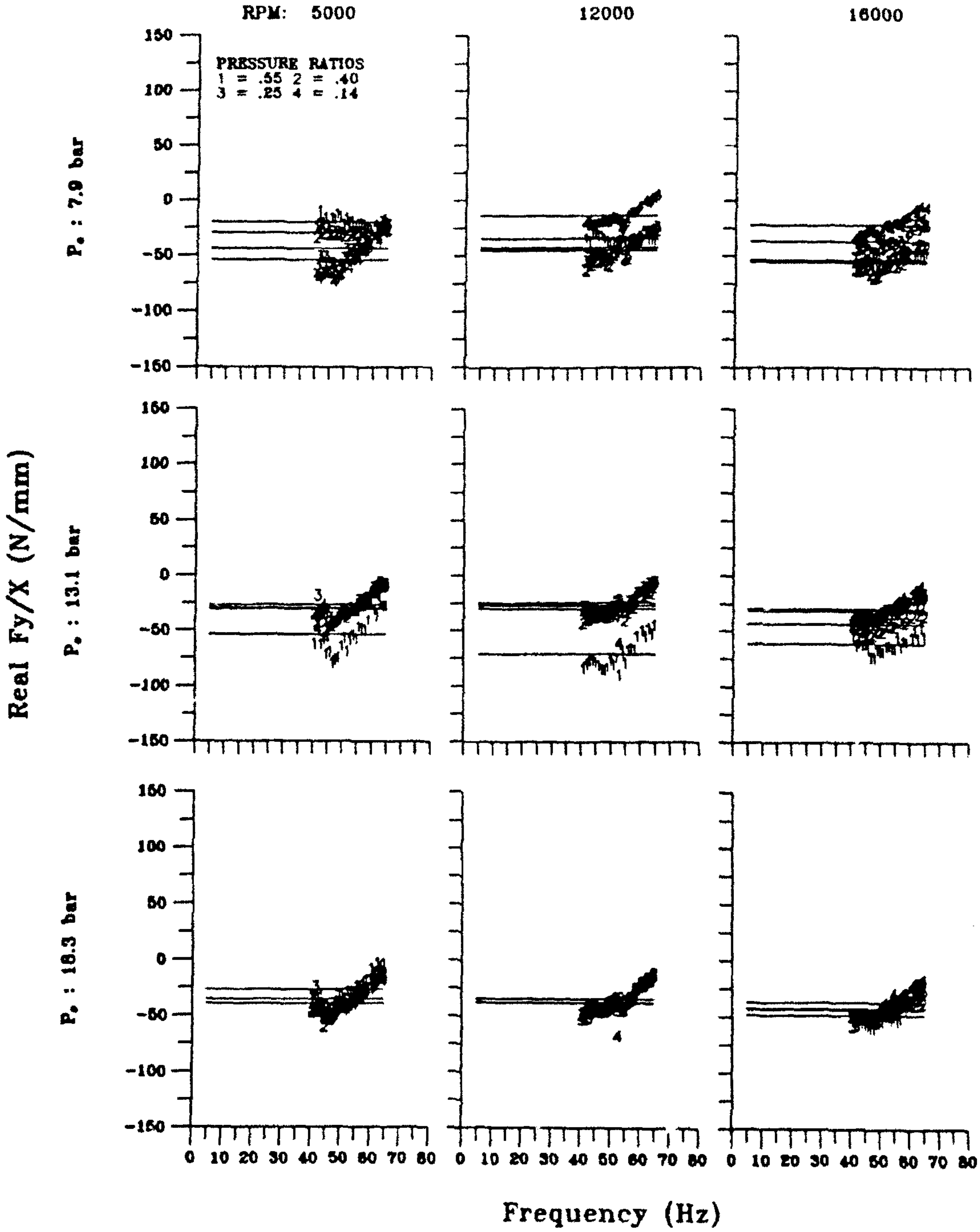

Figure 63 - Cross-coupled stiffness impedance graph for seal 2 with no fluid pre-rotation.

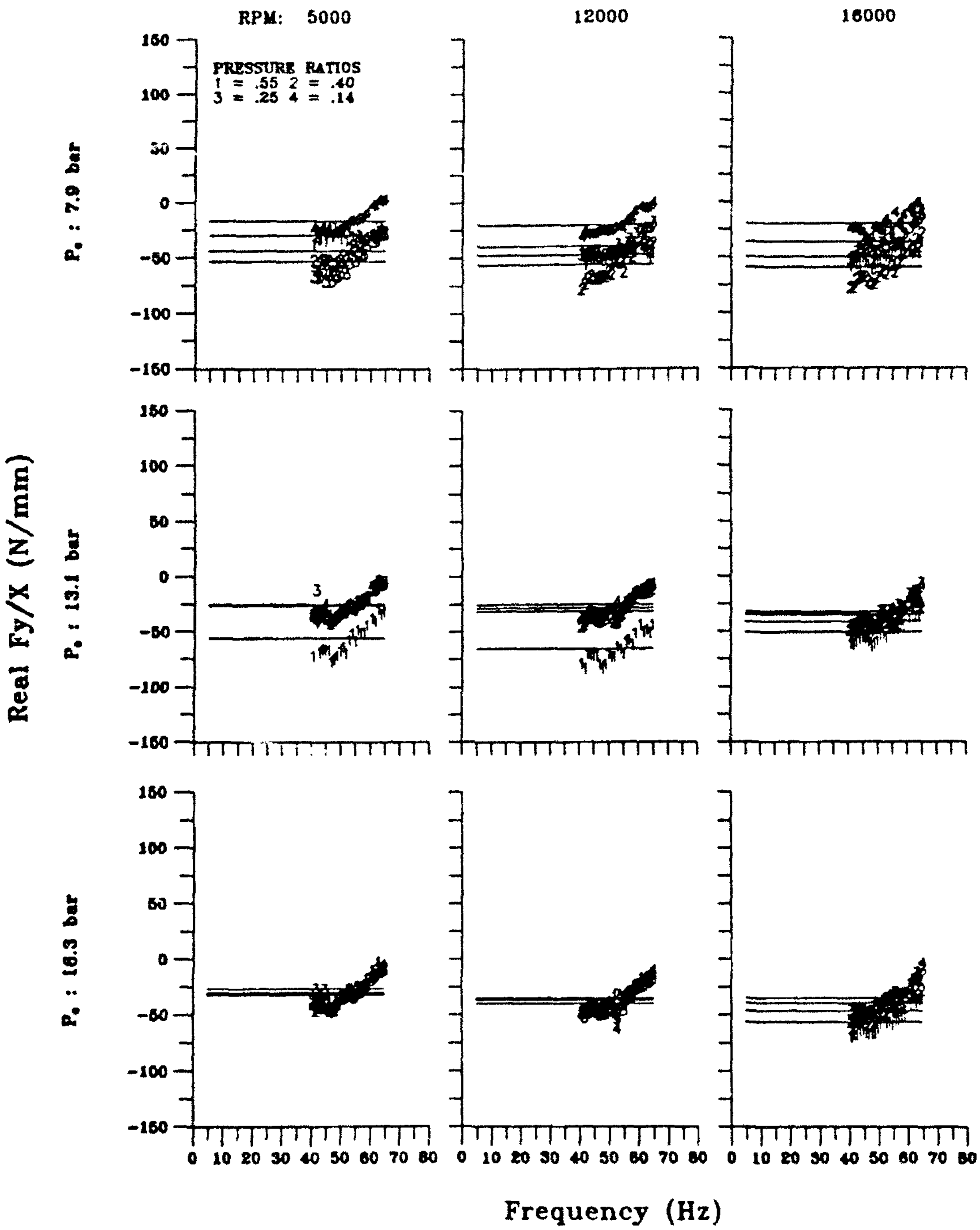

Figure 64 - Cross-coupled stiffness impedance graph for seal 2 with intermediate fluid pre-rotation.

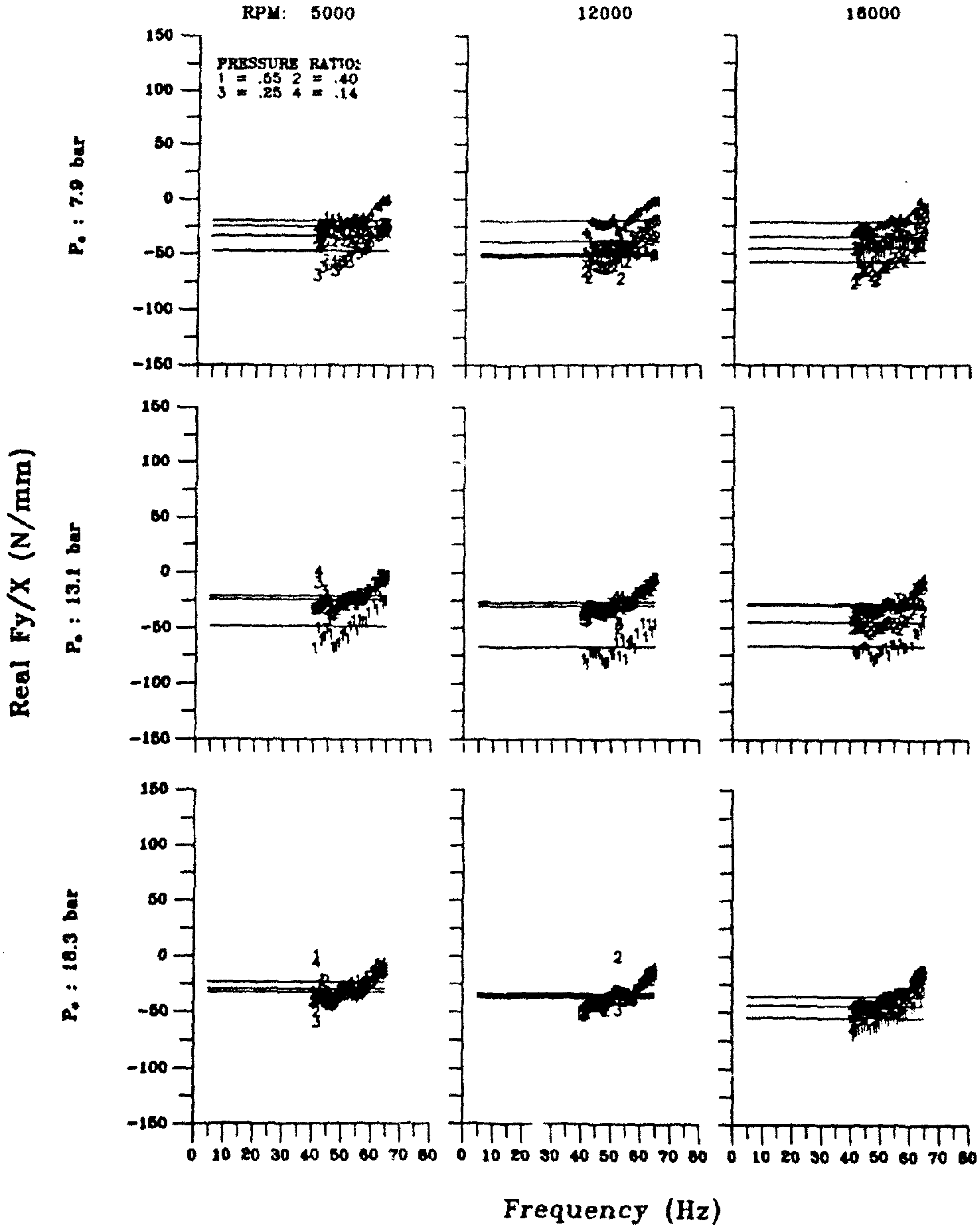

Figure 65 - Cross-coupled stiffness impedance graph for seal 2 with high fluid pre-rotation.

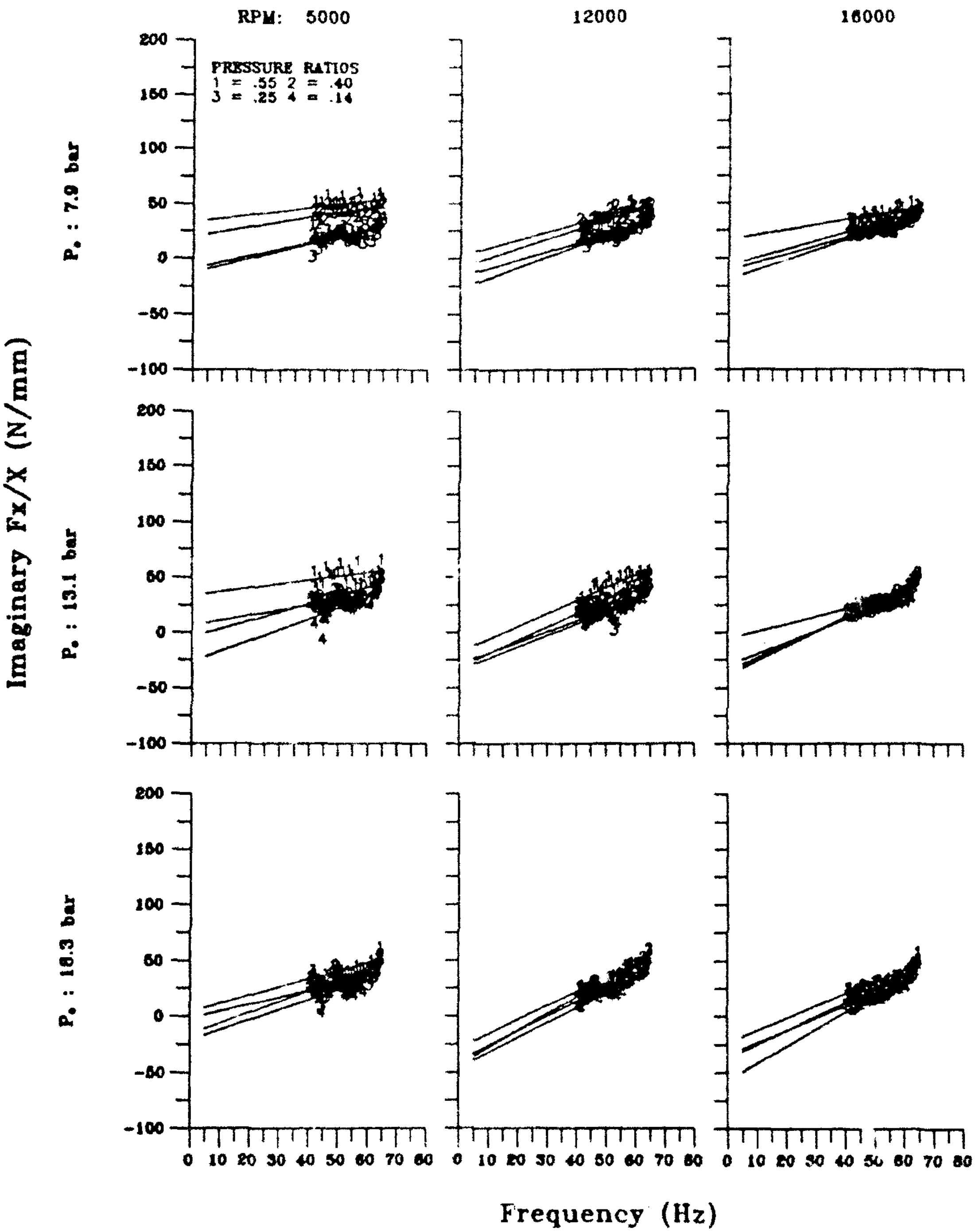

Figure 66 - Direct damping impedance graph for seal 2 with no fluid pre-rotation.

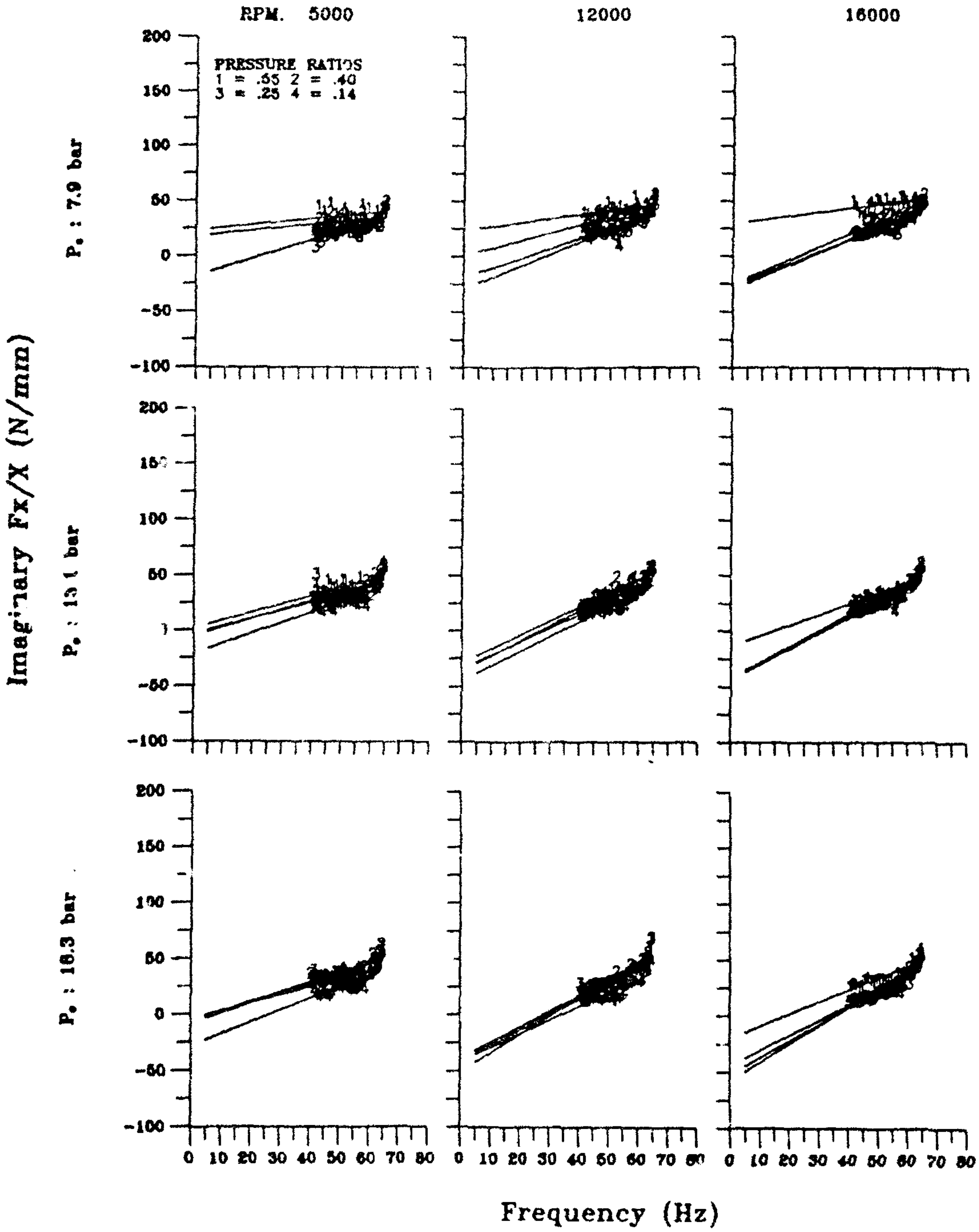

Figure 67 - Direct damping impedance graph for seal 2 with intermediate fluid pre-rotation.

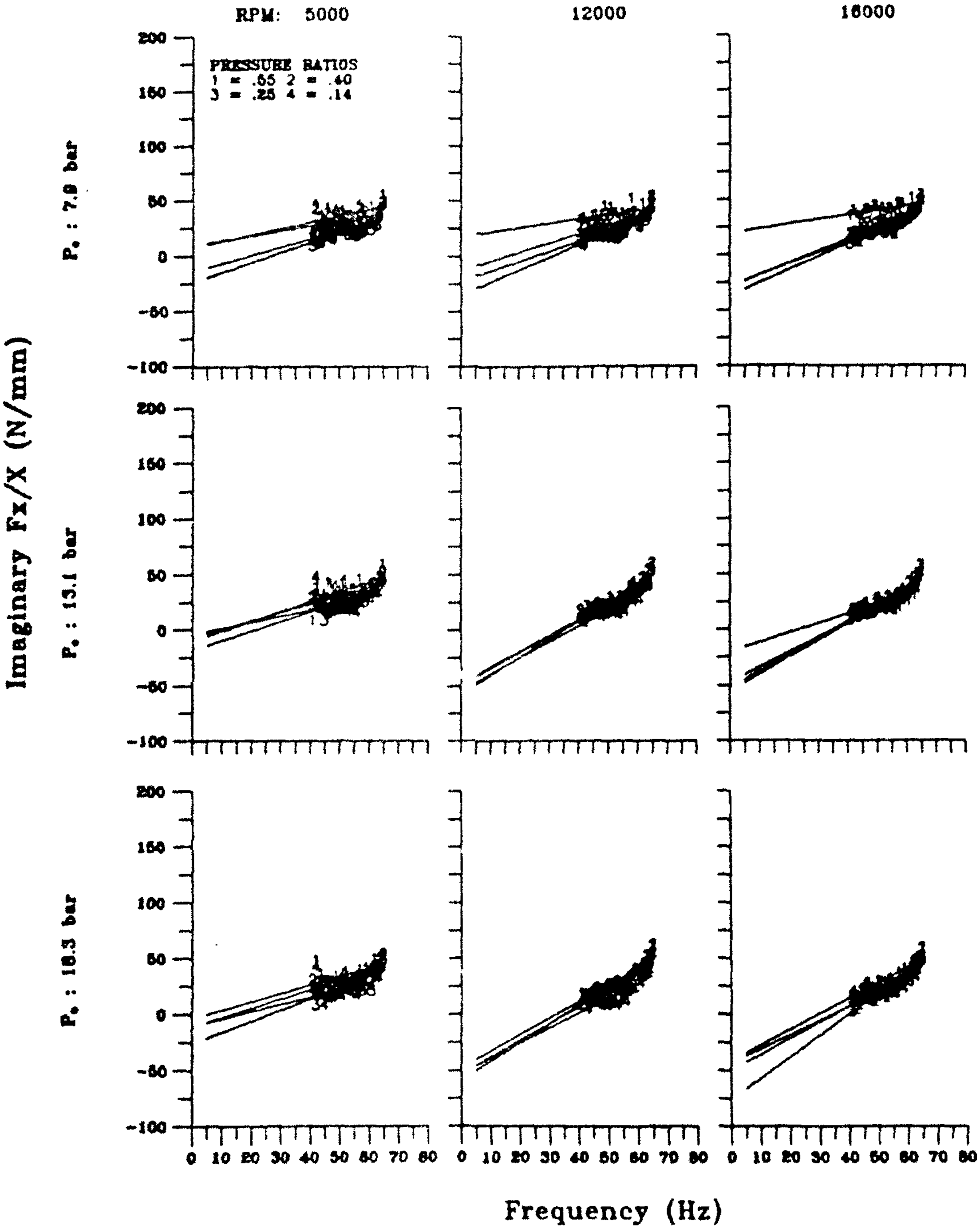

Figure 68 - Direct damping impedance graph for seal 2 with high fluid pre-rotation.

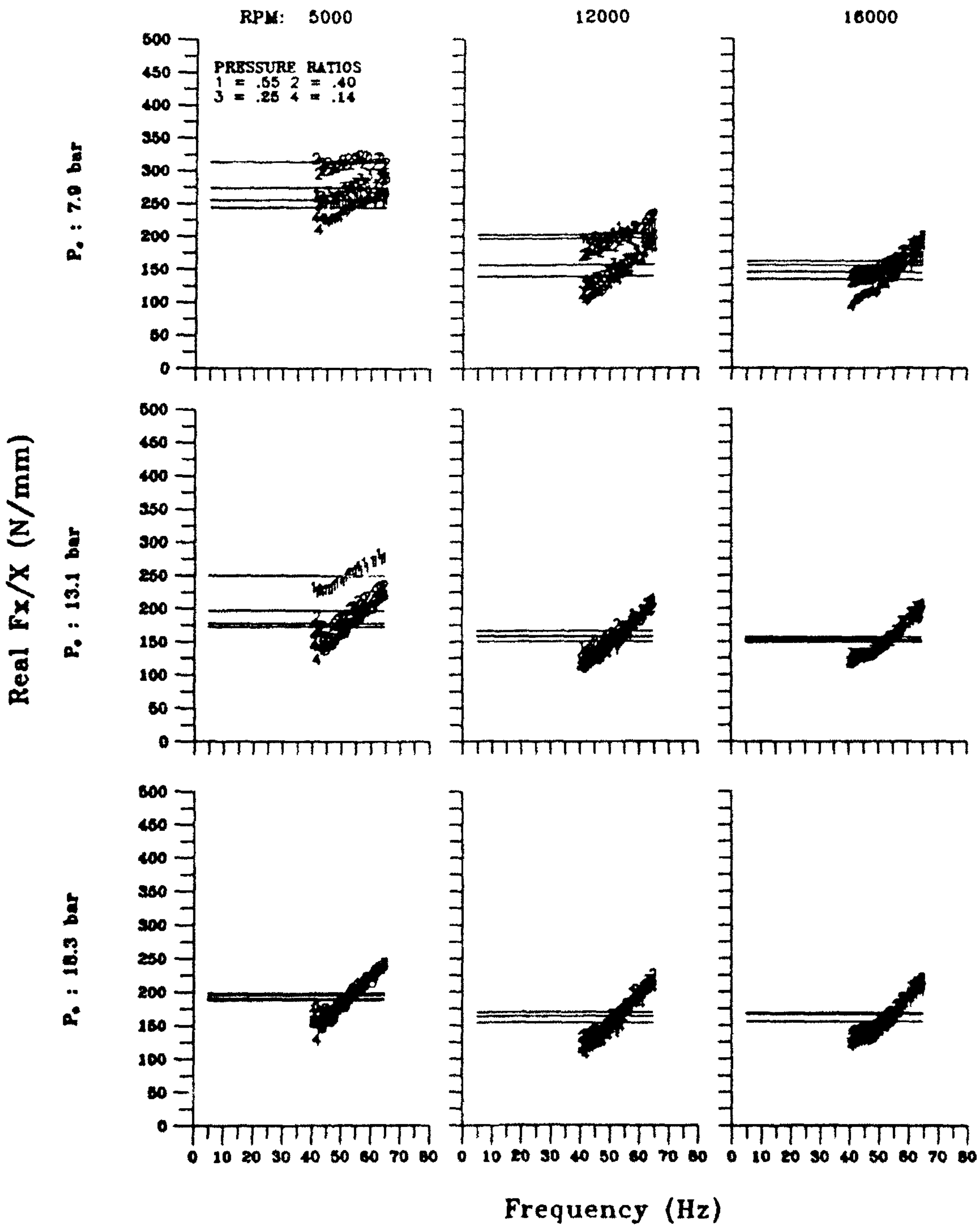

Figure 69 - Direct stiffness impedance graph for seal 3 with no fluid pre-rotation.

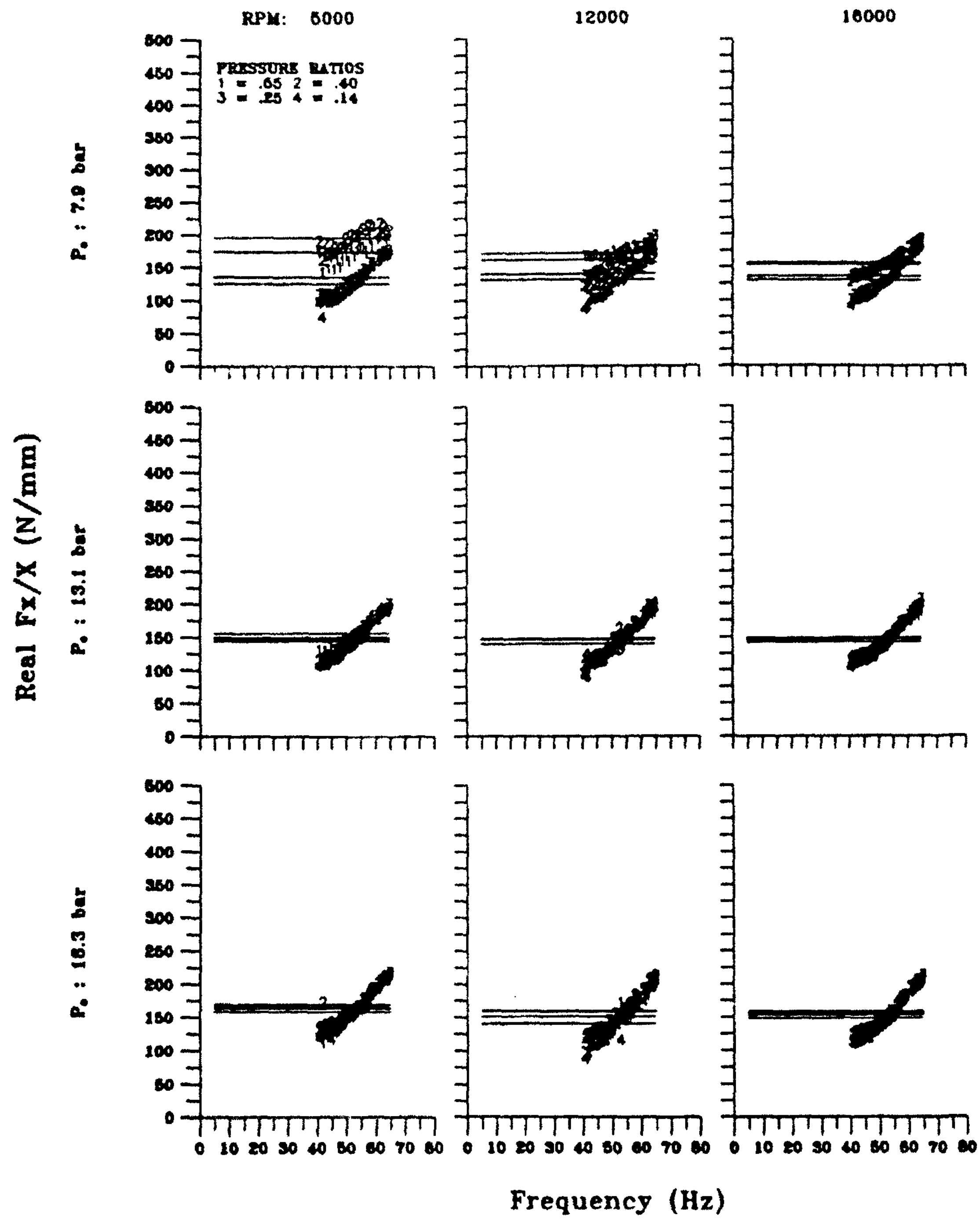

Figure 70 - Direct stiffness impedance graph for seal 3 with intermediate fluid pre-rotation.

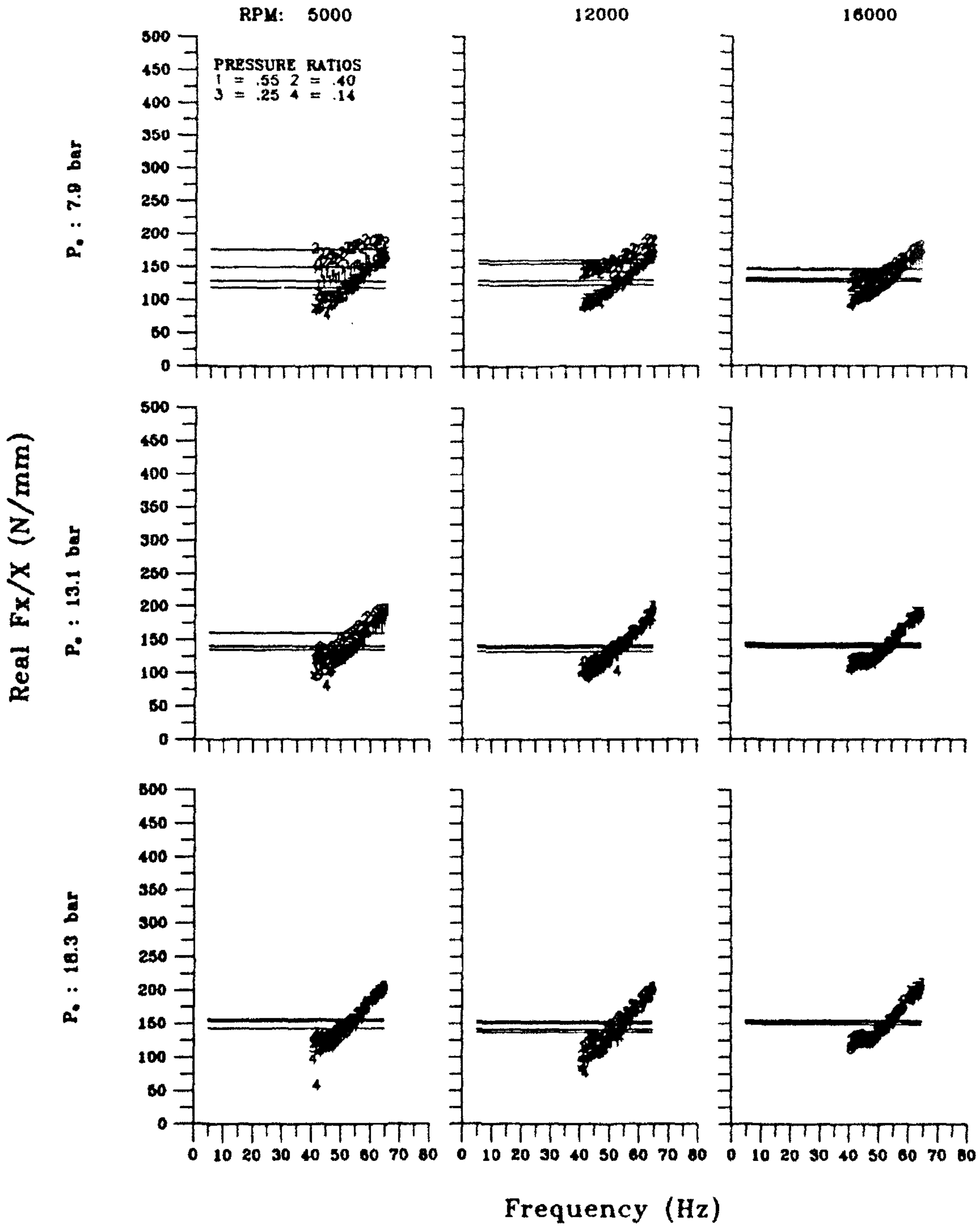

Figure 71 - Direct stiffness impedance graph for seal 3 with high fluid pre-rotation.

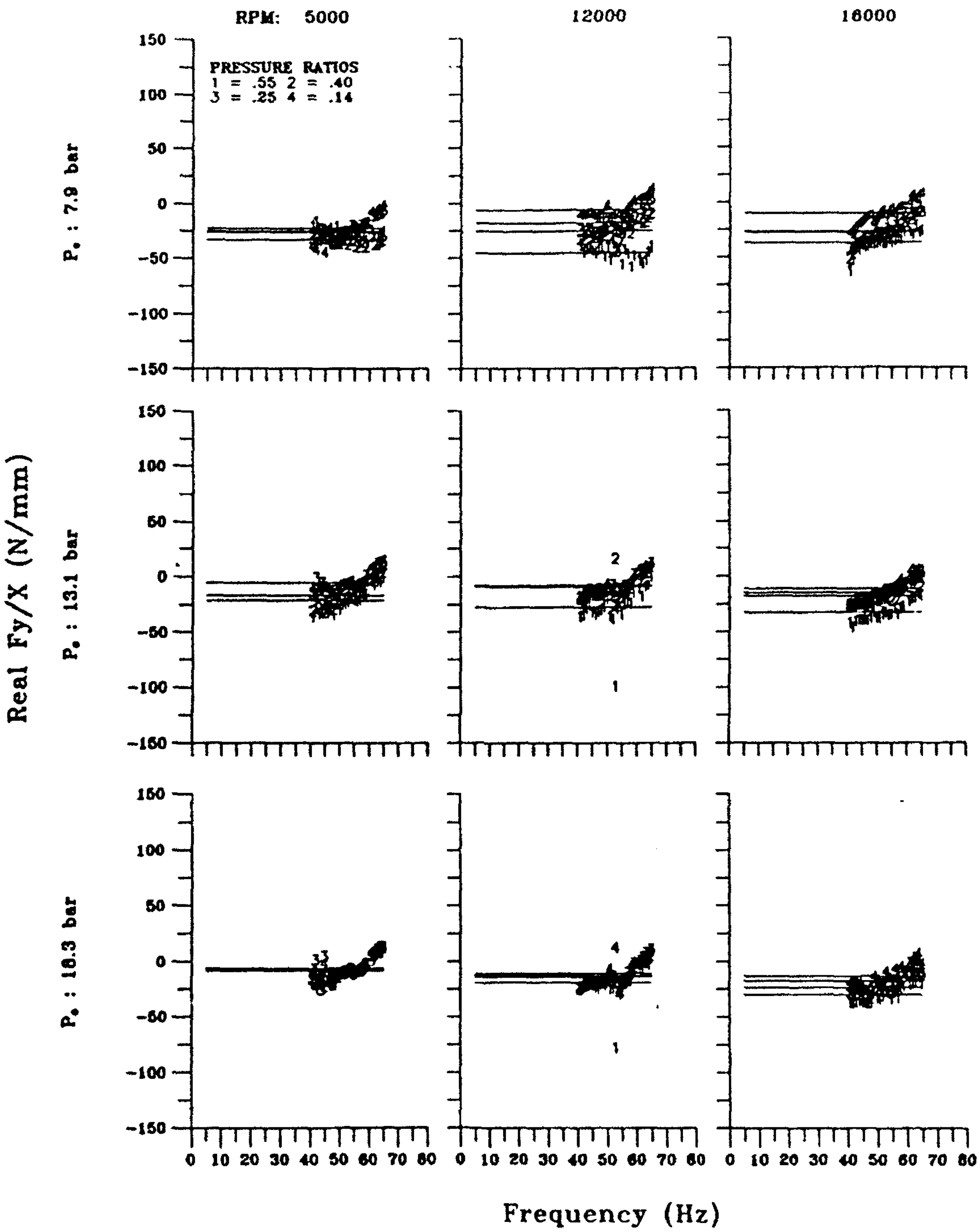

Figure 72 - Cross-coupled stiffness impedance graph for seal 3 with no fluid pre-rotation.

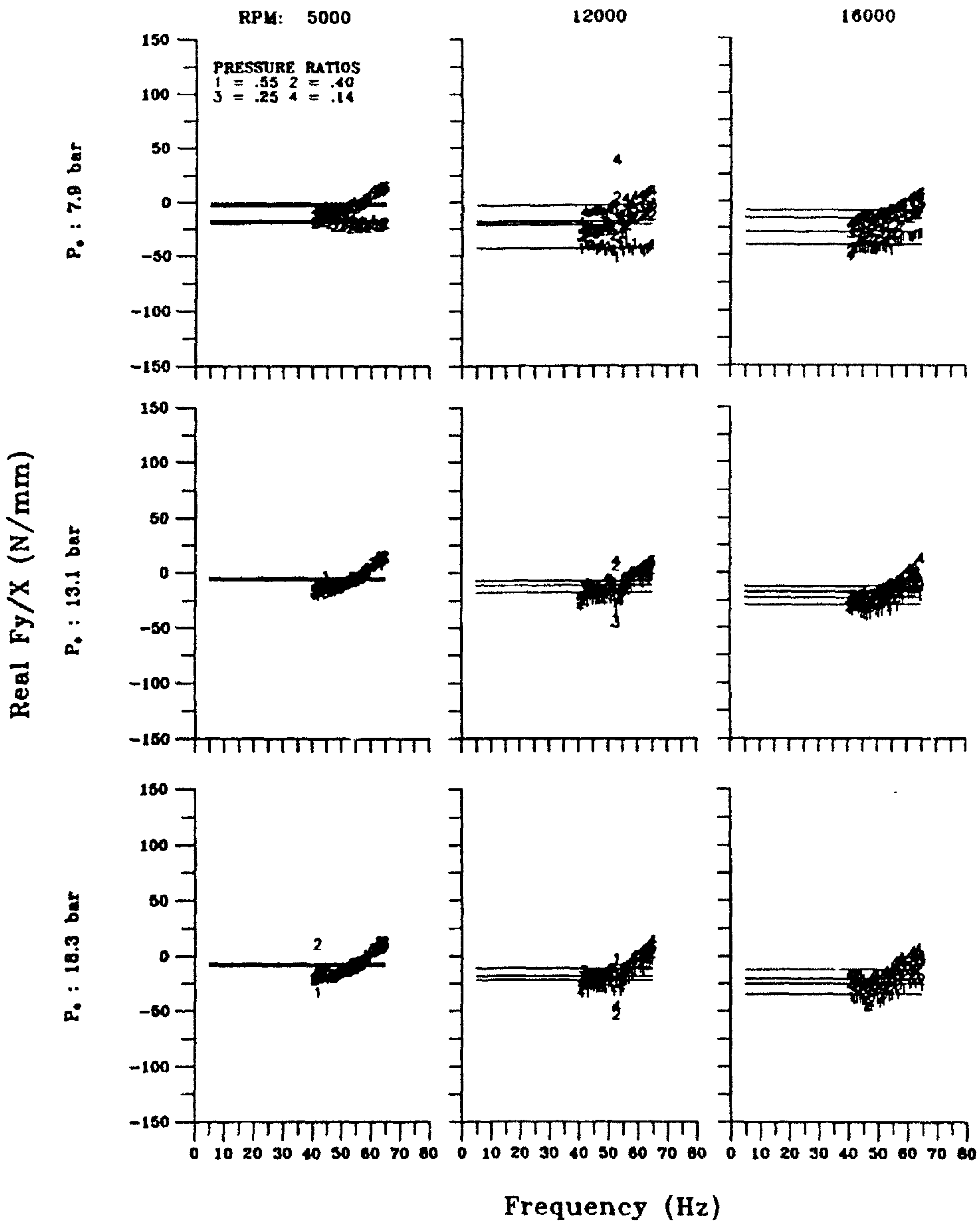

Figure 73 - Cross-coupled stiffness impedance graph for seal 3 with intermediate fluid pre-rotation.

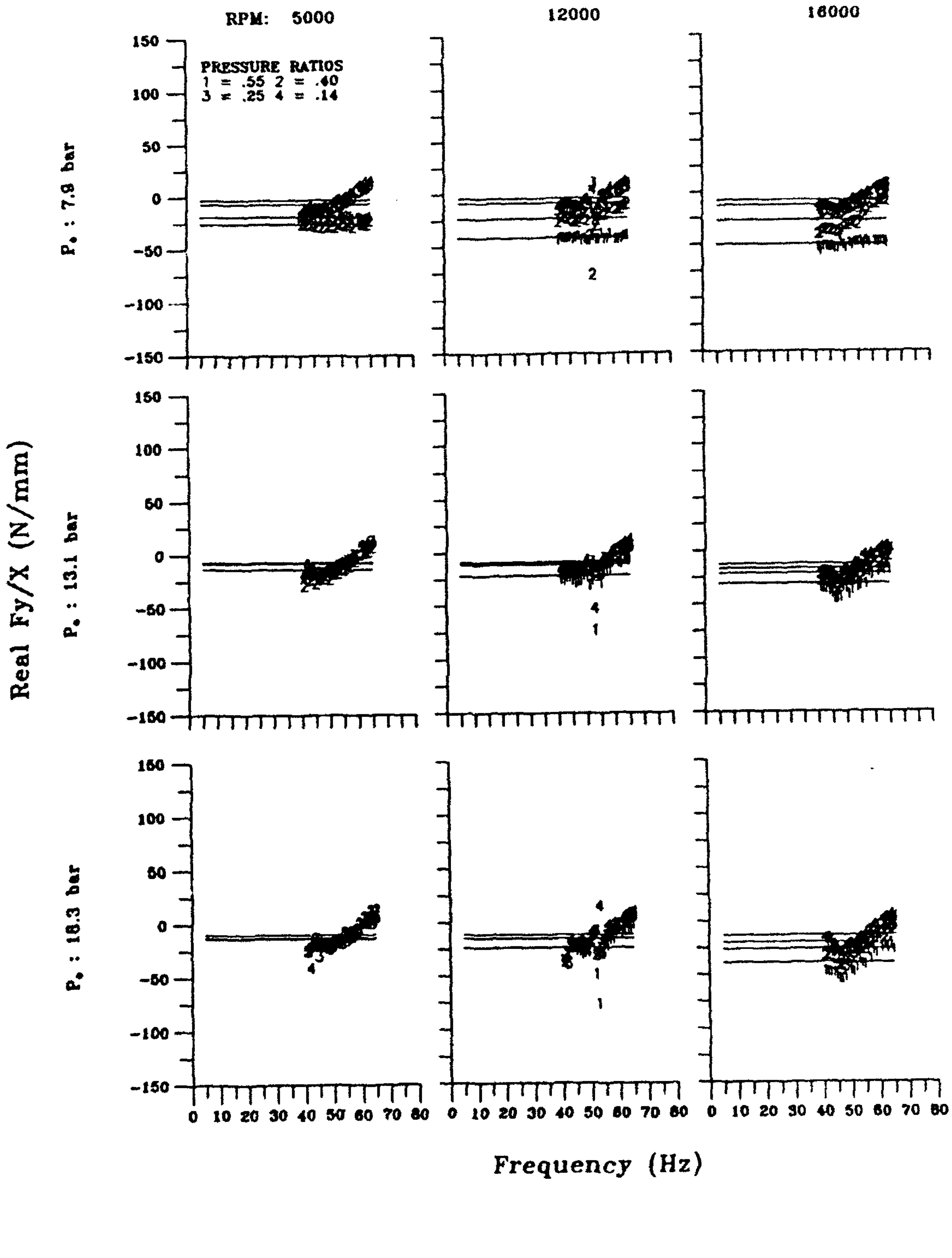

Figure 74 - Cross-coupled stiffness impedance graph for seal 3 with high fluid pre-rotation.

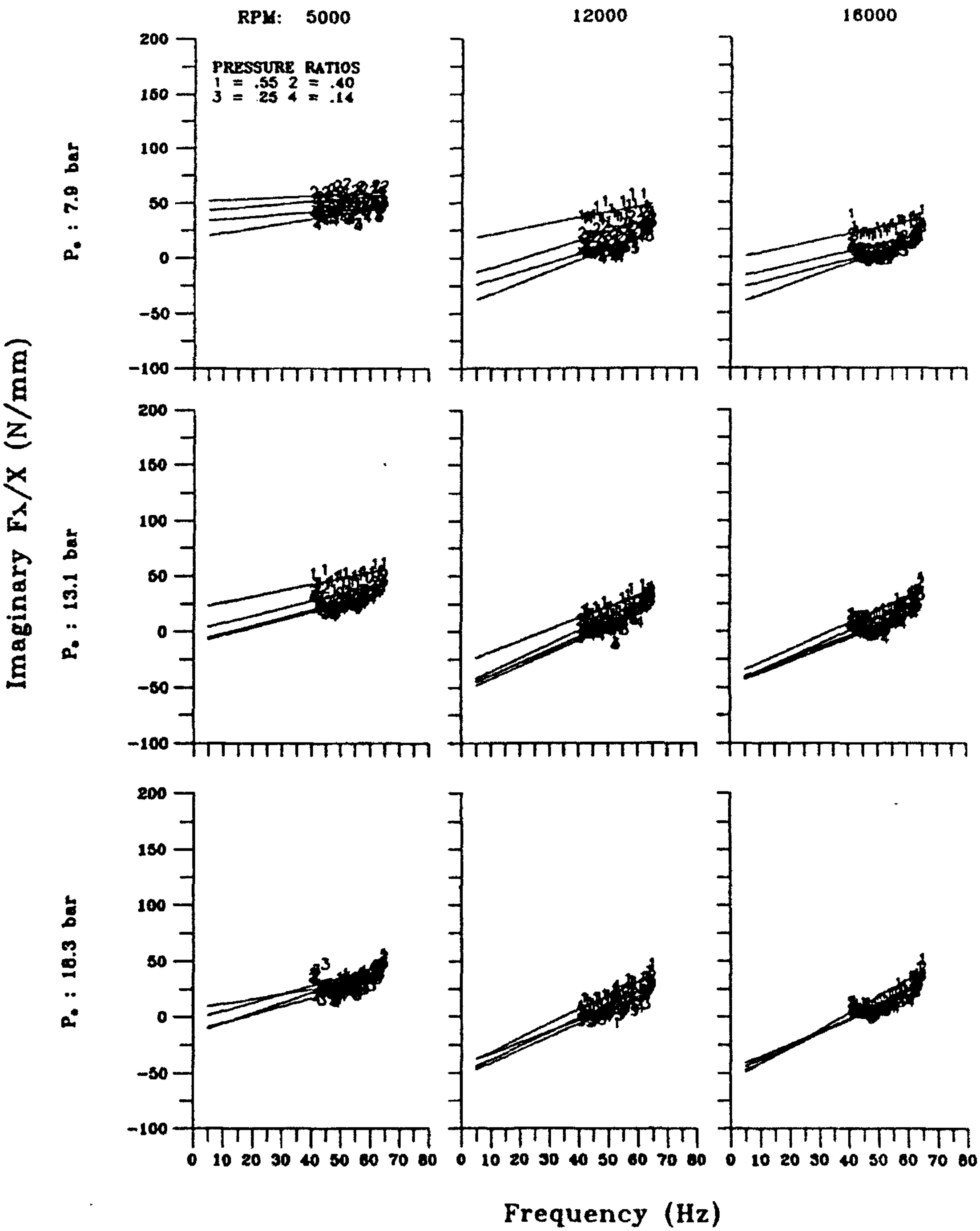

Figure 75 - Direct damping impedance graph for seal 3 with no fluid pre-rotation.

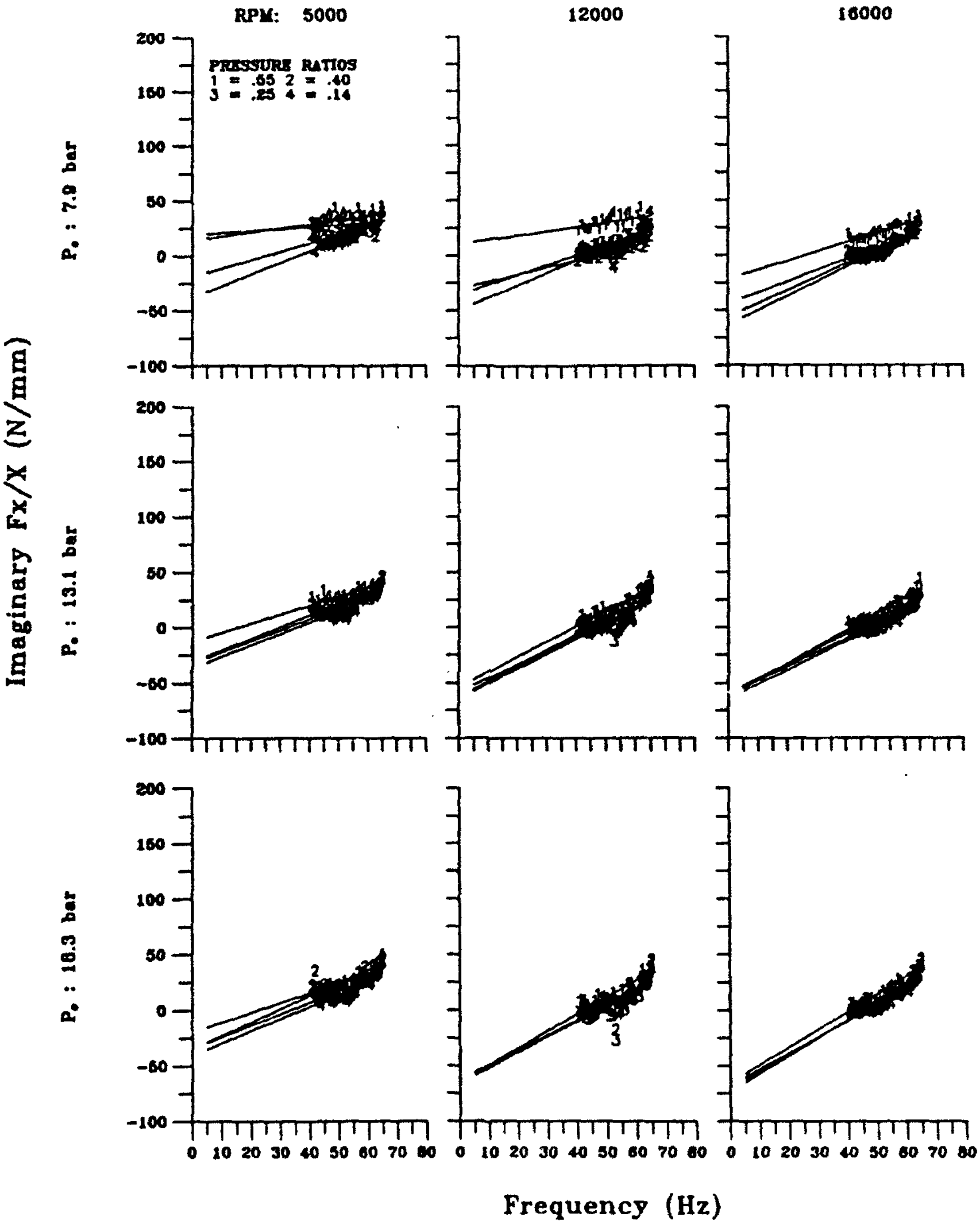

Figure 76 - Direct damping impedance graph for seal 3 with intermediate fluid pre-rotation.

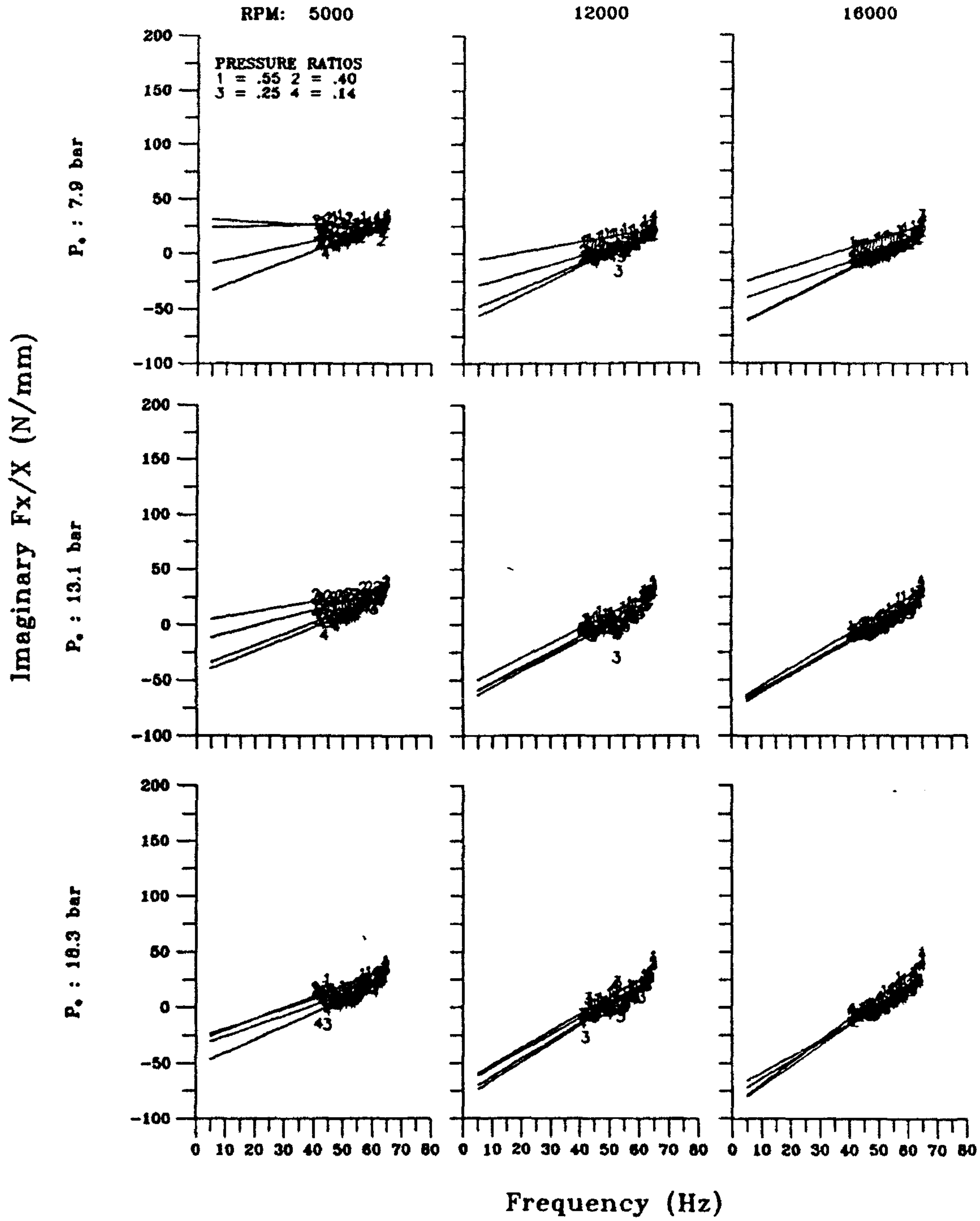

Figure 77 - Direct damping impedance graph for seal 3 with high fluid pre-rotation.

APPENDIX B

TABULATION OF TEST CONDITIONS AND TEST RESULTS

The following 9 tables list the test conditions and test results for each seal configuration. Test results include the mass flow rate, volumetric flow rate, and temperatures before and after the test seal. For seals 2 and 3, cavity pressures between seal stages are listed.

Table B1 - Static and dynamic test data for seal 1 cases with no fluid pre-rotation.

Case	CPM	P_s (bar)	P_b/P_s (-)	T_s (K)	T_b (K)	U_s (m/s)	$\dot{m}$ (kg/s)	q (l/s)
1	5030	7.9575	0.533	299	299	0.00	0.0067	0.7146
2	5030	7.8877	0.387	299	300	0.00	0.0070	0.7473
3	5030	7.9432	0.238	300	300	0.00	0.0071	0.7623
4	5030	7.9486	0.138	300	300	0.00	0.0071	0.7639
5	5030	13.1526	0.539	301	303	0.00	0.0096	0.6243
6	5030	13.1398	0.391	302	305	0.00	0.0103	0.6765
7	5030	13.0518	0.245	303	304	0.00	0.0110	0.7205
8	5030	13.0931	0.134	303	303	0.00	0.0114	0.7485
9	5030	18.2597	0.544	305	305	0.00	0.0136	0.6381
10	5030	18.2499	0.396	305	305	0.00	0.0155	0.7297
11	5030	18.2392	0.249	305	305	0.00	0.0173	0.8111
12	5030	18.2222	0.143	305	303	0.00	0.0182	0.8498
13	12000	7.9091	0.553	305	308	0.00	0.0061	0.6580
14	12000	7.8679	0.400	305	310	0.00	0.0064	0.6937
15	12000	7.8706	0.244	305	311	0.00	0.0066	0.7153
16	12000	7.8732	0.138	305	313	0.00	0.0067	0.7299
17	12000	13.0815	0.535	305	309	0.00	0.0094	0.6163
18	12000	13.1293	0.393	306	311	0.00	0.0102	0.6661
19	12000	13.0331	0.249	306	311	0.00	0.0108	0.7080
20	12000	13.1302	0.139	306	314	0.00	0.0116	0.7614
21	12000	18.2146	0.543	307	310	0.00	0.0136	0.6417
22	12000	18.2068	0.403	307	312	0.00	0.0155	0.7297
23	12000	18.3110	0.241	308	312	0.00	0.0190	0.8903
24	12000	18.1830	0.147	308	313	0.00	0.0221	1.0426
25	16000	7.9111	0.535	308	316	0.00	0.0058	0.6310
26	16000	7.8757	0.395	308	318	0.00	0.0062	0.6775
27	16000	7.9698	0.241	308	322	0.00	0.0063	0.6800
28	16000	7.8980	0.138	308	326	0.00	0.0063	0.6886
29	16000	13.0672	0.542	309	317	0.00	0.0089	0.5886
30	16000	13.0791	0.399	309	319	0.00	0.0097	0.6430
31	16000	13.0737	0.248	309	323	0.00	0.0108	0.7103
32	16000	13.0991	0.138	309	326	0.00	0.0120	0.7899
33	16000	18.2200	0.544	310	317	0.00	0.0136	0.6441
34	16000	18.2385	0.401	310	318	0.00	0.0160	0.7574
35	16000	18.2961	0.254	310	321	0.00	0.0199	0.9320
36	16000	18.1350	0.144	310	321	0.00	0.0244	1.1524

Table B2 - Static and dynamic test data for seal 1 cases with intermediate fluid pre-rotation.

Case	CPM	P_a (bar)	P_b/P_a (-)	T_a (K)	T_b (K)	U_a (m/s)	$\dot{m}$ (kg/s)	q (l/s)
37	5030	7.9317	0.561	307	305	8.71	0.0075	0.8112
38	5030	7.9647	0.414	307	305	9.27	0.0081	0.8637
39	5030	7.9390	0.262	307	305	9.50	0.0082	0.8855
40	5030	7.9584	0.140	307	306	9.7[illegible]	0.0084	0.9048
41	5030	13.1203	0.536	307	304	8.11	0.0116	0.7560
42	5030	13.0967	0.400	307	306	8.72	0.0124	0.8129
43	5030	13.0806	0.252	307	305	9.73	0.0139	0.9065
44	5030	13.0561	0.143	307	305	10.83	0.0155	1.0096
45	5030	18.2253	0.557	308	305	8.68	0.0173	0.8086
46	5030	18.2242	0.397	308	306	10.29	0.0205	0.9590
47	5030	18.2300	0.259	308	305	12.36	0.0248	1.1518
48	5030	18.1928	0.156	308	305	12.74	0.0257	1.1870
49	12000	7.9181	0.565	307	309	8.85	0.0077	0.8249
50	12000	7.8857	0.410	307	310	9.32	0.0080	0.8683
51	12000	7.9087	0.250	307	314	9.47	0.0082	0.8825
52	12000	7.8935	0.143	307	315	9.74	0.0084	0.9070
53	12000	13.1085	0.545	307	310	8.28	0.0118	0.7715
54	12000	13.0349	0.410	307	311	9.06	0.0130	0.8446
55	12000	13.1185	0.254	307	312	9.92	0.0142	0.9244
56	12000	13.0354	0.141	307	313	11.10	0.0160	1.0346
57	12000	18.2242	0.558	307	310	8.74	0.0174	0.8148
58	12000	18.2595	0.401	307	311	10.28	0.0206	0.9582
59	12000	18.1827	0.248	308	311	12.53	0.0251	1.1672
60	12000	18.1760	0.157	308	312	12.74	0.0257	1.1871
61	16000	7.9580	0.539	307	316	8.60	0.0074	0.8014
62	16000	7.8886	0.402	307	317	9.37	0.0080	0.8733
63	16000	7.8184	0.251	307	319	9.60	0.0083	0.8947
64	16000	7.9526	0.143	307	323	9.65	0.0084	0.8990
65	16000	13.0441	0.548	308	316	8.18	0.0113	0.7625
66	16000	13.0925	0.394	308	317	8.74	0.0125	0.8145
67	16000	13.0251	0.260	308	320	9.34	0.0134	0.8705
68	16000	13.1103	0.145	308	322	10.34	0.0148	0.9632
69	16000	18.2938	0.543	308	315	8.38	0.0168	0.7811
70	16000	18.2728	0.400	308	317	9.74	0.0196	0.9074
71	16000	18.1722	0.258	308	318	11.84	0.0238	1.1034
72	16000	18.2124	0.150	308	318	12.73	0.0258	1.1867

Table B3 - Static and dynamic test data for seal 1 cases with high fluid pre-rotation.

Case	CPM	P_e (bar)	P_b/P_e (-)	T_e (K)	T_b (K)	U_e (m/s)	$\dot{m}$ (kg/s)	q (l/s)
73	5030	7.9375	0.549	295	295	18.63	0.0085	0.8677
74	5030	7.9132	0.407	295	296	19.62	0.0090	0.9139
75	5030	7.9486	0.253	295	296	20.38	0.0094	0.9493
76	5030	7.9259	0.147	295	295	20.80	0.0096	0.9684
77	5030	13.1273	0.548	296	295	17.31	0.0130	0.8064
78	5030	13.1593	0.400	296	295	18.47	0.0139	0.8592
79	5030	13.0743	0.248	296	295	19.42	0.0146	0.9042
80	5030	13.1609	0.143	296	295	20.45	0.0155	0.9524
81	5030	18.2925	0.553	297	296	17.10	0.0179	0.7964
82	5030	18.2426	0.403	297	296	19.25	0.0201	0.8963
83	5030	18.3813	0.242	298	296	22.98	0.0244	1.0699
84	5030	18.2979	0.150	298	296	25.36	0.0270	1.1807
85	12000	7.8612	0.564	300	305	21.05	0.0094	0.9803
86	12000	7.8463	0.404	300	305	22.54	0.0102	1.0496
87	12000	7.9533	0.268	301	307	22.88	0.0103	1.0652
88	12000	7.8911	0.151	301	308	23.08	0.0105	1.0746
89	12000	13.0524	0.549	301	305	20.77	0.0154	0.9670
90	12000	13.1159	0.409	300	305	22.04	0.0165	1.0260
91	12000	13.0716	0.256	300	305	23.37	0.0174	1.0887
92	12000	13.0880	0.141	300	305	25.38	0.0193	1.1820
93	12000	18.2460	0.545	300	305	21.25	0.0221	0.9893
94	12000	18.2845	0.389	300	305	24.06	0.0253	1.1203
95	12000	18.2359	0.247	300	304	25.39	0.0271	1.1824
96	12000	18.2448	0.142	300	304	25.36	0.0269	1.1808
97	16000	7.9138	0.563	301	312	17.60	0.0078	0.8192
98	16000	7.8899	0.388	302	314	19.45	0.0087	0.9057
99	16000	7.9503	0.247	302	316	19.90	0.0089	0.9265
100	16000	7.9397	0.147	302	318	20.18	0.0090	0.9399
101	16000	13.0767	0.547	303	312	17.90	0.0131	0.8335
102	16000	13.0756	0.402	303	315	19.41	0.0143	0.9041
103	16000	13.1210	0.245	303	316	20.45	0.0151	0.9526
104	16000	13.0796	0.138	304	317	21.67	0.0160	1.0091
105	16000	18.1726	0.553	305	312	18.84	0.0192	0.8775
106	16000	18.2538	0.399	305	315	20.93	0.0215	0.9749
107	16000	18.2757	0.250	305	315	24.01	0.0248	1.1184
108	16000	18.2159	0.146	306	314	25.45	0.0265	1.1851

Table B4 - Static and dynamic test data for seal 2 cases with no fluid pre-rotation.

Case	CPM	P_o (bar)	P_b/P_o (-)	T_o (K)	T_b (K)	U_o (m/s)	$\dot{m}$ (kg/s)	q (l/s)	P_{cav1} (bar)	P_{cav2} (bar)	P_{cav3} (bar)	P_b (bar)
1	5030	8.0127	0.523	297	296	0.00	0.0057	0.5853	7.7009	7.3903	6.1087	4.1904
2	5030	7.8829	0.407	297	296	0.00	0.0059	0.6221	7.5164	7.1693	5.4147	3.2116
3	5030	7.9104	0.248	297	296	0.00	0.0063	0.6596	7.5837	7.0236	4.7533	1.9607
4	5030	7.8958	0.137	297	297	0.00	0.0066	0.6898	7.3814	6.7079	4.1233	1.0820
5	5030	13.0247	0.555	297	296	0.00	0.0083	0.5284	12.1172	10.9088	9.0561	7.2331
6	5030	13.1021	0.402	297	296	0.00	0.0090	0.5703	11.8656	10.2875	7.7399	5.2673
7	5030	13.1293	0.251	297	297	0.00	0.0097	0.6129	11.6867	9.7119	6.4065	3.3017
8	5030	13.0934	0.135	297	297	0.00	0.0105	0.6669	11.6927	9.6832	5.7529	1.7615
9	5030	18.2435	0.553	298	297	0.00	0.0115	0.5252	16.7636	14.9818	12.3825	10.0843
10	5030	18.1902	0.400	298	297	0.00	0.0126	0.5762	16.1586	13.7116	10.1862	7.2723
11	5030	18.2053	0.248	298	297	0.00	0.0139	0.6337	15.3093	12.2073	7.9877	4.5181
12	5030	18.2542	0.136	298	297	0.00	0.0156	0.7094	14.6648	11.1658	6.3807	2.4868
13	12000	7.7945	0.570	299	304	0.00	0.0048	0.5112	7.2449	6.4561	5.5700	4.4468
14	12000	7.8396	0.401	299	304	0.00	0.0055	0.5797	7.0624	5.9851	4.7488	3.1431
15	12000	7.8396	0.244	299	306	0.00	0.0057	0.6134	6.9013	5.6061	3.9999	1.9161
16	12000	7.9101	0.136	299	310	0.00	0.0060	0.6459	6.6124	5.2275	3.4592	1.0749
17	12000	13.1264	0.546	300	304	0.00	0.0086	0.5502	11.3320	9.6829	8.5910	7.1701
18	12000	13.0203	0.403	300	305	0.00	0.0092	0.5912	11.0828	9.0440	7.1536	5.2525
19	12000	13.1307	0.234	300	307	0.00	0.0102	0.6512	10.7461	8.5151	5.8151	3.0770
20	12000	13.0627	0.130	300	310	0.00	0.0108	0.6938	10.8088	8.3786	4.9422	1.7044
21	12000	18.2292	0.557	301	304	0.00	0.0116	0.5318	15.8460	13.5164	11.9341	10.1454
22	12000	18.2040	0.397	301	304	0.00	0.0127	0.5852	15.3207	12.4079	9.5384	7.2337
23	12000	18.2049	0.245	301	305	0.00	0.0144	0.6617	14.6686	11.2530	7.0912	4.4664
24	12000	18.2100	0.133	301	309	0.00	0.0168	0.7703	13.9074	10.2264	5.3371	2.4221
25	16000	7.8304	0.558	302	313	0.00	0.0045	0.4971	6.5464	5.6965	5.0696	4.3711
26	16000	7.9072	0.409	302	312	0.00	0.0052	0.5564	6.1685	4.9855	4.0994	3.2339
27	16000	7.8631	0.247	302	314	0.00	0.0053	0.5624	6.1632	4.6993	3.4679	1.9398
28	16000	7.8642	0.135	303	322	0.00	0.0053	0.5628	6.2232	4.6473	3.0978	1.0613
29	16000	13.1284	0.542	304	311	0.00	0.0070	0.4542	11.3931	9.5321	8.0948	7.1162
30	16000	13.0898	0.404	304	315	0.00	0.0074	0.4821	11.1100	8.8555	6.6115	5.2851
31	16000	13.1055	0.242	304	319	0.00	0.0079	0.5140	10.7252	8.1794	5.2316	3.1710
32	16000	13.1264	0.127	303	325	0.00	0.0083	0.5315	10.5871	7.8365	4.3169	1.6712
33	16000	18.2571	0.550	305	311	0.00	0.0095	0.4397	15.9942	13.4060	11.2929	10.0486
34	16000	18.2555	0.398	305	317	0.00	0.0120	0.5572	15.0706	12.2000	8.8868	7.2685
35	16000	18.2069	0.244	305	315	0.00	0.0122	0.5652	15.0115	11.4591	7.1681	4.4461
36	16000	18.1924	0.141	305	323	0.00	0.0138	0.6422	14.2010	10.4914	5.6802	2.5680

Table B5 - Static and dynamic test data for seal 2 cases with intermediate fluid pre-rotation.

Case	CPM	P_a (bar)	P_b/P_a (-)	T_a (K)	T_b (K)	U_a (m/s)	$\dot{m}$ (kg/s)	q (l/s)	P_{cav1} (bar)	P_{cav2} (bar)	P_{cav3} (bar)	P_b (bar)
37	5030	7.8570	0.550	303	301	7.29	0.0063	0.6792	6.7128	5.9240	5.3351	4.3214
38	5030	8.0560	0.417	305	304	7.65	0.0066	0.7130	6.3782	5.2684	4.1215	3.3610
39	5030	7.9150	0.240	303	302	8.23	0.0072	0.7672	6.2131	4.7870	3.6272	1.9023
40	5030	7.9772	0.137	303	302	8.33	0.0073	0.7762	6.1792	4.6230	3.2816	1.0909
41	5030	13.0738	0.537	304	302	6.72	0.0096	0.6258	11.1502	9.4306	8.0765	7.0209
42	5030	13.0292	0.397	304	302	7.06	0.0102	0.6576	10.7859	8.6070	6.7262	5.1678
43	5030	13.1400	0.243	304	302	7.43	0.0107	0.6919	10.5266	7.9922	5.4567	3.1866
44	5030	13.0734	0.140	304	303	7.70	0.0111	0.7173	10.3500	7.6288	4.7783	1.8269
45	5030	18.2404	0.545	305	305	6.51	0.0130	0.6067	15.4797	13.2641	11.4087	9.9446
46	5030	18.2138	0.400	305	305	7.11	0.0142	0.6620	14.9439	12.2252	9.4199	7.2835
47	5030	18.2062	0.243	305	304	7.58	0.0151	0.7062	14.4422	11.2041	7.2337	4.4153
48	5030	18.1766	0.137	306	304	8.15	0.0162	0.7594	13.9349	10.3444	5.6315	2.4892
49	12000	7.9748	0.550	305	308	6.29	0.0054	0.5862	6.3421	5.4430	4.8008	4.3874
50	12000	7.9936	0.385	305	308	7.04	0.0061	0.6557	6.1690	4.9418	3.9625	3.0761
51	12000	8.0143	0.253	307	311	7.24	0.0063	0.6748	6.1828	4.6478	3.4790	2.0243
52	12000	7.8891	0.137	307	315	7.34	0.0062	0.6846	6.0409	4.4349	2.9994	1.0798
53	12000	13.0049	0.544	307	311	6.21	0.0088	0.5787	10.8102	9.1255	7.9909	7.0[illegible]18
54	12000	13.0508	0.399	307	311	6.56	0.0093	0.6116	10.7058	8.4404	6.7541	5.2079
55	12000	13.0239	0.247	307	312	6.72	0.0095	0.6263	10.4867	7.9288	5.3128	3.2216
56	12000	13.1017	0.136	308	316	6.93	0.0098	0.6455	10.2835	7.5991	4.2286	1.7827
57	12000	18.2366	0.549	308	312	6.03	0.0119	0.5617	15.4911	12.9411	11.0277	10.0127
58	12000	18.2450	0.402	308	313	6.52	0.0129	0.6075	15.0409	12.1462	9.1377	7.3419
59	12000	18.2009	0.257	309	313	7.18	0.0142	0.6691	14.4814	11.2401	7.0073	4.6768
60	12000	18.2531	0.146	309	316	8.19	0.0162	0.7629	13.9730	10.2986	5.3485	2.6733
61	16000	7.9643	0.541	308	316	5.42	0.0046	0.5055	6.2475	5.3549	4.7098	4.3080
62	16000	7.8611	0.389	309	319	5.99	0.0051	0.5582	6.1480	4.7709	3.8092	3.0596
63	16000	7.8759	0.254	309	321	6.19	0.0053	0.5766	5.9896	4.4133	3.2089	2.0022
64	16000	7.8227	0.135	309	327	6.19	0.0053	0.5769	6.0601	4.4492	2.8444	1.0577
65	16000	13.0805	0.552	310	318	5.19	0.0073	0.4839	10.9090	9.0842	8.0506	7.2206
66	16000	13.0466	0.405	310	320	5.54	0.0078	0.5166	10.7143	8.3105	6.6914	5.2862
67	16000	13.0840	0.247	310	322	5.72	0.0081	0.5332	10.4541	7.9108	5.2648	3.2348
68	16000	13.1189	0.127	310	328	5.98	0.0084	0.5575	10.3346	7.5704	4.0981	1.6712
69	16000	18.2333	0.538	311	318	5.37	0.0106	0.5003	15.4271	13.1026	10.8146	9.8181
70	16000	18.2972	0.396	311	321	6.17	0.0122	0.5752	14.9207	12.1105	8.6876	7.2487
71	16000	18.2355	0.249	311	323	6.85	0.0136	0.6386	14.2876	10.9753	6.7392	4.5447
72	16000	18.1869	0.147	311	330	7.03	0.0139	0.6553	14.0649	10.4140	5.5329	2.6750

Table B6 - Static and dynamic test data for seal 2 cases with high fluid pre-rotation.

Case	CPM	P_e (bar)	P_b/P_e (-)	T_e (K)	T_b (K)	U_e (m/s)	$\dot{m}$ (kg/s)	q (l/s)	P_{cav1} (bar)	P_{cav2} (bar)	P_{cav3} (bar)	P_b (bar)
73	5030	7.8708	0.540	297	296	16.12	0.0073	0.7503	6.3990	5.5108	4.8800	4.2511
74	5030	7.9601	0.384	297	296	15.48	0.0070	0.7209	6.1116	4.9026	4.0313	3.0561
75	5030	7.9585	0.243	297	296	16.39	0.0074	0.7631	5.9641	4.5313	3.4064	1.9361
76	5030	7.8873	0.139	297	296	16.70	0.0075	0.7778	5.9010	4.3546	3.0516	1.0965
77	5030	13.0258	0.545	297	297	13.87	0.0103	0.6456	10.7891	9.2282	8.2296	7.1009
78	5030	13.1427	0.400	297	296	14.69	0.0110	0.6841	10.5653	8.3431	6.8231	5.2566
79	5030	13.0209	0.247	297	296	15.22	0.0113	0.7091	10.3424	7.8079	5.5482	3.2217
80	5030	13.0421	0.136	298	296	15.42	0.0114	0.7180	10.1222	7.4030	4.5775	1.7795
81	5030	18.2731	0.554	299	298	13.37	0.0137	0.6225	15.3608	13.1860	11.2119	10.1258
82	5030	18.3003	0.402	298	297	14.63	0.0151	0.6812	14.7598	11.9540	8.9442	7.3646
83	5030	18.2668	0.246	299	297	15.72	0.0163	0.7320	14.5017	11.2132	6.9331	4.4994
84	5030	18.2704	0.142	298	296	16.25	0.0168	0.7566	14.0463	10.3683	5.6676	2.6007
85	12000	7.9788	0.544	299	302	12.53	0.0055	0.5834	6.4021	5.5121	4.8142	4.3443
86	12000	7.9837	0.401	299	304	13.66	0.0061	0.6364	6.1964	4.8956	3.9838	3.2054
87	12000	7.8889	0.247	299	305	14.16	0.0062	0.6596	5.9753	4.4717	3.3104	1.9497
88	12000	7.9152	0.137	299	308	14.41	0.0064	0.6710	6.0241	4.3615	2.9039	1.0825
89	12000	13.0583	0.545	300	305	12.20	0.0089	0.5684	10.7864	9.0517	7.9777	7.1145
90	12000	13.0472	0.397	300	305	13.11	0.0096	0.6101	10.5245	8.2122	6.5777	5.1741
91	12000	13.0414	0.251	300	305	13.45	0.0098	0.6264	10.3087	7.7943	5.3207	3.2719
92	12000	13.0298	0.136	300	309	13.86	0.0101	0.6451	10.2164	7.5272	4.2850	1.7772
93	12000	18.1772	0.551	301	305	12.10	0.0123	0.5634	15.2897	12.8580	11.1010	10.0109
94	12000	18.2564	0.393	301	306	13.07	0.0134	0.6086	14.8841	11.9905	9.0230	7.1805
95	12000	18.2637	0.250	302	306	14.40	0.0147	0.6706	14.4865	11.1909	7.0219	4.5621
96	12000	18.2178	0.135	302	309	15.82	0.0161	0.7370	13.8656	10.3844	5.4124	2.4524
97	16000	7.9752	0.537	303	313	10.78	0.0048	0.5021	6.3938	5.5070	4.8968	4.2837
98	16000	7.8469	0.401	303	314	12.09	0.0053	0.5633	6.0652	4.7616	3.8127	3.1489
99	16000	7.9295	0.259	303	316	12.30	0.0054	0.5727	6.0286	4.4296	3.1569	2.0499
100	16000	7.9175	0.134	304	323	12.35	0.0054	0.5748	5.9728	4.2941	2.6628	1.0642
101	16000	13.0352	0.552	306	313	10.38	0.0075	0.4834	10.9482	9.1637	7.9373	7.1970
102	16000	13.1050	0.399	306	315	11.11	0.0080	0.5172	10.6905	8.4145	6.4677	5.2283
103	16000	13.0929	0.246	304	320	11.89	0.0086	0.5538	10.4109	7.8775	5.0306	3.2241
104	16000	13.0104	0.134	305	325	12.04	0.0087	0.5608	10.2878	7.5678	4.1652	1.7395
105	16000	18.2691	0.544	306	313	10.34	0.0104	0.4813	15.6707	13.0914	11.0872	9.9449
106	16000	18.2095	0.398	306	317	11.46	0.0115	0.5337	15.0367	12.0227	8.8942	7.2401
107	16000	18.2111	0.246	306	318	12.80	0.0129	0.5960	14.5255	11.2043	7.0696	4.4845
108	16000	18.2171	0.137	307	323	14.28	0.0144	0.6651	14.1003	10.5176	5.7705	2.4977

Table B7 - Static and dynamic test data for seal 3 cases with no fluid pre-rotation.

Case	CPM	P_a (bar)	P_b/P_a (-)	T_a (K)	T_b (K)	U_a (m/s)	$\dot{m}$ (kg/s)	q (l/s)	P_{cav1} (bar)	P_{cav2} (bar)	P_{cav3} (bar)	P_b (bar)
1	5030	7.9185	0.545	298	298	0.00	0.0086	0.9122	7.1108	5.6385	5.2136	4.3129
2	5030	7.8975	0.399	299	298	0.00	0.0090	0.9520	6.8897	5.1251	4.5482	3.1480
3	5030	7.9542	0.248	299	299	0.00	0.0092	0.9682	6.8571	4.8652	4.1351	1.9756
4	5030	7.9472	0.144	299	299	0.00	0.0093	0.9827	6.7940	4.6716	3.8261	1.1465
5	5030	13.1154	0.535	300	299	0.00	0.0124	0.7931	11.7316	9.3840	8.6486	7.0180
6	5030	13.0195	0.405	300	300	0.00	0.0131	0.8453	11.5031	8.7822	7.7630	5.2752
7	5030	13.1384	0.254	301	300	0.00	0.0139	0.8930	11.0345	8.0436	6.6544	3.3312
8	5030	13.0661	0.139	302	300	0.00	0.0142	0.9213	10.7454	7.5765	5.6849	1.8117
9	5030	18.2819	0.548	303	302	0.00	0.0163	0.7559	16.0775	13.2201	11.9359	10.0227
10	5030	18.2276	0.402	303	303	0.00	0.0177	0.8224	15.6091	12.3517	10.4674	7.3265
11	5030	18.2178	0.249	303	302	0.00	0.0188	0.8759	15.1725	11.5491	8.6390	4.5440
12	5030	18.2183	0.140	304	302	0.00	0.0193	0.8983	14.8924	11.0751	7.2495	2.5469
13	12000	7.9033	0.554	303	306	0.00	0.0079	0.8655	6.8899	5.6861	5.1828	4.3802
14	12000	7.8248	0.413	303	306	0.00	0.0086	0.9334	6.7603	5.1672	4.4775	3.2355
15	12000	7.9401	0.247	304	310	0.00	0.0090	0.9691	6.6796	4.9230	4.0494	1.9593
16	12000	7.9586	0.146	304	312	0.00	0.0093	0.9955	6.6040	4.7461	3.7403	1.1608
17	12000	13.0615	0.547	304	308	0.00	0.0130	0.8463	11.5908	9.5511	8.6118	7.1433
18	12000	13.1623	0.389	304	307	0.00	0.0138	0.8975	11.3630	8.9490	7.5571	5.1168
19	12000	13.1020	0.252	305	310	0.00	0.0146	0.9547	11.1576	8.4790	6.5529	3.3060
20	12000	13.0749	0.140	305	311	0.00	0.0153	0.9936	11.0302	8.2080	5.6116	1.8270
21	12000	18.2593	0.547	306	309	0.00	0.0185	0.8617	16.2321	13.6749	12.0599	9.9841
22	12000	18.2000	0.402	306	309	0.00	0.0203	0.9473	15.8058	12.8919	10.3588	7.3111
23	12000	18.2364	0.252	306	310	0.00	0.0220	1.0269	15.3271	12.0898	8.4795	4.5884
24	12000	18.2384	0.139	307	311	0.00	0.0240	1.1219	14.5286	11.2036	6.9366	2.5406
25	16000	7.9024	0.572	306	315	0.00	0.0083	0.8965	6.9899	6.0780	5.3702	4.5168
26	16000	7.9315	0.397	306	314	0.00	0.0089	0.9610	6.8018	5.5520	4.5527	3.1525
27	16000	7.9216	0.258	307	319	0.00	0.0092	0.9824	6.6071	5.2120	3.9615	2.0414
28	16000	7.9232	0.148	307	322	0.00	0.0093	1.0037	6.5594	5.0149	3.5306	1.1690
29	16000	13.0657	0.555	307	315	0.00	0.0126	0.8269	11.4275	9.8681	8.6113	7.2473
30	16000	13.0900	0.409	307	314	0.00	0.0134	0.8759	11.2308	9.1652	7.4179	5.3553
31	16000	13.0334	0.246	307	318	0.00	0.0142	0.9264	10.9533	8.5174	6.0905	3.2011
32	16000	13.1298	0.135	307	322	0.00	0.0148	0.9658	10.6298	8.0128	5.1106	1.7673
33	16000	18.2658	0.544	308	315	0.00	0.0175	0.8183	15.9352	13.6619	11.7931	9.9281
34	16000	18.2301	0.404	308	315	0.00	0.0191	0.8930	15.4741	12.6916	10.0106	7.3651
35	16000	18.2160	0.249	308	318	0.00	0.0212	0.9928	14.7683	11.5152	7.9910	4.5375
36	16000	18.2160	0.136	308	320	0.00	0.0232	1.0882	14.0972	10.6024	6.5141	2.4851

Table B8 - Static and dynamic test data for seal 3 cases with intermediate fluid pre-rotation.

Case	CPM	P_a (bar)	P_b/P_a (-)	T_a (K)	T_b (K)	U_a (m/s)	$\dot{m}$ (kg/s)	q (l/s)	P_{cav1} (bar)	P_{cav2} (bar)	P_{cav3} (bar)	P_b (bar)
37	5030	7.9615	0.531	296	295	11.65	0.0104	1.0853	6.8747	5.9905	5.1611	4.2283
38	5030	7.9184	0.410	296	295	12.46	0.0115	1.1606	6.5498	5.5317	4.6109	3.2501
39	5030	7.9443	0.244	296	295	12.89	0.0117	1.2014	6.4197	5.2200	4.0437	1.9379
40	5030	7.9256	0.154	297	295	13.01	0.0118	1.2120	6.3109	5.0217	3.6691	1.2239
41	5030	13.1029	0.538	297	296	10.63	0.0158	0.9901	11.2824	9.9305	8.7487	7.0503
42	5030	13.1225	0.394	297	296	11.23	0.0167	1.0468	10.9018	9.1635	7.4845	5.1745
43	5030	13.0969	0.244	297	296	11.62	0.0173	1.0832	10.6488	8.4468	6.1415	3.1927
44	5030	13.0638	0.135	298	296	11.84	0.0176	1.1028	10.4384	8.0307	5.1549	1.7697
45	5030	18.3056	0.552	298	297	9.83	0.0203	0.9157	15.8225	13.9153	12.0863	10.1079
46	5030	18.2400	0.401	299	297	10.53	0.0218	0.9814	15.2854	12.7204	10.0796	7.3194
47	5030	18.2998	0.249	299	297	11.34	0.0234	1.0565	14.7252	11.5901	8.0291	4.5480
48	5030	18.2066	0.143	299	296	11.80	0.0243	1.0998	14.2020	10.8027	6.5226	2.6122
49	12000	7.9816	0.573	299	300	11.12	0.0098	1.0363	7.2065	6.3702	5.5804	4.5763
50	12000	7.8218	0.406	301	304	13.49	0.0121	1.2574	6.7364	5.6456	4.3977	3.1766
51	12000	7.9812	0.403	299	302	12.13	0.0108	1.1304	6.4807	5.5647	4.7024	3.2177
52	12000	7.9097	0.154	299	305	12.82	0.0114	1.1949	6.2029	4.9677	3.6109	1.2217
53	12000	13.0951	0.540	300	303	10.77	0.0159	1.0040	11.1704	9.9076	8.6746	7.0688
54	12000	13.0924	0.409	300	303	11.39	0.0167	1.0609	10.8569	9.1449	7.5253	5.3537
55	12000	13.1600	0.248	300	305	11.87	0.0175	1.1059	10.6195	8.4379	5.9978	3.2624
56	12000	13.0598	0.139	300	306	12.28	0.0181	1.1443	10.5517	8.0079	5.0277	1.8094
57	12000	18.2708	0.554	301	304	10.43	0.0213	0.9723	15.8905	13.8106	11.9482	10.1151
58	12000	18.2465	0.402	301	304	11.52	0.0236	1.0736	15.3406	12.6658	9.8940	7.3294
59	12000	18.1566	0.259	301	306	12.66	0.0259	1.1793	14.4577	11.4556	7.7986	4.7111
60	12000	17.9981	0.144	302	306	12.72	0.0259	1.1859	13.7075	10.6033	6.2747	2.5881
61	16000	7.9120	0.543	302	310	10.82	0.0095	1.0084	6.9026	6.0253	5.2365	4.2947
62	16000	7.8906	0.413	302	311	11.37	0.0100	1.0592	6.7158	5.6272	4.6035	3.2606
63	16000	7.9785	0.252	302	316	11.79	0.0104	1.0985	6.5750	5.2771	3.8753	2.0124
64	16000	7.9004	0.154	303	318	12.01	0.0106	1.1194	6.4802	5.0741	3.4107	1.2132
65	16000	12.9893	0.536	303	313	9.97	0.0145	0.9288	11.4462	9.9239	8.4986	6.9635
66	16000	13.0922	0.396	303	312	10.62	0.0154	0.9895	11.1441	9.3071	7.3301	5.1881
67	16000	13.0709	0.253	304	316	11.37	0.0165	1.0592	10.7429	8.4930	5.8570	3.3034
68	16000	13.1174	0.141	304	318	11.94	0.0174	1.1129	10.5546	7.9847	4.8427	1.8455
69	16000	18.2335	0.546	305	313	10.01	0.0202	0.9329	15.8566	13.7863	11.7271	9.9616
70	16000	18.2268	0.396	305	312	11.26	0.0227	1.0495	15.2379	12.6506	9.8141	7.2109
71	16000	18.2659	0.287	305	315	12.23	0.0249	1.1398	14.4956	11.6537	8.0931	5.2472
72	16000	18.2226	0.140	305	316	12.72	0.0260	1.1858	13.6285	10.6390	6.1248	2.5577

Table B9 - Static and dynamic test data for seal 3 cases with high fluid pre-rotation.

Case	CPM	P_o (bar)	P_b/P_o (-)	T_o (K)	T_b (K)	U_o (m/s)	$\dot{m}$ (kg/s)	q (l/s)	P_{cav1} (bar)	P_{cav2} (bar)	P_{cav3} (bar)	P_b (bar)
73	5030	8.0194	0.534	295	295	25.95	0.0122	1.2085	7.0543	6.2456	5.4418	4.2808
74	5030	7.9269	0.431	295	294	26.90	0.0126	1.2529	6.8297	5.8506	4.9207	3.4146
75	5030	7.9349	0.260	295	294	27.66	0.0130	1.2882	6.6551	5.4275	4.1542	2.0618
76	5030	7.9026	0.160	295	294	27.66	0.0130	1.2883	6.6007	5.1920	3.6557	1.2669
77	5030	13.0934	0.538	297	296	22.23	0.0167	1.0352	11.4743	9.9833	8.4481	7.0396
78	5030	13.0909	0.566	295	294	22.97	0.0175	1.0697	11.5584	10.2233	9.0104	7.4108
79	5030	13.1451	0.253	295	294	25.33	0.0194	1.1798	10.7552	8.7055	6.0897	3.3300
80	5030	13.1665	0.134	295	293	25.86	0.0200	1.2039	10.5246	8.1566	4.9107	1.7647
81	5030	18.3112	0.553	297	295	21.01	0.0222	0.9786	15.9721	14.1394	12.0428	10.1301
82	5030	18.2663	0.402	297	295	22.95	0.0243	1.0686	15.3786	13.0012	9.8229	7.3465
83	5030	18.2763	0.245	297	295	25.21	0.0269	1.1740	14.5790	11.6539	7.6581	4.4820
84	5030	18.2315	0.142	297	294	25.36	0.0272	1.1811	13.8049	10.6658	6.3114	2.5886
85	12000	7.9403	0.545	298	301	24.35	0.0111	1.1337	6.8266	6.0384	5.2615	4.3308
86	12000	7.9545	0.407	298	302	25.39	0.0116	1.1826	6.7142	5.6887	4.5739	3.2352
87	12000	7.9084	0.260	299	305	26.39	0.0121	1.2290	6.5248	5.2999	3.8504	2.0540
88	12000	7.8999	0.158	299	305	26.86	0.0123	1.2507	6.4022	5.0575	3.3305	1.2466
89	12000	13.0927	0.557	299	303	22.52	0.0169	1.0489	11.4310	10.0150	8.6772	7.2968
90	12000	13.0902	0.403	299	303	24.60	0.0185	1.1454	10.9888	9.2252	7.2412	5.2691
91	12000	13.0807	0.250	299	304	25.95	0.0197	1.2085	10.6116	8.4648	5.7567	3.2727
92	12000	13.1025	0.137	300	304	26.13	0.0199	1.2168	10.2619	7.9001	4.6966	1.7995
93	12000	18.2335	0.548	301	303	22.73	0.0236	1.0584	15.7103	13.8211	11.7096	9.9833
94	12000	18.2581	0.399	301	304	25.31	0.0266	1.1785	14.8596	12.5712	9.5084	7.2854
95	12000	18.1154	0.246	302	305	25.38	0.0267	1.1821	13.7643	11.3398	7.3124	4.4479
96	12000	17.9507	0.145	302	305	25.40	0.0266	1.1829	13.0398	10.6754	5.8658	2.6051
97	16000	7.9835	0.527	302	310	22.73	0.0102	1.0581	6.9140	5.9632	4.9819	4.2088
98	16000	7.9048	0.403	302	311	23.97	0.0109	1.1164	6.7842	5.6412	4.2994	3.1853
99	16000	7.9327	0.264	303	316	25.16	0.0113	1.1715	6.6649	5.2921	3.6418	2.0904
100	16000	8.0025	0.155	303	317	25.97	0.0117	1.2093	6.5839	5.0559	3.0994	1.2388
101	16000	13.1329	0.536	303	313	21.65	0.0160	1.0081	11.5256	10.0089	8.4332	7.0405
102	16000	13.0309	0.394	304	312	23.42	0.0172	1.0910	11.1333	9.2711	7.0889	5.1404
103	16000	13.0865	0.259	304	316	25.38	0.0187	1.1820	10.5969	8.4722	5.5908	3.3958
104	16000	13.0421	0.136	304	316	26.11	0.0195	1.2160	10.1149	7.8823	4.4321	1.7779
105	16000	18.2592	0.555	305	311	21.69	0.0224	1.0100	15.8392	13.9195	11.7085	10.1294
106	16000	18.2233	0.398	305	312	24.94	0.0258	1.1613	14.6970	12.5228	9.2620	7.2580
107	16000	18.2512	0.246	305	315	25.40	0.0267	1.1828	13.6501	11.2555	6.9475	4.4887
108	16000	18.2297	0.147	305	314	25.39	0.0268	1.1823	13.0646	10.6707	5.7462	2.6832

APPENDIX C

TABULATION OF THE ROTORDYNAMIC COEFFICIENTS AND THE EXPECTED UNCERTAINTIES

The following 18 tables list the rotordynamic coefficients and the calculated related uncertainties for each seal configuration. For direct stiffness and direct damping, the subscripts m, a, and b correspond to the mean, slope, and intercept values respectively. The case numbers refer to the test conditions listed in Appendix B.

Table C1a - Rotordynamic coefficient test data and uncertainties for seal 1 cases with no fluid pre-rotation.

Case	K_m (N/mm)	$\delta(K_m)$ (N/mm)	K_a (Ns/mm)	K_b (N/mm)	k (N/mm)	δ(k) (N/mm)
1	356.35	22.75	0.02	350.11	-53.80	5.46
2	308.15	26.39	0.14	262.57	-64.02	7.24
3	239.30	24.75	0.15	190.61	-26.66	11.30
4	206.14	22.25	0.31	104.56	-12.15	12.18
5	247.05	25.03	0.33	136.54	-12.98	8.56
6	208.98	23.15	0.30	108.99	-8.61	6.85
7	201.72	48.60	0.58	7.35	-2.29	12.84
8	182.45	29.80	0.50	16.51	-4.50	6.70
9	195.16	27.10	0.31	91.23	-9.43	9.68
10	198.85	29.65	0.49	35.25	-7.82	7.77
11	183.92	33.68	0.42	45.20	-8.60	11.27
12	184.20	34.94	0.57	-6.94	-3.22	9.89
13	215.73	18.39	0.07	192.69	-54.55	17.64
14	183.30	31.16	0.34	69.16	-20.24	24.28
15	166.29	36.61	0.35	49.35	-10.08	20.90
16	161.48	39.00	0.41	24.29	-8.37	19.30
17	186.11	34.00	0.36	64.83	-10.61	19.53
18	182.96	41.29	0.44	36.45	-8.22	19.55
19	176.49	50.93	0.53	1.60	-5.72	20.78
20	172.35	55.59	0.61	-29.13	-3.87	21.53
21	193.24	38.74	0.42	54.17	-5.24	20.33
22	190.64	55.94	0.62	-15.58	-2.27	22.07
23	177.34	61.31	0.68	-50.04	-0.48	22.61
24	160.11	64.43	0.71	-75.33	-2.51	23.10
25	211.63	15.72	0.05	195.78	-63.16	14.71
26	172.06	24.74	0.29	76.12	-12.19	33.55
27	163.59	27.23	0.32	57.62	-7.25	36.42
28	159.52	32.66	0.42	19.27	-6.02	32.38
29	177.62	25.90	0.31	74.09	-7.62	36.71
30	184.07	28.07	0.34	71.17	-4.17	37.56
31	175.32	35.44	0.43	30.78	-0.60	40.02
32	165.96	40.29	0.52	-6.80	0.02	40.70
33	188.77	28.09	0.36	70.68	-3.57	37.52
34	186.58	37.11	0.47	30.42	-1.63	46.20
35	174.23	43.95	0.58	-18.76	3.60	50.00
36	159.88	43.31	0.56	-25.94	1.38	48.99

Table C1b - Static and dynamic test data for seal 1 cases with no fluid pre-rotation.

Case	C (Ns/mm)	δ(C) (Ns/mm)	C_b (N/mm)	c (Ns/mm)	δ(c) (Ns/mm)	SEE values C (N/mm)	SEE values c (N/mm)
1	0.1176	.0236	17.43	-0.0002	.0037	35.383	7.481
2	-0.1690	.0224	112.67	-0.1235	.0040	56.531	34.146
3	0.0684	.0180	28.99	-0.0536	.0019	28.139	24.213
4	0.0106	.0174	33.30	-0.1074	.0011	7.641	38.759
5	-0.0266	.0207	69.87	-0.0873	.0010	12.155	29.769
6	0.0339	.0189	32.44	-0.0610	.0013	12.055	24.115
7	-0.0212	.0225	35.24	-0.1097	.0021	20.308	38.803
8	0.1362	.0228	-18.20	-0.0543	.0012	42.213	27.867
9	0.0425	.0190	28.02	-0.0824	.0013	16.044	31.831
10	0.0859	.0228	6.14	-0.0810	.0015	26.175	33.722
11	0.0831	.0232	-1.40	-0.0621	.0014	25.623	27.158
12	0.1427	.0256	-20.04	-0.0522	.0013	43.248	27.079
13	0.0675	.0367	38.42	-0.0444	.0045	20.636	19.850
14	0.1473	.0478	-2.44	-0.0711	.0019	43.971	33.906
15	0.1716	.0633	-22.08	-0.1118	.0013	51.120	49.452
16	0.1579	.0647	-24.96	-0.1330	.0011	46.946	55.828
17	0.1988	.0545	-18.90	-0.0967	.0013	59.101	45.595
18	0.1861	.0677	-23.12	-0.1078	.0016	54.973	48.810
19	0.1626	.0825	-27.66	-0.1203	.0012	48.382	52.023
20	0.1725	.0910	-35.86	-0.1494	.0012	51.139	62.336
21	0.1935	.0626	-18.14	-0.1120	.0013	57.219	50.608
22	0.2067	.0887	-39.05	-0.1254	.0017	61.247	56.490
23	0.2183	.0984	-48.15	-0.1258	.0012	64.886	56.705
24	0.1758	.1028	-40.16	-0.1534	.0012	52.181	64.064
25	-0.0399	.0363	64.08	-0.1397	.0058	12.644	47.069
26	0.0815	.0375	11.20	-0.1489	.0012	24.520	56.899
27	0.1083	.0409	-8.79	-0.1594	.0012	32.080	62.053
28	0.1307	.0441	-19.21	-0.1524	.0016	38.780	61.081
29	0.1337	.0376	-9.60	-0.1940	.0010	39.484	75.576
30	0.1436	.0407	-17.57	-0.1900	.0009	42.433	74.796
31	0.1282	.0496	-20.92	-0.1864	.0010	38.247	72.784
32	0.1601	.0546	-32.76	-0.1845	.0009	47.479	73.795
33	0.1272	.0382	-6.94	-0.2071	.0010	37.618	79.818
34	0.2201	.0508	-48.14	-0.2081	.0009	65.125	85.262
35	0.1709	.0568	-35.11	-0.2198	.0011	50.670	86.598
36	0.1832	.0589	-41.79	-0.2487	.0012	54.381	97.439

Table C2a - Rotordynamic coefficient test data and uncertainties for seal 1 cases with intermediate fluid pre-rotation.

Case	K_m (N/mm)	$\delta(K_m)$ (N/mm)	K_a (Ns/mm)	K_b (N/mm)	k (N/mm)	δ(k) (N/mm)
37	281.37	15.45	-.02	287.51	-33.58	6.35
38	263.10	16.09	-.07	284.96	-37.09	6.38
39	203.76	14.54	0.13	161.41	-14.77	7.01
40	158.10	19.70	0.28	63.63	-4.53	6.84
41	194.01	15.68	0.19	129.26	-4.79	6.12
42	180.88	18.07	0.25	98.22	-6.72	6.96
43	162.56	25.00	0.38	35.72	-4.93	7.66
44	149.06	27.44	0.44	3.89	-2.44	7.65
45	180.02	20.10	0.29	85.20	0.21	8.26
46	173.74	26.66	0.42	34.84	-1.33	8.23
47	161.94	31.18	0.51	-6.85	-3.60	9.62
48	147.64	32.35	0.52	-25.98	-5.54	10.47
49	209.16	17.25	0.02	202.72	-30.34	14.90
50	195.64	23.34	0.18	134.40	-13.47	20.69
51	157.92	37.69	0.34	46.03	-1.00	19.60
52	152.18	40.68	0.37	28.53	-3.55	18.69
53	177.33	30.37	0.26	92.31	-1.00	18.07
54	175.54	38.56	0.34	62.76	-2.78	19.06
55	168.92	50.46	0.49	5.57	-3.32	20.17
56	157.21	53.38	0.53	-18.50	-1.79	20.28
57	191.17	35.82	0.33	81.85	-1.42	18.44
58	182.06	50.53	0.49	17.66	-4.69	19.82
59	167.41	55.55	0.52	-4.70	-0.91	21.86
60	158.21	57.69	0.55	-25.83	-2.21	21.82
61	203.96	13.85	-.03	214.24	-42.89	15.21
62	180.03	18.53	0.20	114.21	-16.68	30.43
63	156.28	30.21	0.37	33.64	-4.67	39.19
64	151.51	32.96	0.41	14.75	-4.40	38.05
65	178.92	24.23	0.27	87.98	-5.97	41.09
66	186.68	30.72	0.37	63.21	-3.15	41.00
67	177.60	37.86	0.49	14.75	-2.21	41.78
68	164.89	41.36	0.54	-14.20	-1.19	44.57
69	197.04	29.64	0.38	71.22	-2.84	34.13
70	189.94	38.75	0.49	28.47	0.22	55.55
71	174.20	44.35	0.59	-22.47	1.28	47.05
72	163.99	45.75	0.60	-36.85	1.34	48.94

Table C2b - Static and dynamic test data for seal 1 cases with intermediate fluid pre-rotation.

Case	C (Ns/mm)	δ(C) (Ns/mm)	C_b (N/mm)	c (Ns/mm)	δ(c) (Ns/mm)	SEE values C (N/mm)	SEE values c (N/mm)
37	-0.0014	.0246	28.18	-0.0432	.0028	7.414	15.536
38	-0.0450	.0243	59.79	-0.1109	.0032	14.264	36.775
39	0.0589	.0211	13.94	-0.1205	.0015	18.796	45.772
40	0.1182	.0204	-16.72	-0.1164	.0009	35.621	47.674
41	0.0464	.0197	31.37	-0.0547	.0011	15.332	22.616
42	0.0762	.0200	8.93	-0.0785	.0014	23.368	32.305
43	0.1571	.0225	-33.21	-0.1180	.0012	46.645	50.347
44	0.1704	.0241	-42.25	-0.1249	.0009	50.576	53.433
45	0.1210	.0211	-8.80	-0.0797	.0015	36.112	35.394
46	0.2134	.0230	-45.00	-0.0972	.0012	63.496	46.393
47	0.1705	.0239	-37.44	-0.1429	.0011	50.570	59.697
48	0.1765	.0251	-44.37	-0.1489	.0011	52.450	62.083
49	-0.0337	.0398	60.53	-0.1467	.0030	12.565	49.627
50	0.0908	.0444	8.70	-0.1146	.0013	27.002	45.440
51	0.1192	.0715	-15.38	-0.1474	.0007	35.345	58.402
52	0.1319	.0766	-24.75	-0.1651	.0010	39.108	65.306
53	0.1288	.0585	-5.80	-0.1695	.0007	38.174	66.609
54	0.1820	.0727	-33.16	-0.1721	.0009	53.802	70.526
55	0.1841	.0910	-43.59	-0.1649	.0013	54.415	68.134
56	0.1630	.0953	-41.62	-0.1723	.0012	48.209	69.550
57	0.1898	.0655	-29.39	-0.1831	.0008	56.013	74.732
58	0.2261	.0878	-53.09	-0.1690	.0013	66.789	71.903
59	0.1928	.1027	-49.15	-0.1626	.0014	57.040	68.421
60	0.1928	.1040	-53.91	-0.1864	.0012	57.234	76.249
61	-0.0155	.0328	41.99	-0.1951	.0038	5.934	67.552
62	0.0880	.0302	-2.62	-0.1813	.0015	26.205	68.444
63	0.1217	.0435	-20.66	-0.1841	.0008	36.069	71.397
64	0.1176	.0471	-22.26	-0.1880	.0010	34.886	72.494
65	0.1295	.0374	-14.23	-0.2162	.0008	38.481	83.078
66	0.1870	.0455	-38.77	-0.1933	.0008	55.202	78.196
67	0.1741	.0519	-38.49	-0.2055	.0009	51.521	81.813
68	0.1790	.0546	-43.19	-0.1765	.0009	52.989	72.120
69	0.1896	.0402	-32.92	-0.2094	.0008	55.912	83.970
70	0.2168	.0535	-51.59	-0.2055	.0007	64.154	84.122
71	0.2132	.0567	-53.88	-0.2012	.0012	62.995	82.508
72	0.2346	.0591	-64.22	-0.1981	.0010	69.230	82.640

Table C3a - Rotordynamic coefficient test data and uncertainties for seal 1 cases with high fluid prerotation.

Case	K_m (N/mm)	$\delta(K_m)$ (N/mm)	K_a (Ns/mm)	K_b (N/mm)	k (N/mm)	δ(k) (N/mm)
73	276.51	20.43	0.20	208.93	-39.16	5.67
74	258.12	16.50	-.04	269.97	-48.48	9.28
75	166.80	19.07	0.26	81.56	-10.57	5.70
76	155.22	19.24	0.28	61.47	-6.68	5.89
77	201.11	19.89	0.31	97.76	-11.68	4.01
78	184.18	18.29	0.27	95.82	-11.23	6.74
79	173.84	22.39	0.35	58.78	-13.48	8.33
80	165.07	26.57	0.44	17.60	-13.76	8.35
81	196.55	19.70	0.28	102.19	-6.48	7.74
82	186.15	25.19	0.42	46.05	-11.09	9.43
83	173.60	27.77	0.47	18.16	-6.92	8.88
84	162.18	30.69	0.51	-6.57	-6.25	9.88
85	186.01	15.70	0.09	154.72	-32.32	16.63
86	160.33	30.72	0.32	52.47	-11.90	23.17
87	148.01	34.53	0.34	34.06	-6.31	19.13
88	144.72	39.60	0.40	11.75	-7.54	19.48
89	171.12	31.70	0.32	64.58	-5.41	18.16
90	171.53	36.49	0.36	51.40	-6.85	19.02
91	167.52	50.68	0.53	-8.65	-2.88	21.59
92	160.93	55.96	0.60	-37.05	-3.08	21.11
93	186.62	34.85	0.35	71.55	-7.92	19.54
94	182.98	49.85	0.52	8.42	-0.23	20.75
95	179.06	57.76	0.62	-26.48	-0.75	22.47
96	164.48	61.44	0.64	-47.18	-5.43	22.54
97	197.31	14.90	0.01	194.55	-43.38	14.84
98	163.03	26.78	0.34	50.32	-11.54	33.30
99	152.83	32.98	0.42	11.56	-7.88	37.17
100	147.92	36.55	0.48	-12.90	-5.75	38.67
101	173.07	26.43	0.32	65.43	-10.01	40.52
102	177.74	33.60	0.44	31.31	-7.01	39.51
103	172.40	42.19	0.57	-18.45	-4.29	48.75
104	161.33	43.92	0.60	-37.21	-3.81	44.71
105	193.36	27.98	0.35	76.04	-10.94	39.90
106	190.97	40.08	0.54	11.21	-1.30	49.02
107	184.19	45.34	0.63	-24.48	-1.77	53.47
108	175.24	46.95	0.64	-38.84	-3.95	55.31

Table C3b - Static and dynamic test data for seal 1 cases with high fluid pre-rotation.

Case	C (Ns/mm)	δ(C) (Ns/mm)	C_b (N/mm)	c (Ns/mm)	δ(c) (Ns/mm)	SEE values C (N/mm)	SEE values c (N/mm)
73	0.0293	.0183	27.26	-0.0762	.0023	13.827	28.742
74	-0.1631	.0173	106.41	-0.1769	.0028	50.594	53.226
75	0.0668	.0143	14.[illegible]3	-0.0975	.0010	20.304	38.378
76	0.0765	.0145	5.48	-0.0903	.0009	23.572	36.638
77	-0.0099	.0150	58.48	-0.1037	.0012	13.719	36.424
78	0.0688	.0152	22.58	-0.0702	.0017	21.682	29.492
79	0.1596	.0169	-20.60	-0.0580	.0022	47.538	30.614
80	0.162[illegible]	.0190	-30.77	-0.0926	.0019	48.481	42.257
81	0.0870	.0164	26.96	-0.0734	.0017	26.267	31.524
82	0.1436	.0176	-10.87	-0.0848	.0020	43.409	38.566
83	0.1977	.0199	-37.42	-0.0778	.0013	58.844	38.845
84	0.1691	.0206	-32.97	-0.1168	.0014	50.754	50.862
85	0.0432	.0319	29.45	-0.1058	.0026	13.767	39.820
86	0.1425	.0487	-16.54	-0.0979	.0011	42.708	42.783
87	0.1171	.0604	-16.78	-0.1376	.0009	34.777	54.915
88	0.1430	.0689	-29.78	-0.1422	.0010	42.591	57.954
89	0.1676	.0547	-21.56	-0.1189	.0009	49.503	51.162
90	0.1527	.0633	-26.71	-0.1452	.0014	45.285	59.568
91	0.1557	.0850	-35.50	-0.1598	.0013	46.197	64.829
92	0.1413	.0930	-35.43	-0.1811	.0016	42.456	71.617
93	0.1850	.0611	-29.38	-0.1342	.0012	54.668	57.553
94	0.1811	.0819	-37.66	-0.1653	.0009	53.698	68.103
95	0.1907	.0944	-47.32	-0.1921	.0014	56.546	78.533
96	0.1700	.1051	-46.52	-0.1928	.0018	50.621	77.480
97	-0.0146	.0340	42.16	-0.2291	.0044	5.956	79.461
98	0.1422	.0373	-22.17	-0.2009	.0015	42.069	78.500
99	0.1503	.0444	-30.29	-0.1887	.0012	44.313	74.60[illegible]
100	0.1790	.0477	-42.24	-0.1765	.0010	52.850	71.931
101	0.1834	.0370	-36.74	-0.2279	.0011	54.109	90.126
102	0.2233	.0435	-55.37	-0.2090	.0011	65.848	85.852
103	0.1877	.0518	-48.48	-0.2228	.0013	55.534	88.593
104	0.2284	.0548	-62.28	-0.2081	.0011	67.400	85.867
105	0.2954	.0376	-76.57	-0.2439	.0018	87.035	101.947
106	0.2988	.0494	-83.34	-0.2037	.0009	88.013	88.192
107	0.2575	.0547	-69.92	-0.1873	.0013	75.926	80.216
108	0.2256	.0574	-63.38	-0.1649	.0016	66.749	70.576

Table C4a - Rotordynamic coefficient test data and uncertainties for seal ? cases with no fluid pre-rotation

Case	K_m (N/mm)	$\delta(K_m)$ (N/mm)	K_a (Ns/mm)	K_b (N/mm)	k (N/mm)	$\delta(k)$ (N/mm)
1	328.02	12.39	-.01	331.93	-20.82	5.71
2	379.02	16.70	0.10	344.65	-30.10	4.76
3	309.65	29.07	0.44	164.20	-44.31	13.03
4	241.29	33.55	0.56	53.64	-53.05	14.92
5	295.93	28.32	0.41	159.68	-53.29	16.58
6	226.94	28.63	0.49	65.44	-29.85	11.59
7	222.35	35.34	0.57	34.06	-26.16	12.02
8	215.13	58.24	0.79	-45.97	-27.76	17.82
9	231.73	34.93	0.56	44.27	-25.95	13.76
10	230.09	38.11	0.63	20.32	-34.20	14.85
11	216.63	32.01	0.53	41.80	-35.68	11.99
12	197.63	36.27	0.60	-2.25	-39.33	11.13
13	290.21	18.70	0.10	257.61	-34.75	7.21
14	251.22	36.55	0.42	112.24	-44.92	16.66
15	214.65	46.96	0.58	22.76	-42.07	16.77
16	168.93	46.40	0.51	0.29	-13.15	17.79
17	246.22	42.07	0.47	89.78	-70.74	17.20
18	191.56	47.80	0.52	19.42	-29.82	18.03
19	188.59	54.27	0.61	-15.47	-23.73	19.64
20	181.85	56.28	0.62	-25.23	-26.40	20.89
21	210.02	48.60	0.53	33.75	-34.08	16.70
22	209.43	56.63	0.62	2.80	-34.30	18.63
23	203.57	59.90	0.62	-2.52	-37.63	20.08
24	190.96	64.23	0.68	-35.46	-37.56	20.85
25	308.77	22.74	0.19	246.10	-53.69	14.44
26	270.42	32.93	0.41	134.62	-55.54	16.74
27	202.26	36.68	0.49	39.18	-36.75	24.82
28	184.20	40.54	0.54	4.55	-21.67	27.61
29	252.18	40.52	0.55	69.98	-61.56	26.93
30	220.82	38.26	0.46	66.34	-42.81	31.17
31	209.11	43.88	0.55	24.80	-30.76	34.26
32	206.57	49.06	0.63	-3.21	-29.21	38.30
33	242.19	34.89	0.40	108.10	-48.41	29.54
34	212.24	41.53	0.50	44.62	-42.91	36.65
35	217.00	47.86	0.59	19.22	-42.22	38.54
36	205.84	50.46	0.61	1.74	-36.87	41.73

Table C4b - Static and dynamic test data for seal 2 cases with no fluid pre-rotation.

Case	C (Ns/mm)	δ(C) (Ns/mm)	C_b (N/mm)	c (Ns/mm)	δ(c) (Ns/mm)	SEE values C (N/mm)	SEE values c (N/mm)
1	0.0667	.0210	28.78	0.0393	.0015	20.927	10.776
2	0.0700	.0244	19.89	0.0771	.0023	21.625	23.313
3	0.0718	.0239	-4.09	0.0381	.0037	23.371	10.191
4	0.1229	.0197	-17.86	-0.0231	.0041	36.962	15.393
5	0.0443	.0244	36.53	0.0139	.0039	15.343	5.600
6	0.0263	.0198	22.42	-0.0780	.0023	23.688	29.733
7	0.0367	.0215	17.09	-0.0986	.0021	15.284	37.108
8	0.0986	.0230	-10.47	-0.1051	.0025	32.895	43.043
9	0.1115	.0201	5.72	-0.0773	.0020	33.063	33.510
10	0.1661	.0226	-19.77	-0.0762	.0029	49.223	36.294
11	0.0646	.0235	7.94	-0.0935	.0028	21.968	36.720
12	0.1808	.0249	-32.42	-0.0735	.0032	54.413	36.311
13	0.1439	.0345	-10.63	0.0945	.0032	42.679	25.263
14	0.1106	.0540	3.39	0.0564	.0049	32.790	14.906
15	0.1168	.0668	-16.04	-0.0321	.0045	34.570	18.444
16	0.1478	.0759	-26.43	-0.0885	.0017	43.619	39.768
17	0.2046	.0639	-23.49	0.0591	.0073	60.633	10.184
18	0.1984	.0767	-32.93	-0.0600	.0035	58.537	33.251
19	0.1545	.0858	-28.15	-0.1141	.0026	46.029	49.254
20	0.1760	.0903	-36.94	-0.0947	.0028	52.165	43.839
21	0.1981	.0771	-27.69	-0.0416	.0037	58.340	26.080
22	0.2526	.0921	-46.95	-0.0644	.0040	74.517	37.076
23	0.2261	.1039	-44.39	-0.0825	.0046	66.767	41.887
24	0.2173	.1087	-47.60	-0.1178	.0043	64.076	53.733
25	0.0721	.0390	16.43	0.0631	.0044	21.555	18.506
26	0.1196	.0441	-7.30	0.0146	.0052	35.408	4.715
27	0.1206	.0471	-12.46	-0.0679	.0033	35.639	31.037
28	0.1561	.0530	-23.70	-0.1173	.0023	46.196	50.145
29	0.1183	.0487	-9.36	-0.0443	.0048	35.172	22.667
30	0.2210	.0538	-42.52	-0.1028	.0037	65.157	48.666
31	0.2044	.0612	-38.70	-0.1194	.0028	60.307	53.337
32	0.1600	.0662	-28.42	-0.1501	.0028	47.283	61.726
33	0.1732	.0510	-23.24	-0.1078	.0041	51.062	47.778
34	0.2557	.0586	-61.52	-0.1069	.0037	75.401	52.016
35	0.1965	.0680	-37.50	-0.1404	.0041	57.939	60.460
36	0.1695	.0738	-33.49	-0.1603	.0036	50.063	65.764

Table C5a - Rotordynamic coefficient test data and uncertainties for seal 2 cases with intermediate fluid pre-rotation.

Case	K_m (N/mm)	$\delta(K_m)$ (N/mm)	K_a (Ns/mm)	K_b (N/mm)	k (N/mm)	δ(k) (N/mm)
37	285.32	19.21	0.22	210.59	-29.73	5.40
38	275.18	24.96	0.38	149.69	-43.23	11.57
39	238.98	27.88	0.45	89.67	-53.25	13.88
40	178.83	28.83	0.51	10.28	-16.46	10.38
41	269.83	23.62	0.34	157.29	-55.78	14.80
42	209.13	26.84	0.43	66.04	-26.82	10.96
43	210.40	36.57	0.54	29.56	-23.73	13.68
44	196.07	35.10	0.60	-2.83	-24.35	12.07
45	217.03	27.85	0.46	62.45	-26.30	11.60
46	217.93	29.99	0.49	54.58	-30.03	11.23
47	212.18	30.92	0.47	55.80	-30.58	11.14
48	198.95	33.59	0.57	10.81	-31.44	12.17
49	324.31	20.00	0.09	293.87	-47.68	6.89
50	254.64	37.50	0.39	124.80	-55.59	18.56
51	209.25	45.37	0.48	49.22	-39.61	16.77
52	182.20	48.30	0.49	18.61	-19.84	17.70
53	263.10	48.33	0.53	87.79	-65.10	17.85
54	209.54	53.31	0.55	25.38	-30.36	18.19
55	209.10	55.08	0.53	31.87	-27.89	19.70
56	202.46	56.81	0.54	21.46	-25.38	20.24
57	230.26	46.33	0.41	93.50	-34.49	18.16
58	229.71	56.70	0.54	51.64	-36.01	19.06
59	220.05	60.55	0.57	29.42	-39.31	20.15
60	204.49	64.55	0.61	0.28	-35.15	21.15
61	338.63	23.79	0.18	280.39	-50.43	14.07
62	262.35	31.71	0.37	139.25	-59.69	19.40
63	207.15	35.35	0.47	50.84	-36.19	25.85
64	187.05	39.07	0.52	14.10	-20.28	32.05
65	233.73	34.80	0.46	81.31	-51.05	26.29
66	225.64	35.14	0.43	81.96	-41.39	29.57
67	217.18	40.28	0.51	48.15	-32.22	32.99
68	211.79	45.36	0.57	21.23	-34.66	36.47
69	245.69	36.08	0.46	94.11	-56.09	27.05
70	229.38	38.52	0.46	76.50	-46.69	36.05
71	221.95	44.30	0.55	37.50	-34.61	38.46
72	217.52	48.59	0.62	11.80	-38.92	39.25

Table C5b - Static and dynamic test data for seal 2 cases with intermediate fluid pre-rotation.

Case	C (Ns/mm)	δ(C) (Ns/mm)	C_b (N/mm)	c (Ns/mm)	δ(c) (Ns/mm)	SEE values C (N/mm)	SEE values c (N/mm)
37	0.0332	.0202	25.74	-0.0254	.0021	12.187	11.698
38	0.0577	.0220	13.63	0.0212	.0033	18.610	5.684
39	0.1399	.0202	-20.79	0.0187	.0043	41.510	4.791
40	0.1291	.0181	-17.73	-0.1018	.0014	38.276	42.964
41	0.1513	.0225	-8.03	-0.0037	.0044	45.871	10.406
42	0.0330	.0200	21.97	-0.1337	.0022	24.595	49.123
43	0.1466	.0222	-12.71	-0.0979	.0022	44.518	42.706
44	0.2176	.0225	-40.63	-0.1175	.0021	66.354	53.621
45	0.1608	.0205	-11.71	-0.0986	.0021	47.717	43.693
46	0.0769	.0221	10.67	-0.1414	.0023	27.934	54.047
47	0.1143	.0244	-4.06	-0.1268	.0026	34.313	50.933
48	0.2310	.0255	-46.11	-0.1048	.0027	69.824	49.940
49	0.0554	.0400	24.14	0.0370	.0042	16.998	10.426
50	0.0825	.0602	8.95	0.0095	.0062	25.748	8.175
51	0.1291	.0731	-15.63	-0.0730	.0041	38.331	33.086
52	0.1776	.0827	-31.80	-0.1362	.0026	52.729	57.860
53	0.1836	.0742	-24.09	-0.0541	.0071	54.318	29.649
54	0.2183	.0881	-36.37	-0.1300	.0035	64.421	58.321
55	0.1981	.0973	-34.85	-0.1432	.0030	58.547	61.673
56	0.2132	.1021	-45.33	-0.1436	.0031	62.888	62.478
57	0.2312	.0858	-42.01	-0.1093	.0040	68.392	51.871
58	0.2631	.1010	-51.22	-0.1383	.0040	77.569	63.449
59	0.2303	.1107	-44.57	-0.1586	.0042	68.210	68.601
60	0.2048	.1165	-44.32	-0.1677	.0039	60.526	70.683
61	0.0713	.0428	24.97	-0.0284	.0042	21.720	14.487
62	0.1667	.0457	-21.00	-0.0497	.0056	49.517	27.031
63	0.1850	.0451	-31.82	-0.1310	.0035	54.569	56.377
64	0.1619	.0500	-25.73	-0.1566	.0019	47.817	64.240
65	0.1496	.0435	-13.27	-0.1116	.0043	44.163	47.634
66	0.2455	.0490	-47.41	-0.1381	.0036	72.456	62.236
67	0.2173	.0551	-41.84	-0.1649	.0032	64.115	70.205
68	0.2282	.0634	-46.36	-0.1783	.0035	67.465	75.540
69	0.1660	.0472	-18.02	-0.1725	.0049	49.108	69.721
70	0.2624	.0551	-59.40	-0.1388	.0042	77.324	63.471
71	0.2303	.0609	-51.14	-0.1746	.0034	67.933	74.172
72	0.1998	.0664	-40.94	-0.1827	.0040	59.048	75.498

Table C6a - Rotordynamic coefficient test data and uncertainties for seal 2 cases with high fluid pre-rotation.

Case	K_m (N/mm)	$\delta(K_m)$ (N/mm)	K_a (Ns/mm)	K_b (N/mm)	k (N/mm)	δ(k) (N/mm)
73	284.44	27.98	0.35	167.21	-24.65	6.29
74	317.56	25.10	0.38	192.80	-34.32	4.46
75	228.81	32.51	0.51	60.62	-47.07	13.46
76	171.54	32.63	0.56	-15.42	-19.87	9.87
77	250.56	25.78	0.38	123.64	-47.97	13.28
78	194.15	28.39	0.47	39.50	-24.03	9.49
79	187.92	28.40	0.45	37.98	-21.33	11.00
80	179.51	33.50	0.39	50.62	-22.51	12.01
81	207.42	25.18	0.37	85.51	-23.52	11.59
82	207.71	31.13	0.48	47.26	-29.12	9.75
83	200.14	34.27	0.52	27.14	-32.89	11.01
84	194.01	33.13	0.46	41.96	-32.69	12.10
85	329.36	20.85	0.07	307.34	-50.41	5.51
86	249.97	37.41	0.41	114.89	-52.00	15.94
87	199.55	47.58	0.52	25.50	-38.75	16.30
88	174.93	50.94	0.52	1.84	-19.90	17.30
89	258.15	46.70	0.48	99.97	-67.08	16.95
90	201.09	50.85	0.49	38.36	-30.30	18.11
91	199.49	56.95	0.56	12.26	-26.78	18.89
92	197.87	59.67	0.59	2.98	-26.69	19.59
93	224.64	48.75	0.46	72.87	-37.07	17.30
94	223.24	58.41	0.58	31.64	-34.40	21.02
95	215.00	64.32	0.63	5.28	-35.84	20.83
96	203.82	64.42	0.60	5.78	-33.13	22.15
97	336.82	27.11	0.24	256.92	-46.04	16.01
98	259.78	33.83	0.39	129.00	-58.16	19.17
99	202.38	36.62	0.47	45.22	-35.12	28.48
100	184.93	40.32	0.52	10.58	-21.97	35.06
101	264.50	42.65	0.58	71.70	-66.86	25.86
102	225.95	37.31	0.46	74.28	-44.41	33.84
103	210.90	44.28	0.57	21.86	-28.08	38.67
104	207.15	48.07	0.62	-0.13	-28.95	41.74
105	248.08	35.62	0.43	104.50	-54.63	30.76
106	231.92	40.65	0.49	68.32	-43.40	38.59
107	225.81	47.05	0.60	25.40	-35.54	43.13
108	211.37	49.57	0.63	0.56	-35.08	47.30

Table C7a - Rotordynamic coefficient test data and uncertainties for seal 3 cases with no fluid pre-rotation.

Case	K_m (N/mm)	$\delta(K_m)$ (N/mm)	K_a (Ns/mm)	K_b (N/mm)	k (N/mm)	δ(k) (N/mm)
1	257.82	14.09	0.07	235.30	-26.90	6.32
2	315.01	16.16	0.09	286.05	-33.94	6.08
3	272.66	23.49	0.21	202.86	-23.61	8.52
4	244.05	23.56	0.32	136.13	-25.49	12.12
5	256.45	34.47	0.47	100.30	-20.14	12.53
6	199.38	30.50	0.49	36.04	-17.08	10.97
7	178.78	32.21	0.50	11.89	-6.06	10.11
8	176.33	38.39	0.65	-39.23	-4.97	9.45
9	202.35	31.75	0.52	30.72	-7.45	10.35
10	197.18	34.52	0.58	4.95	-7.58	10.20
11	191.32	37.04	0.54	12.02	-7.86	11.73
12	194.37	47.86	0.76	-58.77	-4.08	12.62
13	203.70	19.11	0.13	161.42	-46.65	10.56
14	198.11	34.88	0.39	68.43	-25.58	15.46
15	158.45	48.08	0.51	-11.98	-18.18	18.58
16	140.81	53.60	0.56	-44.18	-6.32	19.85
17	170.61	50.83	0.57	-17.79	-26.87	22.87
18	162.05	55.79	0.60	-37.08	-9.06	21.70
19	157.82	59.00	0.58	-35.83	-8.82	21.79
20	153.30	63.82	0.67	-69.89	-8.76	22.18
21	164.46	52.87	0.58	-27.44	-19.26	22.32
22	171.00	56.82	0.61	-30.74	-14.09	21.14
23	164.92	62.12	0.66	-54.81	-12.08	22.62
24	155.10	65.09	0.67	-67.59	-10.74	24.73
25	146.42	19.50	0.20	78.69	-37.72	15.80
26	163.00	31.66	0.38	35.80	-28.02	24.09
27	158.49	39.39	0.49	-4.36	-26.51	31.84
28	135.91	45.15	0.57	-55.17	-10.12	37.53
29	152.72	37.61	0.50	-14.83	-32.52	33.48
30	153.84	39.93	0.51	-14.30	-18.06	42.39
31	159.88	45.23	0.57	-29.46	-14.61	45.79
32	155.23	48.94	0.62	-50.39	-11.37	47.73
33	157.68	40.05	0.54	-20.56	-29.80	38.85
34	172.54	45.84	0.59	-24.28	-22.51	47.76
35	170.21	47.87	0.62	-35.84	-16.95	50.01
36	158.19	49.01	0.64	-53.21	-12.76	52.47

Table C6b - **Static and dynamic test data for seal 2 cases with high fluid pre-rotation.**

Case	C (Ns/mm)	δ(C) (Ns/mm)	C_b (N/mm)	c (Ns/mm)	δ(c) (Ns/mm)	SEE values C (N/mm)	SEE values c (N/mm)
73	0.1896	.0188	-20.79	-0.0058	.0017	60.656	14.062
74	0.0386	.0215	18.41	0.0180	.0026	15.773	5.421
75	0.0584	.0223	2.72	-0.0049	.0040	23.035	7.470
76	0.1377	.0208	-22.18	-0.0949	.0017	40.864	41.002
77	0.1637	.0244	-16.11	0.0268	.0039	48.936	3.920
78	0.1347	.0228	-11.01	-0.0727	.0020	40.033	33.094
79	0.1783	.0242	-30.03	-0.0381	.0020	53.702	23.923
80	0.0882	.0244	-4.28	-0.0810	.0019	27.297	33.682
81	0.0734	.0241	9.69	-0.0693	.0020	25.394	28.928
82	0.1547	.0263	-17.18	-0.1093	.0022	45.975	47.134
83	0.0808	.0284	-3.78	-0.1298	.0026	30.767	50.191
84	0.0875	.0287	-5.98	-0.0720	.0029	27.154	30.621
85	0.0379	.0431	24.07	0.0384	.0044	13.300	11.935
86	0.1056	.0592	-6.47	0.0071	.0054	32.060	5.883
87	0.1494	.0777	-25.48	-0.0559	.0041	44.184	28.165
88	0.1704	.0867	-33.02	-0.1295	.0022	50.430	55.221
89	0.2397	.0765	-51.45	-0.0113	.0068	70.682	18.880
90	0.2684	.0912	-59.92	-0.1009	.0033	79.145	50.435
91	0.2284	.1003	-49.33	-0.1351	.0031	67.354	60.163
92	0.2402	.1072	-57.49	-0.1427	.0032	70.967	63.534
93	0.2450	.0981	-50.06	-0.1235	.0038	72.232	56.934
94	0.2531	.1020	-54.32	-0.1369	.0041	74.670	62.153
95	0.2191	.1137	-47.56	-0.1612	.0041	64.872	68.755
96	0.2335	.1213	-57.93	-0.1474	.0039	69.248	64.829
97	0.0617	.0469	20.69	-0.0086	.0037	18.631	7.796
98	0.1825	.0496	-32.02	-0.0346	.0054	53.943	22.509
99	0.1868	.0488	-36.60	-0.0845	.0033	55.136	40.132
100	0.1695	.0544	-30.38	-0.1328	.0021	50.066	56.059
101	0.1249	.0511	-16.83	-0.0686	.0052	37.318	31.157
102	0.2533	.0534	-56.50	-0.1014	.0040	74.724	49.760
103	0.2395	.0593	-55.07	-0.1561	.0027	70.661	68.087
104	0.2407	.0651	-54.80	-0.1501	.0030	71.214	66.158
105	0.2215	.0502	-41.34	-0.1217	.0048	65.302	54.984
106	0.2997	.0585	-75.33	-0.1161	.0041	88.296	57.504
107	0.2035	.0632	-43.65	-0.1476	.0035	60.276	63.134
108	0.1963	.0673	-42.60	-0.1612	.0034	57.987	67.507

Table C8a - Rotordynamic coefficient test data and uncertainties for seal 3 cases with intermediate fluid pre-rotation.

Case	K_m (N/mm)	$\delta(K_m)$ (N/mm)	K_a (Ns/mm)	K_b (N/mm)	k (N/mm)	$\delta(k)$ (N/mm)
37	177.57	24.57	0.36	59.00	-17.27	5.41
38	196.56	20.17	0.26	110.03	-20.57	5.07
39	137.99	29.32	0.52	-33.36	-3.30	8.05
40	128.91	34.85	0.62	-76.77	-0.17	8.64
41	157.69	28.23	0.48	-2.85	-6.71	8.88
42	152.05	32.35	0.57	-37.82	-4.47	9.84
43	150.88	34.20	0.60	-47.89	-5.58	9.42
44	145.31	36.13	0.62	-59.64	-4.88	8.74
45	166.63	33.26	0.57	-23.08	-7.58	10.38
46	170.16	31.77	0.50	5.20	-6.62	11.25
47	168.11	36.88	0.64	-44.19	-8.24	10.16
48	161.64	39.20	0.67	-62.64	-8.02	10.43
49	172.52	14.57	0.09	143.84	-44.22	5.10
50	140.86	30.21	0.30	42.14	-22.07	16.09
51	162.58	37.02	0.39	32.83	-19.21	15.74
52	132.24	55.98	0.59	-62.33	-3.57	21.91
53	149.82	46.07	0.51	-18.36	-17.71	18.01
54	149.15	53.39	0.57	-40.57	-11.75	20.26
55	148.44	58.74	0.64	-65.30	-11.47	21.06
56	143.08	63.85	0.70	-88.51	-7.45	22.19
57	161.82	50.89	0.55	-22.66	-21.62	19.31
58	161.52	56.24	0.62	-43.45	-17.68	20.43
59	153.06	62.03	0.68	-73.02	-11.49	21.88
60	142.57	65.37	0.72	-97.42	-10.28	22.62
61	155.58	22.04	0.29	58.57	-40.78	14.66
62	158.99	32.24	0.43	17.21	-28.44	23.62
63	138.02	40.71	0.55	-44.24	-15.95	35.79
64	131.61	45.11	0.60	-68.50	-8.51	40.12
65	144.94	40.18	0.52	-28.68	-29.04	36.76
66	151.61	43.27	0.56	-33.21	-22.25	40.73
67	150.10	49.95	0.65	-64.96	-16.91	45.58
68	145.89	52.52	0.68	-80.35	-11.98	44.70
69	156.45	43.80	0.59	-40.16	-33.94	40.57
70	161.25	46.26	0.61	-40.83	-24.74	45.31
71	158.21	50.84	0.67	-63.41	-19.84	48.71
72	150.36	52.19	0.68	-76.15	-11.62	50.96

Table C7b - **Static and dynamic test data for seal 3 cases with no fluid pre-rotation.**

Case	C (Ns/mm)	δ(C) (Ns/mm)	C_b (N/mm)	c (Ns/mm)	δ(c) (Ns/mm)	SEE values C (N/mm)	SEE values c (N/mm)
1	0.0012	.0221	52.48	0.0425	.0021	9.956	15.468
2	0.0716	.0267	36.82	0.0640	.0028	25.122	19.[illegible]51
3	0.0593	.0249	25.87	0.0730	.0027	19.016	22.716
4	0.1102	.0236	5.77	0.0815	.0031	34.329	23.085
5	0.1018	.0246	16.30	0.0303	.0025	30.614	6.215
6	0.1072	.0243	0.27	-0.0160	.0024	31.993	13.022
7	0.1062	.0260	-7.14	-0.0427	.0016	31.762	21.628
8	0.0861	.0266	-3.65	-0.0993	.0012	26.535	39.828
9	0.1399	.0246	-7.66	-0.0383	.0014	41.692	21.747
10	0.1582	.0257	-18.26	-0.0594	.0014	46.837	30.026
11	0.0418	.0271	15.51	-0.1009	.0014	16.815	38.041
12	0.1393	.0302	-18.86	-0.1122	.0015	41.819	47.257
13	0.0661	.0344	20.14	0.1243	.0044	20.668	40.203
14	0.1254	.0542	-16.69	0.0039	.0029	37.349	9.243
15	0.1540	.0819	-37.07	-0.0559	.0024	46.176	29.882
16	0.1691	.0926	-45.19	-0.1116	.0014	50.101	48.838
17	0.1187	.0745	-16.46	-0.0448	.0033	36.650	24.606
18	0.1961	.0912	-48.70	-0.1086	.0015	57.857	49.202
19	0.1870	.1019	-52.34	-0.1173	.0017	55.419	51.897
20	0.1346	.1081	-40.20	-0.1496	.0019	41.795	60.343
21	0.1803	.0823	-38.10	-0.1055	.0024	53.772	47.649
22	0.1847	.0936	-47.60	-0.1090	.0019	54.522	48.825
23	0.2041	.1032	-58.13	-0.1150	.0021	60.435	52.520
24	0.1397	.1073	-37.67	-0.1330	.0024	41.824	55.361
25	0.1055	.0312	-6.07	0.0326	.0041	31.630	6.127
26	0.0864	.0452	-16.48	-0.0619	.0035	26.118	26.571
27	0.1370	.0556	-38.13	-0.0947	.0031	41.226	40.972
28	0.1737	.0621	-50.20	-0.1519	.0018	51.765	63.117
29	0.1887	.0464	-40.19	-0.0727	.0032	55.686	36.099
30	0.2042	.0545	-51.69	-0.1464	.0021	60.454	62.858
31	0.1616	.0621	-44.60	-0.1697	.0020	47.892	68.508
32	0.1818	.0681	-52.94	-0.1907	.0017	54.015	77.024
33	0.2497	.0489	-59.55	-0.1293	.0030	73.636	59.342
34	0.1670	.0570	-41.75	-0.2157	.0025	50.519	85.101
35	0.1545	.0627	-40.05	-0.1965	.0020	46.032	77.589
36	0.1559	.0647	-41.32	-0.2138	.0017	46.710	83.672

Table C9a - Rotordynamic coefficient test data and uncertainties for seal 3 cases with high fluid pre-rotation.

Case	K_m (N/mm)	$\delta(K_m)$ (N/mm)	K_a (Ns/mm)	K_b (N/mm)	k (N/mm)	δ(k) (N/mm)
73	149.32	17.78	0.26	64.29	-19.63	3.67
74	179.23	19.56	0.25	97.29	-25.95	3.46
75	129.52	26.87	0.47	-26.16	-6.95	8.43
76	121.31	34.47	0.61	-80.22	-2.09	10.02
77	145.01	28.45	0.47	-11.07	-6.49	11.18
78	161.88	27.10	0.47	6.88	-13.49	9.85
79	143.65	37.15	0.65	-72.91	-7.42	10.97
80	139.55	40.62	0.70	-91.80	-6.18	11.12
81	155.98	30.08	0.52	-17.46	-8.98	11.27
82	158.57	32.06	0.55	-24.63	-9.29	10.84
83	156.73	35.95	0.61	-45.40	-11.74	10.65
84	146.29	44.81	0.79	-116.66	-12.45	10.86
85	156.05	13.13	0.10	122.79	-41.87	3.68
86	161.56	29.11	0.35	45.94	-23.27	16.42
87	130.06	47.11	0.51	-40.32	-7.71	18.75
88	123.73	50.42	0.55	-57.57	-3.25	18.50
89	143.44	39.90	0.44	-2.87	-21.73	18.46
90	144.44	51.49	0.57	-44.90	-10.99	18.72
91	140.35	57.63	0.62	-64.58	-9.42	20.53
92	135.58	63.07	0.69	-94.14	-8.36	22.05
93	155.81	50.97	0.56	-31.62	-22.75	21.04
94	153.18	57.66	0.66	-66.52	-14.29	19.51
95	142.47	62.36	0.73	-99.84	-14.04	21.58
96	139.71	66.52	0.77	-117.87	-10.11	23.40
97	146.16	17.40	0.20	78.92	-50.61	12.35
98	147.99	33.73	0.42	9.18	-26.99	26.99
99	133.73	41.72	0.55	-48.34	-12.27	38.47
100	129.99	44.26	0.58	-63.37	-7.00	41.77
101	142.90	37.88	0.48	-16.77	-30.78	36.89
102	148.34	42.11	0.53	-27.68	-20.81	41.85
103	146.22	47.31	0.60	-53.08	-16.24	44.39
104	141.20	50.21	0.63	-68.15	-12.23	46.74
105	155.32	40.66	0.52	-16.18	-38.59	38.71
106	156.63	43.67	0.53	-20.19	-25.52	44.58
107	157.46	51.80	0.67	-66.57	-18.72	48.17
108	152.20	51.56	0.66	-66.57	-12.49	49.78

Table C8b - Static and dynamic test data for seal 3 cases with intermediate fluid pre-rotation.

Case	C (Ns/mm)	δ(C) (Ns/mm)	C_b (N/mm)	c (Ns/mm)	δ(c) (Ns/mm)	SEE values C (N/mm)	SEE values c (N/mm)
37	0.0287	.0148	22.44	0.0291	.0012	12.794	10.004
38	0.0265	.0175	19.40	0.0556	.0013	10.273	18.268
39	0.0861	.0181	-9.50	-0.0436	.0008	26.969	20.672
40	0.1896	.0197	-44.55	-0.0564	.0006	56.123	30.704
41	0.1261	.0181	-11.50	-0.0168	.0010	37.365	13.399
42	0.1831	.0206	-35.22	-0.0383	.0010	54.143	24.026
43	0.1587	.0224	-32.00	-0.0557	.0010	46.990	28.668
44	0.1774	.0236	-40.38	-0.0653	.0009	52.618	33.158
45	0.2136	.0221	-41.07	-0.0374	.0011	63.161	25.517
46	0.1023	.0223	-8.56	-0.0423	.0013	32.071	21.818
47	0.1453	.0249	-28.58	-0.0735	.0013	43.341	34.155
48	0.1732	.0275	-39.90	-0.0781	.0013	51.277	37.290
49	0.0434	.0273	15.76	0.0561	.0039	14.387	17.753
50	0.0945	.0494	-27.85	-0.0011	.0027	28.204	8.686
51	0.1300	.0582	-31.75	-0.0233	.0024	38.707	16.627
52	0.1649	.0881	-45.56	-0.1321	.0013	49.175	56.129
53	0.2162	.0734	-53.11	-0.0882	.0023	64.012	43.505
54	0.2132	.0850	-59.29	-0.1268	.0018	63.120	56.523
55	0.1878	.0937	-55.11	-0.1414	.0018	55.813	60.190
56	0.2074	.1018	-62.53	-0.1503	.0016	61.426	64.645
57	0.2506	.0810	-66.21	-0.0908	.0025	73.930	45.998
58	0.2222	.0906	-64.61	-0.1321	.0024	65.967	58.916
59	0.1956	.0998	-58.84	-0.1492	.0019	58.644	64.036
60	0.2138	.1028	-62.49	-0.1561	.0018	63.232	67.033
61	0.1356	.0274	-23.36	0.0515	.0036	40.043	10.577
62	0.1732	.0418	-48.26	-0.0413	.0030	51.094	24.409
63	0.2004	.0516	-59.32	-0.1185	.0019	59.102	52.814
64	0.1940	.0578	-60.15	-0.1511	.0014	57.370	63.871
65	0.2459	.0522	-64.72	-0.1056	.0025	72.420	51.014
66	0.2139	.0573	-59.90	-0.1545	.0021	63.063	66.190
67	0.2088	.0657	-62.65	-0.1549	.0018	61.583	66.052
68	0.1929	.0690	-60.66	-0.1668	.0017	57.002	69.374
69	0.2603	.0530	-66.51	-0.1439	.0027	76.656	65.092
70	0.2482	.0589	-69.94	-0.1679	.0021	73.186	72.931
71	0.2429	.0654	-69.68	-0.1829	.0020	71.552	77.764
72	0.2164	.0689	-63.45	-0.1907	.0014	63.899	79.002

Table C9b - Static and dynamic test data for seal 3 cases with high fluid pre-rotation.

Case	C (Ns/mm)	δ(C) (Ns/mm)	C_b (N/mm)	c (Ns/mm)	δ(c) (Ns/mm)	SEE values C (N/mm)	SEE values c (N/mm)
73	0.0108	.0145	23.70	0.0541	.0012	6.287	18.669
74	-0.0303	.0163	33.74	0.0564	.0017	10.617	21.661
75	0.0959	.0177	-13.12	-0.0016	.0010	28.439	7.167
76	0.1557	.0191	-36.92	-0.0370	.0009	46.011	22.364
77	0.1355	.0170	-21.48	-0.0014	.0011	40.489	9.686
78	0.0392	.0182	12.62	0.0515	.0016	14.455	16.381
79	0.1021	.0220	-21.52	-0.0642	.0012	33.770	29.141
80	0.1254	.0232	-32.34	-0.0557	.0013	38.933	27.820
81	0.1603	.0201	-30.30	-0.0063	.0014	47.392	12.285
82	0.1436	.0220	-28.74	-0.0258	.0013	42.508	17.667
83	0.1376	.0241	-32.53	-0.0388	.0014	41.204	21.967
84	0.1753	.0250	-48.86	-0.1258	.0013	52.012	54.001
85	0.0621	.0217	-5.48	0.0414	.0036	18.892	11.366
86	0.1093	.0404	-30.63	-0.0092	.0021	32.436	12.499
87	0.1795	.0727	-55.04	-0.0850	.0014	53.176	40.734
88	0.2095	.0816	-65.09	-0.1088	.0011	61.873	50.188
89	0.2120	.0625	-56.85	-0.0556	.0025	62.677	31.966
90	0.2422	.0824	-72.60	-0.1143	.0015	71.644	53.790
91	0.2169	.0941	-69.43	-0.1317	.0017	64.457	58.890
92	0.1931	.0984	-62.29	-0.1406	.0017	57.220	60.319
93	0.2335	.0770	-64.50	-0.1219	.0027	68.978	56.463
94	0.2296	.0865	-67.29	-0.1568	.0024	67.719	68.396
95	0.2346	.0927	-72.49	-0.1834	.0022	69.725	78.197
96	0.2720	.0965	-85.09	-0.1561	.0026	80.329	70.334
97	0.1203	.0250	-25.88	0.0508	.0041	35.631	11.397
98	0.1240	.0471	-38.95	-0.0483	.0028	36.919	24.111
99	0.1972	.0527	-62.88	-0.1155	.0016	58.333	51.636
100	0.2021	.0577	-66.13	-0.1437	.0011	59.691	61.751
101	0.2280	.0496	-64.32	-0.1187	.0027	67.464	54.743
102	0.2363	.0563	-72.69	-0.1247	.0021	69.650	57.155
103	0.2300	.0637	-73.78	-0.1425	.0018	67.819	63.016
104	0.2263	.0692	-73.37	-0.1571	.0016	66.685	67.952
105	0.2975	.0519	-83.78	-0.1335	.0035	87.685	63.690
106	0.3035	.0602	-91.96	-0.1203	.0025	89.393	59.472
107	0.2609	.0671	-80.12	-0.1093	.0020	76.937	53.381
108	0.2519	.0696	-78.23	-0.1190	.0015	74.399	56.146

☆ U.S. GOVERNMENT PRINTING OFFICE 1993 — 750-113--80200